EFFECT OF SURFACE TREATMENT OF ZIRCONIA-CERAMIC DENTAL RESTORATIONS

FIRAS ABDULAMEER FARHAN

FACULTY OF DENTISTRY
UNIVERSITY OF MALAYA
KUALA LUMPUR

2018

EFFECT OF SURFACE TREATMENT OF ZIRCONIA-CERAMIC DENTAL RESTORATIONS

FIRAS ABDULAMEER FARHAN

THESIS SUBMITTED IN FULFILMENT OF THE REQUIREMENTS FOR THE DEGREE OF DOCTOR OF PHILOSOPHY

FACULTY OF DENTISTRY
UNIVERSITY OF MALAYA
KUALA LUMPUR

2018

UNIVERSITY OF MALAYA
ORIGINAL LITERARY WORK DECLARATION

Name of Candidate: Firas Abdulameer Farhan

Registration/Matric No: DHA140004

Name of Degree: Doctor of Philosophy

Title of Thesis ("this Work"): Effect of Surface Treatment of Zirconia-Ceramic Dental Restorations

Field of Study: Dentistry (Prosthodontics)

I do solemnly and sincerely declare that:

(1) I am the sole author/writer of this Work;
(2) This Work is original;
(3) Any use of any work in which copyright exists was done by way of fair dealing and for permitted purposes and any excerpt or extract from, or reference to or reproduction of any copyright work has been disclosed expressly and sufficiently and the title of the Work and its authorship have been acknowledged in this Work;
(4) I do not have any actual knowledge nor do I ought reasonably to know that the making of this work constitutes an infringement of any copyright work;
(5) I hereby assign all and every rights in the copyright to this work to the University of Malaya ("UM"), who henceforth shall be owner of the copyright in this Work and that any reproduction or use in any form or by any means whatsoever is prohibited without the written consent of UM having been first had and obtained;
(6) I am fully aware that if in the course of making this Work I have infringed any copyright whether intentionally or otherwise, I may be subject to legal action or any other action as may be determined by UM.

Candidate's Signature Date:

Subscribed and solemnly declared before,

Witness's Signature Date:

Name:

Designation:

EFFECT OF SURFACE TREATMENT OF ZIRCONIA-CERAMIC DENTAL RESTORATIONS

ABSTRACT

The zirconia-ceramic restoration (ZCR) is used as substitutes for the metal-ceramic restoration. Clinical studies of ZCRs showed a high fracture incidence of veneering layer than metal-ceramic restorations. This attributed to the low bond strength of zirconia to veneering ceramic as a result of lacking glass content in its matrix. Surface treatment was proposed to improve the bonding strength between zirconia and veneering ceramic. Several studies revealed that surface treatment such as airborne particle abrasion (APA) is responsible for generating chipping of veneering ceramic. The study aimed to develop a new zirconia coating to increase the bonding strength between zirconia substrate and veneering porcelain. Three groups of 150 zirconia specimens (discs, rods and crowns) were divided according to the type of surface treatments. Group M1, the unsintered zirconia specimens were coated with a mixture of glaze porcelain powder and partially-sintered zirconia powder prepared at 1100 °C. Group M2 was coated with a mixture of ceramic liner paste and partially-sintered zirconia powder. The APA group (control), the sintered zirconia specimens were abraded with 50 µm aluminium oxide powder. Group M1 and M2 were further subdivided according to partially sintered zirconia powder with two selected particle sizes, A (26 ± 0.3 µm) and size B (47 ± 0.5 µm) into M1A, M1B, M2A and M2B respectively. Surface area roughness (S_a) was measured by surface texture analyser. Surface morphology and elemental composition were analysed by scanning electron microscope (SEM). Crystallographic phases were identified by X-ray diffraction (XRD). The coefficient of thermal expansion (CTE) was assessed with a thermomechanical analyser. Shear bond strength (SBS) test was evaluated by a universal testing machine (UTM). Fracture strength (FS) test prepared by Cercon CAD/CAM system and measured with UTM. Fractographic analysis of SBS and FS were examined by a stereomicroscope and SEM, where for each test and measurement, 10 specimens were used per group. Finite element analysis (FEA) was simulated and predicted the stress distributions of the static oblique load in coated and non-coated zirconia crown models. The collected data were analysed by one-way ANOVA and Tukey HSD test at ($P<0.05$). Surface roughness results showed significant differences among all groups ($P<0.000$). The M1B group exhibited a higher S_a value (10.33 ± 0.59 µm) among the tested groups. XRD analysis showed *tetragonal* and *monoclinic* phases in the control group while only *tetragonal* was detected in the coated groups. The SBS of the coated groups were higher than those of the control group. The M1B group showed significantly higher SBS (37.54 ± 4.38 MPa) compared to other tested groups ($P<0.05$). The FS of the coated M1B group (647.92 ± 97.33 N) had higher FS compared to other groups ($P<0.00$). FEA showed the coated crown models have lower stress level than the non-coated model. The new coating (M1B) by airbrush spray technique can be considered as an alternative method to APA treatment to improve the bond strength of zirconia substrate to veneering ceramic. It is an applicable surface treatment for improving the clinical performance of the coated ZCR.

Keywords: Zirconia ceramic-restoration, New zirconia coating, Airbrush spray technique, Airborne particle abrasion, Finite element analysis.

EFFECT OF SURFACE TREATMENT OF ZIRCONIA-CERAMIC DENTAL RESTORATIONS

ABSTRAK

Sistem seramik zirkonia digunakan sebagai pengganti sistem konvensional logam-seramik. Kajian klinikal restorasi seramik zirkonia telah menunjukkan kejadian fraktur lapisan venir yang tinggi berbanding restorasi logam seramik. Ini disebabkan oleh kekuatan ikatan zirkonia yang rendah kepada venir seramik disebabkan kekurangan kaca dalam matriks zirkonia. Rawatan permukaan dicadangkan untuk meningkatkan kekuatan ikatan antara zirkonia dan venir seramik. Kajian menunjukkan rawatan seperti lelasan zarah udara (APA) bertanggungjawab menghasilkan keretakan dan serpihan venir seramik. Kajian ini bertujuan membina salutan permukaan zirkonia yang baru untuk meningkatkan kekuatan ikatan di antara substrat zirkonia dan venir porselin. Tiga kumpulan 150 spesimen zirkonia (cakera, rod dan korona) dibahagikan mengikut jenis rawatan permukaan. Kumpulan M1, spesimen zirkonia yang tidak disinter disalut dengan campuran serbuk porselin glasir dan serbuk zirkonia separuh sinter yang disediakan pada 1100 ° C. Kumpulan M2 disalut dengan campuran lapisan seramik dan serbuk zirkonia separuh sinter. Kumpulan APA (kawalan), spesimen zirkonia sinter dirawat dengan serbuk aluminium oksida 50 µm. Kumpulan MI dan M2 dibahagikan pula mengikut dua saiz serbuk zirkonia terpilih; sizes A (26 ± 0.3 µm) and size B (47 ± 0.5 µm) ke dalam subkumpulan M1A, M1B, M2A dan M2B. Kekasaran kawasan permukaan (S_a) diukur oleh analyser tekstur permukaan. Morfologi permukaan dan komposisi unsur dianalisis dengan mengimbas mikroskop elektron (SEM). Fasa krystallografik telah dikenalpasti dengan difraksi X-ray (XRD). Pekali pengembangan haba (CTE) dinilai oleh analyser termomekanik. Ujian kekuatan ikatan ricih (SBS) dinilai oleh mesin ujian universal (UTM). Ujian kekuatan fraktur (FS) disediakan dan diukur oleh sistem Cercon CAD / CAM dan UTM. Analisis fraktografi untuk SBS dan FS diperiksa oleh stereomicroscope dan SEM. Bagi setiap ujian dan pengukuran, 10 spesimen digunakan setiap kumpulan. Finite element analysis (FEA) digunakan untuk mensimulasikan dan meramalkan pengagihan tekanan beban serong statik dalam model korona zirkonia bersalut dan tidak bersalut. Data yang dikumpulkan dianalisis dengan ujian ANOVA dan Tukey HSD sehala ($P<0.05$). Hasil kekasaran permukaan menunjukkan perbezaan yang signifikan antara semua kumpulan ($P<0.000$). Kumpulan M1B menunjukkan nilai S_a yang lebih tinggi (10.33 ± 0.59 μm) di kalangan kumpulan yang diuji. Analisis XRD menunjukkan fasa tetragonal dan monoklinik dalam kumpulan kawalan manakala hanya tetragonal dikesan dalam kumpulan bersalut. Nilai SBS untuk kumpulan bersalut lebih tinggi daripada kumpulan kawalan. Kumpulan M1B menunjukkan SBS yang ketara tinggi (37.54 ± 4.38 MPa) dibandingkan dengan kumpulan lain yang diuji ($P<0.05$). Ujian FS menunjukkan bahawa kumpulan bersalut M1B (647.92 ± 97.33 N) menghasikan FS yang lebih tinggi berbanding kumpulan lain. FEA menunjukkan model korona bersalut mempunyai tahap stress yang lebih rendah daripada model tidak bersalut. Rawatan permukaan salutan baru boleh dianggap sebagai cara alternatif untuk rawatan lelasan partikel udara untuk meningkatkan kekuatan ikatan substrat zirkonia kepada venir seramik, menunjukkan potensinya sebagai rawatan permukaan yang sesuai untuk meningkatkan prestasi klinikal korona seramik zirkonia bersalut.

Kata kunci: Sistem seramik zirkonia, Salutan zirkonia baru, Teknik semburan Airbrush, Lelasan zarah udara airborne, Finite element analysis

ACKNOWLEDGEMENTS

First and foremost, my thanks and gratitude goes to “ALLAH” for allowing me to finish the PhD study with his blessing.

I would be deeply gratefully appreciation to my supervisors Associate Professor Dr Eshamsul Bin Sulaiman and Senior Lecturer Dr Muralithran A/L Govindan Kutty, for their guidance, encouragement and valuable support that allowed me to complete this PhD project.

I am thankful for the scholarship sponsored by the government of the Republic of Iraq / Ministry of Higher Education and Scientific Research / University of Baghdad.

I will be continuously appreciative to loveliest father and mother; I have been nothing without your prayers and inducements. Great gratitude to the father’s in law for generosity and fabulous encouragement during my study.

Last great thanks to my life partner and wonderful wife; Rasha and my children; Ali, Zainab and Hayder, they stood up with me to pass the difficult times throughout the study years. I am so grateful for my brothers and sister for their support and valuable prayers.

My Special thanks go to my friend Dr Haki Ismail for its keen kind interest and support.

TABLE OF CONTENTS

CHAPTER 3: MATERIALS AND METHODS 47

LIST OF FIGURES

LIST OF TABLES

LIST OF SYMBOLS AND ABBREVIATIONS

APA : Airborne particle abrasion

ASTM : American society for testing and materials

BMP : Bitmap image

°C/min : Degree Celsius per minute

CAD/CAM : Computer aided design/computer aided manufacturing

dB : Decibel

DICOM : Digital Imaging and Communications in Medicine

FITS : Flexible Image Transport System

FS : Fracture strength

GIF : Graphics Interchange Format

GPa : Gigapascal

ISO : International organization for standardization

JPEG : Joint photographic experts group

Kgf/cm^2 : Kilogram-force per square centimeter

mL : milliliter

MPa : Megapascal

N : Newton

Psi : Pound per square inch

Rpm : Round per minute

S_a : Surface area roughness

TIFF : Tagged Image File Format

wt% : Weight percentage

YSZ : Yttria stabilised zirconia

LIST OF APPENDICES

CHAPTER 1: INTRODUCTION

1.1 Background of study

Yttria-stabilized zirconia (YSZ) are used as all-ceramic restorations owing to their high flexural strength, superior biocompatibility and better aesthetic (metal-free substructure). They have become suitable alternatives to the metal-ceramic restoration in situations of high mechanical stress, such as the framework substructure for fixed dental prostheses like crowns, bridges, and post/core systems (Guazzato et al., 2004; Della Bona & Kelly, 2008). The material used as a framework for zirconia-ceramic fixed dental restorations is the tetragonal structure of YSZ because of these superior properties (Piconi & Maccauro, 1999; Manicone et al., 2007).

Furthermore, introduction of computer aided design/computer aided manufacturing (CAD/CAM) technologies in dentistry have facilitated the design and fabrication of zirconia-ceramic fixed restorations with minimal flaws and in lesser time (Li et al., 2014). In general, the flexural strength of the coping materials fabricated by CAD/CAM is higher than those produced by the conventional approach (Miyazaki et al., 2009).

The using of the zirconia-ceramic system was met with some technical complications which were related to the weak coping/veneer bond strength at the interface area. These complications lead to decrease in the efficacy of zirconia-ceramic restorations to tolerate the functional stresses applied on an aesthetic part of veneering porcelain which is transferred to the underlying framework (Aboushelib et al., 2008). Therefore, the chipping incidence in zirconia-ceramic restorations is higher than the metal-ceramic restorations which have been recognised as the main cause of clinical failure (Della Bona & Kelly, 2008; Triwatana et al., 2012).

To improve the bonding of veneering porcelain to zirconia coping, several means have been proposed, such as surface treatment which can be achieved by either removing or adding materials on the zirconia surface to increase the microroughness and thus improving the micromechanical interlocking between zirconia and the veneering porcelain (Yoon et al., 2014).

Airborne particle abrasion (APA) (Yang et al., 2010), grinding with discs or diamond rotary instruments (Ohkuma et al., 2011), selective infiltration etching (Aboushelib et al., 2007) and laser etching (Liu et al., 2013) were methods used as surface treatments to increase roughness by removing a thin layer from zirconia surface to create a microroughness surface. APA by aluminium oxide particles is considered a common surface treatment method used for zirconia restoration because it can be applied to simple and complex shapes. Many studies proposed that the APA approach causing the phase transition of the zirconia surface from tetragonal to monoclinic which is combined with volume increase produces stresses on veneering porcelain layer that leads to microcracks and chipping susceptibility (Kosmač et al., 2008; Casucci et al., 2010; Tholey et al., 2010; Arami et al., 2014).

In order to avoid undesirable phase transition associated with APA, other kinds of surface treatments are performed by adding a thin film to the zirconia surface such as tribochemical silica coating (Scherrer et al., 2011), plasma spraying (Sun et al., 2001) and sputtering (Yang et al., 2005). Moreover, new surface treatment by adding a thin layer of micron sized zirconia powder that is mixed with a glue and applied to the zirconia surface. After sintering, this will provide the microroughness required for mechanical interlocking between zirconia surface and veneering porcelain. It has been shown that surface modification by zirconia particles could significantly improve the bond strength between zirconia substrate and veneering porcelain compared to the APA approach (Teng et al., 2012).

1.2 Statement of problems

The general complications related to zirconia-ceramics restorations that are detected frequently after clinical use and *in vitro* study are listed below:

1. Several clinical studies investigated that the incidence rate of veneering ceramics chipping of zirconia-ceramic restorations ranges from 11.4% to 25% of all fixed dental prostheses (Sailer et al., 2009b; Wolfart et al., 2009; Raigrodski et al., 2012).
2. Zirconia-ceramic systems do not yet reach the same bond strength in metal-ceramic systems. Therefore, the bonding between the porcelain and zirconia core is still an interesting issue to investigate for the long-term success of the zirconia restoration.
3. It has been proposed that APA surface treatment resulted in a phase transition of zirconia from tetragonal to monoclinic and lead to increased tensile stress on the veneering ceramic, causing microcrack and chipping (Fischer Jens et al., 2008).
4. There is no alternative surface treatment available to produce a rougher zirconia surface and improved bonding to veneering ceramic without any adverse effect such as cracks and fracture.

1.3 Hypothesis

The coating of zirconia substrate with the new zirconia powder using spraying method will improve the bonding strength of the zirconia-ceramic restoration.

1.4 Aim and objectives of the study

A. To develop new surface coatings by spraying method on the zirconia surface substrate and evaluate their surface and physical properties.

Objectives:

1. To synthesise new coating mixture (two particle sizes of partially-sintered zirconia powder mixed with glazing porcelain powder).
2. To synthesise new coating mixture (two particle sizes of partially-sintered zirconia powder mixed with ceramic liner paste).
3. To use a new coating method by airbrush spraying.
4. To measure the surface roughness, morphology, the crystal phase changes and microstructure characterization of treated zirconia specimens

B. To assess the effect of new surface coatings on the mechanical and bonding properties of zirconia substrate to veneering ceramic

Objectives:

1. To measure the coefficient of thermal expansion of treated zirconia specimens.

2. To assess the bonding strength of the treated zirconia specimens by using shear bond strength method.
3. To evaluate the effect of different surface treatments on the fracture strength of zirconia-ceramic crowns.
4. To examine the fractured specimens through fractographic analysis.

C. To predict the effect of new surface coatings on the stress distribution of zirconia-ceramic crowns using finite element analysis (FEA).

Objectives:

1. To simulate and evaluate the stress distribution along the surface of the treated zirconia-ceramic crown under oblique load and compare with the non-coated crown.

1.5 Significance of study

Metal-ceramic restorations have been in use by a dentist for more than 50 years. The desired strength of a metal framework may improve the clinical performance, but the dark colour and oxides of metal make it difficult to match the aesthetic look of a natural tooth. Currently, all-ceramic restorations are preferred, especially when superior aesthetic is required.

Zirconia is used as a coping material for crown and bridge in all-ceramic restoration, because of superior aesthetic, higher mechanical strength and improved biocompatibility properties. Furthermore, the introduction of CAD/CAM systems in dentistry have facilitated the design and fabrication of zirconia-ceramic restorations with minimal flaws and advanced dimensional accuracy.

The clinical performance of zirconia-ceramic restorations have been evaluated and showed a high incidence rate of veneer ceramic chipping compared to the metal-ceramic restorations. This was due to the weak bonding strength of zirconia coping to veneering ceramic and in order to improve this, surface treatments have been suggested.

Airborne particle abrasion (APA) with aluminium oxide is a common surface treatment used to zirconia. APA is often used to increase the microroughness which lead to improved micromechanical interlocking between zirconia coping and the veneering porcelain. However, this approach causes a phase transition from tetragonal to monoclinic of the zirconia surface that leads to increased generation of stress on veneering porcelain which produced microcracks and chipping susceptibility.

In this study, APA method was selected as a control group because it was commonly used in zirconia-ceramic restoration by dental technicians to provide a surface roughness to increase micromechanical interlocking to veneering porcelain. In order to increase~~s~~ the success rate of the zirconia-ceramic system and avoid the microcracks created from APA treatment, new zirconia coatings were developed as an alternative surface treatment to produce microroughness on zirconia surface without phase transformation and improve bonding strength to veneering porcelain. The surface roughness value, surface morphology, physical and mechanical properties of coated zirconia specimens were evaluated and compared with APA surface treatment.

CHAPTER 2: REVIEW OF LITERATURE

2.1 Definition and history of dental ceramics

The word *Ceramic* originates from the Greek word *Keramos*, which means pottery or overcooked raw material. Historically, three basic types of ceramic materials have been developed; earthenware, stoneware and porcelain. China, in about 100 B.C., industrialised stoneware by firing at higher temperatures to improve their strength and resistance to water infiltration. The porcelain material is obtained by fluxing white china clay with *China stone* to produce pottery structures with high strength and translucency (Jones, 1985).

The first fixed dental prostheses (FPDs) were introduced at the end of the nineteenth century. In 1889, doctor Charles H. Land designed a technique to fabricate porcelain jacket crowns and within the same time, Jan Adriaansen advanced the method of building up porcelain powder with a brush. The widespread use of metal-ceramic restorations did not become practical until 1962 when M. Weinstein and S. Katz developed the use of gold alloys to support the brittleness of veneer porcelain (Land, 1904; Asgar, 1988).

Ceramics have been used for centuries due to their colour stability, durability, low thermal conductivity and good optical properties. Conventional dental ceramics is a solid material with an amorphous structure based on silica (quartz (SiO_2)), kaolin (clay) ($Al_2O_3.2SiO_2.2H_2O$), metallic pigments, potash feldspar ($K_2O.Al_2O_36SiO_2$) and soda feldspar ($Na_2O.Al_2O_36SiO_2$) (Craig & Powers, 2002).

Ceramics can be classified into four categories: (1) silicates, (2) oxides, (3) non-oxides, and (4) glass. Silicate ceramics are characterised by an amorphous glass phase and can have a porous structure. The main component is SiO_2 with small additions of crystalline Al_2O_3, MgO, ZrO_2 and/or other oxides. Oxide ceramics composed of a major crystalline phase such as Al_2O_3, MgO and ZrO_2 either without glass phase or a small amount of glass phase. Non-oxide ceramics are unworkable for use in dentistry because of high processing temperatures, complex processing methods, and unaesthetic colour and opacity. Glass-ceramics are partially crystallised glasses, which occur by nucleation and growth of crystals in the glass matrix (Anusavice, 2003).

The term ceramic is defined as a compound made basically from nonmetallic minerals as clay which is fired at a high temperature to achieve desired properties (Blarcom & Clifford, 2008). The term porcelain refers to a ceramic material formed of infusible elements joined by lower fusing materials. Most dental porcelains are glasses and are used in the fabrication of teeth for dentures, laminate veneer, inlays, onlays and veneering layer of metal or all-ceramic crown/bridge fixed restorations. Ceramic used in dental restorations belong to this family and are commonly referred to as dental porcelain (Craig & Powers, 2002; Blarcom & Clifford, 2008).

In dentistry, dental ceramics can be classified according to the substructure materials which is called coping or core for the single crown and ~~called~~ framework for the bridge of more than one unit that supported the veneering porcelain layer. The substructure is either fabricated from metal (the restoration termed metal-ceramic restoration) or from ceramic (the restoration termed all-ceramic restoration) (Blarcom & Clifford, 2008). Metal-ceramic restoration contains a cast metallic coping onto which at least two layers of ceramic are baked to provide aesthetic and function of restoration as shown in Figure 2.1. The first layer applied is the opaque layer, its role is to mask the darkness of the metal oxidation layer reproduced during porcelain sintering to obtain suitable aesthetics. The subsequent layers are dentine and enamel porcelain to give a restoration appearance as a natural tooth (Craig & Powers, 2002).

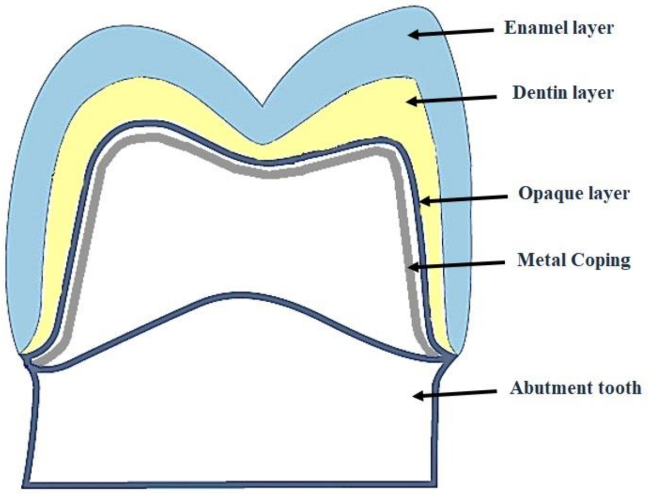

Figure 2.1: Diagram showed the metal-ceramic crown layers

The first alloy used for casting the metal coping or framework is usually gold-based alloy which contains a high percentage of gold. Due to an increase in gold price, different alloys were introduced with less percentage of gold in their composition such as the gold-palladium, silver-palladium and nickel-chromium alloys to produce restorations with low cost and high strength (Kelly et al., 1996; Anusavice, 2003).

Metal-ceramic restorations are still considered as the gold standard because of their biocompatibility, high survival rate and superior strength. In addition, metal-ceramic restorations are durable and long-lasting due to good bonding with veneering porcelain (Pjetursson et al., 2007; Sailer et al., 2007b).

2.2 Definition and history of all-ceramic systems

An all-ceramic restoration is defined as a ceramic fixed dental restoration that covered a prepared clinical crown that supported by ceramic (metal free) framework. The use of metal-ceramic restorations has declined due to poor aesthetic caused by the presence of metal. The metal acts as a barrier to the light transmission and reduces the translucency of restoration which giving an opaque appearance with the darkening line at the cervical region (Raigrodski, 2004).

McLean and Hughes (1965) introduced ceramic material to substitute the metal coping of a metal-ceramic restoration with high strength properties and aesthetic quality. The first material used was aluminium oxide (Al_2O_3) as a reinforced substrate in porcelain restoration. They fabricated alumina with 95% purity as an aluminous ceramic core which consisted of a glass matrix with 45-50% Al_2O_3 (McLean & Hughes, 1965).

A high-strength alumina coping was introduced in 1985 by Sadoun, contained over 85% alumina and was planned for anterior and posterior single crowns as well as anterior three-unit bridges (Yoshinari & Dérand, 1994). In 1993 Andersson manufactured a densely sintered alumina coping for porcelain restorations, currently known as Procera All-Ceram Alumina (Andersson & Odén, 1993).

The all-ceramic systems have been widely used in dentistry as FDPs to improve aesthetics compared to metal-ceramic restorations (Pjetursson et al., 2007; Sailer et al., 2009a). The wide range of the all-ceramic systems shading properties, especially feldspathic ceramic which composed of a translucency amorphous matrix that makes it look like the natural tooth colour (Giordano, 2006). In addition to aesthetic, all-ceramic restorations are assumed to be preferable as an alternative to the metal-ceramic system to avoid adverse reactions, such as metal toxicity and hypersensitivity (van Noort et al., 2004).

2.3 Classification of all-ceramic systems

All-ceramic systems were designed to replace the metal coping with a more aesthetic and adequate strength material. Different classifications were introduced after using all-ceramic systems to cover the requirements of restorative dentistry. All-ceramic systems can be classified according to their sintering temperatures, chemical compositions, and fabrication methods as shown in Figure 2.2 (Craig & Powers, 2002; Anusavice, 2003).

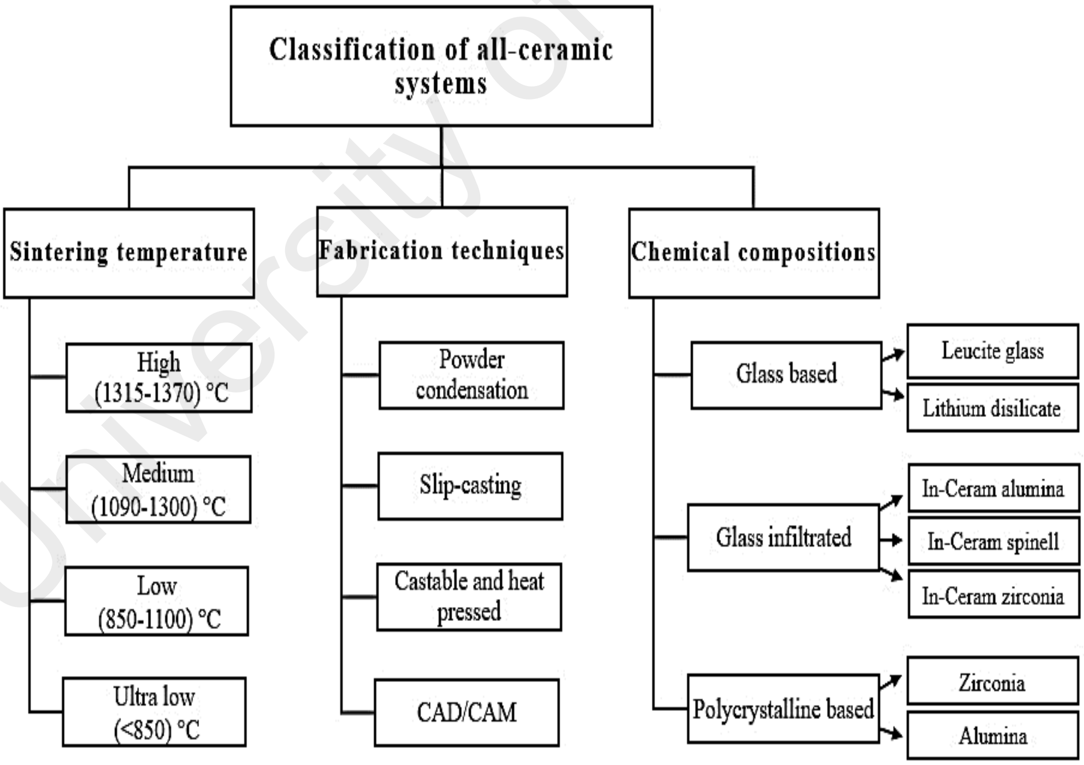

Figure 2.2: Classification of all-ceramic systems

2.3.1 Classification of all-ceramic based on their sintering temperature

Dental ceramics are divided according to the firing temperature into high-sintering (1315-1370°C), medium sintering (1090-1300°C), low sintering (850-1100°C), and ultra-low sintering (<850°C) ceramics (Anusavice, 1996). This classification was related to earlier dental ceramic compositions, which contained three main ingredients: quartz, feldspar, and clay (or kaolin). The sintering temperature is decided by the proportional amount of these three ingredients (Craig & Powers, 2002).

2.3.2 Classification of all-ceramic based on fabrication techniques

2.3.2.1 Powder condensation technique (Hand layering)

This is the traditional method used for the fabrication of ceramic restorations. It involves applying a wet porcelain after mixing the ceramic powder with a special liquid to produce a slurry and is placed over the coping which is either metal or all-ceramic material by using a special ceramic brush to build up the crown similar to the natural tooth shape. The porcelain powder is compressed by using vibration to remove the excess moisture and porosity before sintering. The final shape of porcelain crown is sintered by vacuum hot furnace which allows further porcelain condensation and vitrification (Griggs, 2007; Powers & Wataha, 2013).

Feldspathic porcelain is utilised for this technique with a high degree of translucency. Powder condensation method is used mainly for constructing a veneer layer to the metal and all-ceramic restorations (Antonson & Anusavice, 2001).

2.3.2.2 Slip-casting technique

A slip is a ceramic powder with low-viscosity mixed with water to form a suspension. The slip casting in dentistry is applied over a die, commonly fabricated from gypsum products and sintered at high temperature 1120 °C for 10 hours to produce porous coping (Pröbster, 1992; Pröbster & Diehl, 1992).

The resulting coping with this technique is very weak due to the porous structure. It is then infiltrated with a molten glass. A low viscosity lanthanum oxide (La_2O_3) glass is used to fill the porosity of slip coping, which sintered at 1100°C for 4-6 hour to produce a dense ceramic coping with high strength and low crack susceptibility (McLean, 2001; Naji et al., 2016).

Ceramics fabricated by the slip casting have higher fracture resistance than those produced by powder condensation because the strengthening glass particles produce a continuous and dense network throughout the matrix of the coping. Use of this method in dentistry has been limited probably because the method requires a complex series of steps, which provides, a difficulty in achieving an accurate fit and may result in internal flaws that weaken the material from incomplete glass infiltration (Yeo et al., 2003; Walter et al., 2006; Griggs, 2007).

2.3.2.3 Castable and heat pressed ceramics

Castable ceramic was introduced in the 1982 and the first commercially available material used was Dicor ceramic (Dentsply International Inc. York, PA) (Habelitz et al., 2001; Höland et al., 2006). In 1990 Ivoclar Vivadent introduced heat-pressed ceramics (IPS Empress I and II), a leucite-reinforced glass ceramic. The ceramics were reinforced by leucite crystal which acts as a barrier to prevent crack propagation and to improve the ceramic strength. In 2005, IPS e.max Press was introduced with better aesthetic and physical properties than IPS Empress I and II (Heffernan et al., 2002; Altamimi et al., 2014).

This technique allows the dental technician to produce the restoration by the lost wax method, in which the restoration is waxed to full contour over the master die cast. The wax pattern is invested with special investment materials and burnt-out in a furnace at 800ºC. The ceramic available for lost wax technique (moulding) is in the form of glass ceramic ingots.

The ingots have a similar composition with improved mechanical properties than conventional porcelains used with hand layer technique and it comes with different colour shades and sizes that are heated at 1100 ºC to press inside the investment mould. For castable ceramic, a special centrifugal machine is used (Dong et al., 1992), whereas for pressed ceramic a special ceramic plunger is utilised and the temperature is maintained for 20 minutes in a designed automatic press furnace (Gorman & Hill, 2003). Two finishing techniques can be applied, including a staining or layering technique that leads to the compatible look of the final restoration with a natural tooth colour (Denry & Holloway, 2010).

2.3.2.4 Machinable ceramics technique (CAD/CAM system)

The clinical approaches used to produce all-ceramic crown and bridge by conventional technique include impression taking, die or model construction. The model is sent to a dental laboratory to fabricate crown or bridge by using one of the conventional manufacturing methods which need long laboratory steps and time.

In the mid-1990, Nobel Biocare introduced the first all-ceramic substructure coping with 99.9% alumina produced by the CAD/CAM which was veneered with a feldspathic ceramic. The development strategy of CAD/CAM techniques included automating the production process and optimizing the quality of fixed dental prostheses by using new biocompatible materials, especially high-performance all-ceramic materials, such as zirconia and lithium disilicate (Luthardt et al., 2002).

The CAD systems function is to scan the tooth surfaces to be restored inside the patient mouth to collect digital data and for designing of the restoration. There are several approaches to gather data for CAD including; intraoral scanning, contact and non-contact digitisation and computed tomography (CT) scan or magnetic resonance imaging (MRI).

Intraoral scanning is used to create three-dimensional simulated picture directly of the prepared tooth/teeth from the patient's mouth and the adjacent structures. This scanning is also called a digital impression. The contact and non-contact digitisation are achieved by taking a conventional impression to produce a model, the data was generated and transferred into the CAD system through probe digitisation (contact) or laser light (non-contact). CT and MRI are new methods used the individual images of the object to produce data. CT scan utilizes radiation for data acquisition while MRI used a magnetic field. For soft tissue modelling, MRI data is suitable and for hard tissue like bone modelling, CT data is used (Davidowitz & Kotick, 2011).

The data is then converted into STL (stereolithography) format which is used to design the coping using the CAD software. The final design data of coping is transferred to the CAM and a milling machine is used to cut out a material block using rotary instruments (burs) to produce the restoration or copings (Beuer et al., 2008; Miyazaki et al., 2009).

An advantage of the CAD/CAM system is that a restoration can be produced and cemented on the tooth in one visit with the least technical inaccuracies compared with the other fabrication processes. Therefore, a temporary restoration is not needed, leading to a reduction in laboratory fees (Tinschert et al., 2004). Another advantage is that the CAD/CAM system can produce a higher strength coping with a short time and less porosity compared to that produced by conventional ceramic techniques (Anusavice, 2003).

CAD/CAM restorations can be produced by three different methods. These are Chairside production, Laboratory production and Centralised production (Beuer et al., 2008)*;*

Chairside production includes taking of intraoral optical impression at chairside and creating the final restoration without need participation of the laboratory and the restoration was fixed in the patient mouth at the same visit of one session. It saves times but the system is expensive and may put extra cost on the patient. The *Laboratory production* is similar to the conventional method of producing all-ceramic restoration but the dentist takes the impression and refers it to the laboratory which scanning of models, designing and fabrication of the final restoration using the CAD/CAM system. The *Centralised production*, involves taking of an impression and digitisation a master cast by the scanner and sending the data to an outsourced laboratory through the internet. The final restoration is fabricated and returned back to the dentist. The advantages of this technique are that only requires digitizer device and software to perform a high-quality restoration.

According to these classifications, there are many CAD/CAM systems available in dentistry, such as CEREC System (chairside production), Cercon Smart Ceramic System, Celay System, CICERO System, LAVA TM System (laboratory production) and Procera All-Ceramic System (centralised production).

(a) CEREC System

The CEREC system name was derived from CERamic REConstruction introduced by Siemens/Sirona Dental Systems, Bensheim, Germany. It was developed at the University of Zurich by Mörmann and Brandestini in 1980 (Mörmann et al., 1989). The materials used with the CEREC system are Vita Mark II fine-grained, feldspathic ceramic (Vita Zahnfabrik, Bad Säckingen, Germany), ProCAD leucite-reinforced ceramic (Ivoclar Vivadent, Amherst, N.Y.) and Paradigm™ MZ100 composite block (3M ESPE). The software for three-dimensional virtual display became available in 2003 with the CEREC inLab CAD/CAM system (Santos Jr et al., 2013). The different types of hard and aesthetic ceramic materials are available for this system: SPINELL™, ALUMINA™, ZIRCONIA™, Invizion™, and new Yttrium-stabilised Zirconia (YZ™).

(b) Cercon smart ceramic system

The Cercon system was introduced by DeguDent, Dentsply (Germany) based on the development done by Swiss investigators from the Federal Institute of Technology Zurich, in coordination with the Dental School of Zurich (Filser et al., 1997).

It has the ability to fabricate crown copings, bridge frameworks, dental implant and abutment from zirconia. The Cercon system components are (a) Cercon eye: laser scanner, (b) Cercon brain: milling unit and (c) Cercon heat: sintering furnace. The procedure for producing core using this system begins with a laser scanner to scan the model followed by designing and milling unsintered zirconia block to produce crown coping using software and milling machine of cercon brain unit. The milled coping is sintered in the Cercon heat unit based on automatic thermal process reaching a final temperature of 1350°C for six hours (Popa et al., 2015).

Several studies have evaluated the clinical application of this system in the crowns and bridges, and they proposed that three important aspects which supported the use of Cercon system: aesthetic, fracture resistance and marginal adaptation. The Cercon restorations showed a natural appearance and there are no changes in colour or fractures (Lou et al., 2004; Sailer et al., 2007a). The marginal integrity of the zirconia restorations produced by this system was considered as more favourable than other systems based on the clinical literature review by Kelly 2007, who examined clinically different CAD/CAM systems restorations (Kelly, 2007).

(c) Copy milling system (Celay system)

The Celay machinable system is designed to produce the inlays, onlays, and veneers from prefabricated ceramic blocks. It was introduced in the 1990s and developed by Mikrona Technologie, Spreitenbach, Switzerland (Davidowitz & Kotick, 2011). The system is manually controlled rather than computer controlled by a hand-operated contacting probe that touches the external contour of prefabricated precision wax or acrylic mould of the final restoration. A milling arm following the probe by means of a pantographic arm with eight degrees of freedom, which cuts a copy of the prefabricated mould from the ceramic block. The crown manufactured by the Celay system using In Ceram material Vita-Celay alumina blocks (Qualtrough & Piddock, 1995).

(d) CICERO system (Computer Integrated Ceramic Reconstruction)

The CICERO system can produce a ceramic core and two porcelain layers (opaque and translucent porcelain) with even thickness. All-ceramic restorations manufactured by this system consist of a glass saturated aluminium oxide ceramic core with a thickness 0.6 to 0.8 mm (Dozić et al., 2003).

(e) LAVA TM all-ceramic system

The LAVA all-ceramic system was introduced by 3M ESPE (USA) in 2002. It has a special scanner (Lava scan), a computerised milling machine (CAM) (Lava Form), a sintering furnace (Lava Therm) and CAD/CAM software technology. The Lava^{TM} all-ceramic system uses CAD/CAM technology to produce a densely sintered and high-strength zirconia framework from the green blank block (3 mol partially yttria-stabilized zirconia) (Piwowarczyk et al., 2005).

(f) Procera all-ceramic system

The Procera system was introduced by Nobel Biocare, Goteborg, Sweden and it was considered as a common CAD/CAM systems that used aluminium oxide as core material (Andersson & Odén, 1993). The all-ceramic core produced by this system was densely sintered at 1600 °C, high purity 99.9% aluminium oxide core combined with the matched mechanical properties of veneering porcelain. The core ceramic form is dry-pressed onto the die, sintered and veneered. The usual shrinkage of the core ceramic during sintering is 15-20% and this was compensated by fabricating an oversized ceramic core. Procera

All Ceram can be used for anterior and posterior crowns, veneers, onlays, and inlays (Anusavice et al., 2013).

(g) DCS system (digitising computer system)

The DSC system consists of two main parts; a Preciscan laser scanner (to produce three-dimension CAD file) and Precimill CAM a multi-tool milling (to cut different material). This system is one of the limited CAD/CAM systems that can mill titanium and fully sintered zirconia (Liu, 2005).

The DCS software automatically recommended the sizes for the connector and pontic forms of the fixed dental bridge. An *in vitro* study conducted by Martin and Bhasin showed that the marginal discrepancies of alumina and zirconia based posterior fixed bridge milled by the DCS system was between 60 μm to 70 μm. There is no shrinkage involved in the milling process, but microcracks may be introduced to the infrastructure (Luthardt et al., 2004; Mantri & Bhasin, 2010).

2.3.3 Classification all-ceramic system based on their composition

All-ceramic can be categorized into three main groups based on the composition of glass to crystalline ratio into; glass based ceramics, glass-infiltrated ceramics and polycrystalline ceramics (Raigrodski, 2005; Shenoy & Shenoy, 2010).

2.3.3.1 Glass-based all-ceramic systems

The glass-based system is a solid material formed by controlled crystallization of a glass amorphous. The glasses were manufactured by nucleation and development of the crystals in the glass matrix phase. The feldspathic porcelain is the most common porcelain under this system which is an aluminosilicate glass derived from the ternary system K_{20}-Al_2O_3-SiO_2. A typical composition of a feldspathic porcelain is 52-62 wt% SiO_2, 11-16 wt% Al_2O_3, 9-11 wt% K_2O, 5-7 wt% Na_2O, and additives (Höland & Beall, 2012).

However, feldspathic porcelain is brittle and has the low flexural strength (60-70 MPa). It can be reinforced by adding leucite material which is incorporated within the glassy component of feldspathic porcelain to improve its strength and increase their opacity. Thus, this kind of ceramic is used as veneering porcelain over metal or ceramic coping (Saint-Jean, 2013).

The first commercial glass-ceramic used for the castable method was Dicor ceramic which is fluormica glass-ceramic. It consists of a 55% volume fraction of small tetrasilicic fluormica platelets crystals ($K_2Mg_5Si_8O_{20}F_4$) which interlocking with the glassy matrix. Glass based ceramics have high translucency, high chemical resistance and reasonable flexural strength 150 MPa (Saint-Jean, 2013). However, the flexural strength value of glass ceramic is not adequate to use for constructing bridge framework and it was restricted to producing the single crown restoration (Rizkalla & Jones, 2004; McCabe & Walls, 2008).

Glass-ceramic materials have been strengthened by adding filler particles to their glass matrix to improve mechanical properties and increase the opacity of the material. The fillers are usually crystalline particles such as leucite ($KAlSi_2O_6$) and lithium disilicate ($Li_2Si_2O_5$) that stop the crack propagation because these crystalline phases are more resistance to the cracks. The increase in crystalline particles gives the ceramic high flexural strength with low translucency which leads to poor aesthetic (Denry & Holloway, 2010; Monmaturapoj et al., 2013).

(a) Leucite glass ceramic

Leucite glass-based systems are made from ceramic materials that contain mainly silicon dioxide, which contains various amounts of alumina. This ceramic system was introduced by the IPS-Empress® in 1991 (Vivadent, 2009; Helvey, 2010). The leucite ($KAlSi_2O_6$) crystal is available as an ingot which is added to the glass in order to reinforce and improve fracture strength. Leucite glass-ceramics consist of 35-45% volume fraction of leucite randomly dispersed in the glassy matrix which acts as a reinforcing phase (Brochu & El-Mowafy, 2002). The leucite crystals volume was limited within this range because a high crystal amount results in higher opacity (poor aesthetic). The IPS Empress ceramics were used for fabricating a single crown, inlays, onlays, and veneering layer by using either heat-pressing or CAD/CAM techniques (Craig & Powers, 2002).

A leucite glass-ceramics used as machinable blocks for CAD/CAM restorations which have a similar composition and mechanical properties of the pressable glass-ceramics. The moulding technique takes advantage of the flow properties of glass-ceramic to produce the shape that was formed by the wax (Denry et al., 1996; Denry & Holloway, 2010).

(b) Lithium disilicate glass-ceramics

Lithium-disilicate glass ceramic is a recent type of glass-ceramic introduced by Ivoclar as IPS Empress® II (now called IPS e.max®) (Vivadent, 2009; Helvey, 2010) where the aluminosilicate glass has lithium oxide added in order to improve the strength of glass-based ceramic. It consists of a large volume fraction 70% of the fine rod of Lithium disilicate ($Li_2Si_2O_5$) crystals with a small amount of lithium orthophosphate (Li_3PO_4) crystals that are randomly spread in the glassy matrix (Qualtrough & Piddock, 2002).

The flexural strength of lithium disilicate glass systems is superior to the leucite glass system, with a range of 350-450 MPa and fracture toughness approximately three-times than that of the leucite glass ceramic (Shenoy & Shenoy, 2010). Depending on the approaches or technique, lithium disilicate glass ceramics was manufactured in two different forms either as ceramic blocks for a machinable milling technique or as pressable ingots for the hot pressing technique (Van Noort & Barbour, 2013).

2.3.3.2 Glass-infiltrated all-ceramics system

Glass-infiltrated all-ceramic system is a ceramic consisting of glass which is infiltrated the partially sintered alumina to fill the pores and improve strength. The system was introduced in 1988 as a ceramic composite and contains 40-50 vol% alumina that formed onto a refractory die after mixing a fine slurry of alumina powder with water by a process known as slip casting. After the die has dried, it is sintered for 10 hours at 1120°C. The porous coping is then infiltrated with a lanthanum oxide (La_2O_3) glass to make it stronger. The molten glass is able to penetrate into the pores, producing a dense ceramic (Shenoy & Shenoy, 2010; Naji et al., 2016). The addition of small alumina crystals into the glass ceramic in concentrations of 40-50 vol% increases the flexural strength of about 2-3 times. Alumina particles are stronger than the glass matrix and are more successful than quartz crystals in preventing crack propagation (Pröbster, 1992).

According to Thompson and Rekow (2004), the reinforced aluminium oxide with glass matrix increases the fracture strength of the all-ceramic fixed prostheses comparable to leucite crystals (Thompson & Rekow, 2004). The In-Ceram coping is veneered with a feldspathic ceramic to achieve a final aesthetic restoration with high translucency and visual qualities, but it has poor physical properties and needs a high strength coping that can be provided with infiltrated ceramics. The In-Ceram systems are classified into three different materials to achieve regularity between strength and aesthetics. These are In-ceram alumina, In-ceram spinell and In-ceram zirconia.

(a) In-Ceram alumina

In-Ceram Alumina was first introduced by Sadoun as a core material in 1988. In-Ceram alumina core containing about 70% alumina infiltrated with 30% sodium lanthanum glass which is used for crown and bridge substructures (Sadoun, 1988; Claus, 1990). Alumina has limited aesthetics due to the semi-opaque coping, therefore, the application in dental restoration is restricted (Della Bona et al., 2008).

Vita In-Ceram Alumina coping material contains 75% alumina, fabricated through the slip-casting technique. In-Ceram alumina coping has flexural strengths of between 400 and 700 MPa, depending on the amount of alumina in their structure (Quinn et al., 2003). Higher value aluminous porcelain systems used for fabricating stronger copings include Vita In-Ceram (Vita Zahnfabrik, Sackingen, Germany) and Procera (Nobel Biocare AB, Goteborg, Sweden) (Pröbster, 1992; Al-Sanabani et al., 2014).

However, crowns fabricated by the glass-infiltrated alumina showed low adhesion to the tooth preparation during cementation process due to the resistance of the material to acid etching procedure used before cementation as a result of high crystalline content. Moreover, these materials are relatively expensive and have a long processing time (O'Brien, 2002).

(b) In-Ceram spinell

Spinell is a natural crystal containing aluminium oxide and magnesium oxide ($MgAl_2O_4$) that normally originates together with limestone (Figure 2.3). It has an extremely high melting point (2135°C) combined with high strength. Spinell is chemically inactive, has low electrical and thermal conductivity. It has a moderate strength of about 350 MPa with superior translucency to In-Ceram alumina because its crystalline phase has a high refractive index which is close to that of glass. Therefore, In-Ceram spinell is suggested for inlays and anterior crown (Heffernan et al., 2002; Saint-Jean, 2013).

Hwang and Yang (2001), found that In-Ceram alumina and In-Ceram zirconia showed higher flexural strength than In-Ceram spinel. The flexural strength value of In-ceram alumina is 500 MPa which resulted from the higher flexural strength of the alumina (Hwang & Yang, 2001).

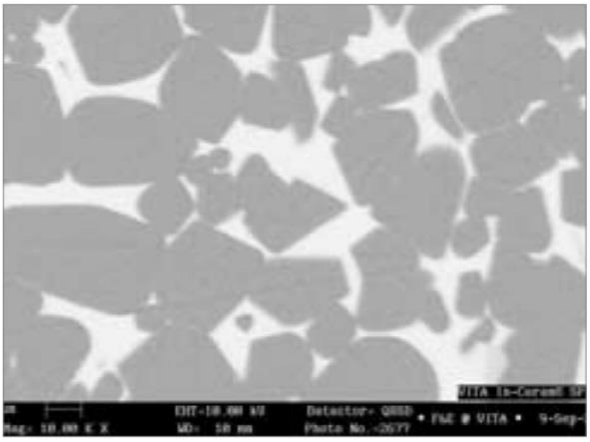

Figure 2.3: VITA In-Ceram Spinell, glass-infiltrated structure: Magnification x 500. (Spinell, 2002)

(c) In-Ceram zirconia

This system was introduced in 1999 and produced a noticeable increase in the flexural strength of the substructure of crown and bridge. In-Ceram zirconia contains 35% partially sintered stabilised zirconia with glass infiltrated alumina. Aluminium oxide form about two-thirds of the crystalline structure and the remaining structure consists of tetragonal zirconium oxide. The proportion of glass phase amounts approximately 20–25% of the total structure (Piconi & Maccauro, 1999). The high flexural strength of In-Ceram zirconia is 700 MPa due to the presence of zirconium oxide particles which protect the material against the crack initiation and propagation. However, this system showed poor translucency due to the opacity of zirconia crystalline (Hwang & Yang, 2001).

According to a study by Guazzato (2001), In-Ceram zirconia was tougher than In-Ceram alumina as a result of high toughness value of zirconia. The process of fabrication is achieved either by milling or slip-cast technique. Due to higher strength and fracture toughness, this material is recommended for the posterior single crown and three unit bridge replacement (Guazzato et al., 2001).

In-Ceram zirconia is considered as the strongest material of the slip-casting and CAD/CAM technique. Nonetheless, it has high opacity with poor translucency due to there is low glass contain which cannot use for anterior crowns (Raigrodski, 2004; Yilmaz et al., 2007). In-Ceram zirconia is considered the strongest of three frameworks of the slip-casting and CAD/CAM technique (Raigrodski, 2004; Sundh & Sjögren, 2004).

2.3.3.3 Polycrystalline based all-ceramic system

The polycrystalline ceramic material defined as a solid ceramic material composed of densely sintered particles with no glass components. Under this system, there are two main ceramic materials used to fabricate fixed partial denture (FPD) framework in dentistry; aluminium oxide ceramic (alumina) and zirconium oxide ceramics (zirconia) (Guess et al., 2011).

However, alumina still had a risk of fracture either during laboratory work or in clinical use (Walter et al., 2006). Therefore, zirconia has been used as an alternative material with higher flexural strength (900-1200 MPa). The development of CAD/CAM technologies has facilitated using of zirconia block material to produce coping and framework (Denry & Kelly, 2008).

2.4 Zirconia-based ceramic

2.4.1 Definition and history

The term zirconium denotes the metal, while zirconia refers to zirconia dioxide (ZrO_2). The name “Zirconium” comes from the Arabic word “Zargon” which means “golden in colour.” Zirconia was originally discovered by the chemist Martin Heinrich Klaproth in Germany in 1789 while working with certain processes of heating some gems and was isolated by the Swedish chemist Jöns Jacob Berzelius in 1824 (Piconi & Maccauro, 1999).

Zirconium is a transition metal with corrosion resistant and it does not exist in nature in a pure state, but only as a free oxide (ZrO_2) or in conjunction with silicate called Zircon ($ZrSiO_4$). Zircon is composed of 67.2% of ZrO_2 and 32.8% of SiO_2, which is considered as the main source of zirconia found primarily in Australia, South Africa, Brazil, India, Russia, and the United States (Hisbergues et al., 2009).

The first reported biomedical application of zirconia was in 1969 for biomedical implants by Helmer and Driskell (Helmer & Driskell, 1969). In 1988, Christel et al utilised zirconia as a material for total hip replacement (Christel et al., 1988). In the early 1990s zirconia was used in dentistry as orthodontic brackets (Springate & Winchester, 1991), endodontic posts (Meyenberg et al., 1995) and hard copings for crowns and fixed partial dentures (Luthardt et al., 2002) and more recently as implant abutments (Kohal et al., 2006; Guess et al., 2012).

Zirconia has a characteristic called transformation toughening by changing the zirconia microstructure phase from brittle to the denser structure by heating to a specific temperature. This transformation phenomena give higher flexural strength and toughness to zirconia compared with other ceramics (Hutchinson, 1989).

2.4.2 Zirconia transformation toughening

Zirconia is a polymorphic structure which exists in three crystallographic phases depending on the temperature; monoclinic phase (*m*) at room temperature which is a deformed prism with parallelepiped sides;, tetragonal phase (*t*) above 1170 °C which is a straight prism with rectangular sides and cubic (***c***) beyond 2370 ° C which is square sides as shown in Figure 2.4 (Pittayachawan, 2009).

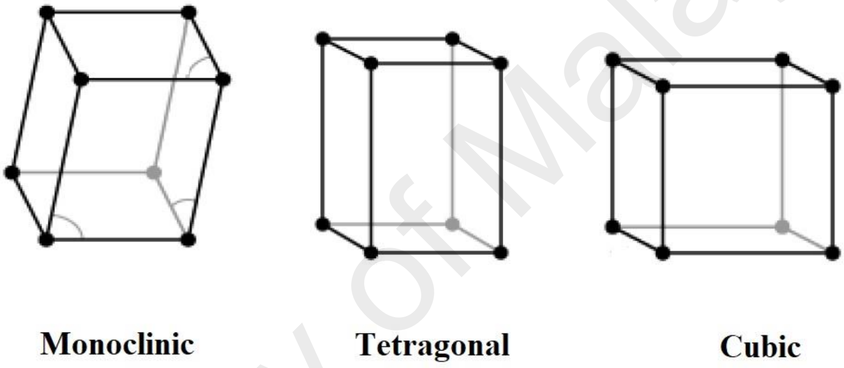

Figure 2.4: Crystallographic phases of zirconia (Pittayachawan, 2009)

The phase transformation of zirconia was discovered in 1975 (Garvie et al., 1975) and it supposed to be martensitic, which is a change in the crystal structure (a phase change) in the solid state of the material that involves simultaneous and cooperative movement of atoms over the distances less than the atomic diameter (Jin, 2005). These movements are usually less than the interatomic distances and the atoms hold the same microstructural relations. Martensitic transformation only leads to changes in crystal structure and not in the composition of the phases (Anderson et al., 1990; Porter, 1992).

Pure zirconia is a monoclinic phase at room temperature and transforms to a denser tetragonal form when sintered using the furnace. This process promotes volume changes as shown in Figure 2.5. Different metal oxides are added to pure zirconia to control the phase stability of the crystalline structure such as Magnesia (MgO), Yttria (Y_2O_3), Calcium oxide (CaO), and Ceria (CeO) (Seghi et al., 1995; Helvey, 2008).

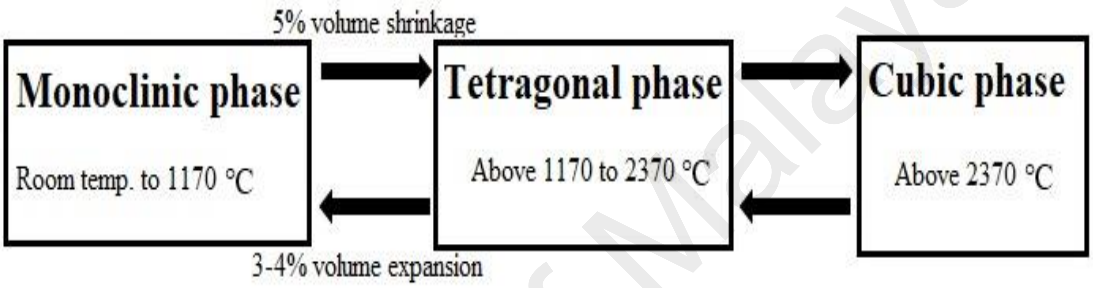

Figure 2.5: Transformation toughening of zirconia phases (Pittayachawan, 2009)

Yttrium oxide (3 mol) was added to zirconia as a stabilizer that helps to retain tetragonal zirconia phase at room temperature, producing yttria stabilised zirconia (YSZ) with a flexural strength from 900 to 1200 MPa and fracture toughness of 9 to 10 $MPa.m^{1/2}$. YSZ was introduced in 1969s as a ceramic biomaterial instead of alumina for medical purposes such as orthopaedic applications as the new material used in hip-head replacement because of its biocompatibility and excellent strength (Helmer & Driskell, 1969).

The YSZ was introduced to dentistry in the early of 1990 and became a popular material used in dentistry as a substructure material for fabrication of fixed all-ceramic restorations (crowns and bridges), implant fixtures, and implant abutments due to their superior strength, wear resistance, biocompatibility, and aesthetics (Thompson et al., 2007; Marinis et al., 2013). Furthermore, YSZ was also used in the fabrication of orthodontic brackets (Winchester, 1991) and endodontic posts (Meyenberg et al., 1995).

Sintering of the pure zirconia without stabilisers at a temperature of above 1170°C leads to the generation of the tetragonal phase. Subsequently, in cooling, the phase transformation from tetragonal to monoclinic occurs and is accompanied by 3-5% volume expansion of the crystalline phase, which causes stress in the sintered material. This stress generates intense cracking of the material during cooling, thus pure zirconia cannot be used as a bulk material (Chevalier et al., 2009).

The transformation of zirconia from tetragonal into monoclinic phase can also occur when it is exposed to mechanical stress such as grinding, grit blasting (Kosmač et al., 1999; Curtis et al., 2006) and thermal cycling (thermal ageing) (Deville et al., 2006; Chevalier et al., 2009). The transformation of zirconia phases led to the development of localised compressive stresses produced around and at the crack tip, preventing further crack propagation (Porter & Heuer, 1977). This mechanism is known as transformation toughening and makes zirconia-based ceramics exhibit high strength and toughness compared to other ceramics (Guazzato et al., 2004).

YSZ was used by CAD/CAM technologies because of its superior mechanical properties as block material which is either fully sintered or unsintered to fabricate copings or crowns. Although the superior mechanical properties of the YSZ material, it has the low bond strength to the other ceramic materials which have been reported as a significant cause that affect its clinical performance because there is no inherent glass content, in addition, a nonpolar covalent bond in its chemical structure (Christel et al., 1989).

2.5 Veneering porcelain

Veneering porcelain refers to a layer of ceramic material applied over the metal or all-ceramic coping to optimise function and aesthetic of the restoration. The main material used to fabricate a veneer is feldspathic dental porcelain which is usually leucite-reinforced type. Veneering porcelain is typically sintered under vacuum in order to decrease the porosity of the final porcelain product (Claus, 1989). The flexural strength of a commonly used veneering porcelain is about 90-120 MPa (Guess et al., 2011).

The adhesion between the zirconia coping and the veneering porcelain is determined by several factors including, the chemical bond strength, mechanical coping/veneer interlocking or surface roughness, type and amount of defects at the interface, wetting properties, and the degree of compressive stress in the veneering layer due to a difference in the coefficients of thermal expansion between zirconia and the veneering porcelain (Aboushelib et al., 2005; Fischer Jens et al., 2008).

Several clinical studies have evaluated zirconia-ceramic restorations performance in short (3 years) and medium (5 years) trial periods. These studies concluded that chipping and delamination of the veneering porcelain as the common failure cause of zirconia ceramic restorations. Furthermore, the chipping incidence rate (11.4% to 25% of all FDPs) in zirconia ceramic restorations is generally higher than that of metal-ceramic restorations (Sailer et al., 2007b; Raigrodski et al., 2012; Triwatana et al., 2012).

In order to encourage adequate bonding between the zirconia substrate and veneer ceramic, surface treatments for the zirconia surface have been suggested. This can be attained by the increased surface roughness of zirconia substructure and improve the mechanical interlocking of the veneering layer to the rougher surface. The roughness could achieve either by removing a layer from the zirconia surface or adding materials to the zirconia surface (Elsaka, 2013; Yoon et al., 2014).

2.6 Zirconia surface treatment

Surface treatments on the zirconia substrate prior to veneering play an important role in the enhancing of bond strength and durability by converting a non-retentive surface to retentive one. Surface preparation considered as one of the important parameters which are directly related to the material properties and activation of surface elements to join with other material. According to this, the efficiency of the surface treatment is highly dependent on the composition of materials (Ghumatkar et al., 2016).

Several studies have reported that the bond strength of zirconia coping to veneering porcelain is affected by different surface treatments (Aboushelib et al., 2008; Fischer Jens et al., 2008; Kim et al., 2011). The high flexural strength and toughness of the zirconia polycrystalline structure will resist surface modification by chemical treatment such as acid etching. The target of zirconia surface treatments is to produce a microroughness surface to improve its bonding strength to the veneering porcelain (Christel et al., 1989; Kelly et al., 1996). However, different surface treatments have been used on the zirconia surface to create microroughness including mechanical, chemical and surface coatings.

2.6.1 Mechanical surface treatments

Numerous mechanical surface treatments have been used for zirconia-ceramic restoration such as grinding by diamond rotary instruments, airborne particle abrasion (APA) and silicon deposition method. Grinding by round or diamond rotary instrument is used to create superficial roughness to increase the bonding strength between zirconia and veneer porcelain. Past research suggests that when grinding is applied, a thin layer of compressive residual stress may be produced and caused damage to the zirconia surface. This stress can trigger the phase transformation from tetragonal to monoclinic which results in a volumetric expansion around the superficial defects, consequently inducing arresting crack propagation (Kosmač et al., 2008; Jing et al., 2014).

The APA is a common surface treatment used in dental laboratories to clean and create a rough surface to increase the micromechanical interlocking between zirconia and the veneering porcelain, which is important to improve the bonding strength. APA is applied to metals and zirconia frameworks as an effective method to produce micromechanical roughness and improve the contact area between treated materials and the veneering porcelain. Aluminium oxide particles (Al_2O_3) of various particle sizes (ranging from 50 to 110 µm) are used as a grit material (Kim et al., 2011). Several parameters control abrasion treatment such as Al_2O_3 particle size, pressure, working time and distance from the ceramic surface (Kern & Thompson, 1993).

Several studies have revealed that low bond strength value related with APA treatment or even spontaneous chipping after artificial ageing by immersion in water storage and repeated thermocycling (Kern & Wegner, 1998; Fischer Jens et al., 2008; Casucci et al., 2009). According to the Kosmač et al (2008), the APA treatment promotes a phase transition at the zirconia surface from tetragonal to monoclinic phase, which attended with volume change that generated the tensile stress and cracks susceptibility of veneering porcelain (Kosmač et al., 2008). In addition, Guazzato et al (2004), concluded that the phase transformation from tetragonal to monoclinic is accompanied by a generation of localized stresses, which may create microcracks in the glass phase of the veneer (Guazzato et al., 2004). On the other hand, Fischer et al. recommended that APA was not an essential surface pretreatment to enhance the bond strength between zirconia and veneering porcelain (Fischer et al., 2008).

The other mechanical surface treatment is a silicon deposition methods which started with the silicoater technology and the Rocatec system. These systems are based on the use of 110 μm (Rocatec) or 30 μm (CoJet) Si-coated alumina particles that are blasted by air abrasion onto the ceramic surface (Kern & Thompson, 1995). Si deposition produced reactive surface but it attends to produce a lower surface roughness and consequently lower mechanical interlocking. This technique mainly used to increases the bond strength of glass-infiltrated ceramic or zirconia materials to resin cement (Matinlinna et al., 2006).

2.6.2 Chemical surface treatment

The most common chemical surface treatment used for zirconia-ceramic restorations is etching by hydrofluoric acid (HF) or phosphoric acid (H_3PO_4) to clean and produce nanoroughness to improve the adhesive properties of zirconia surface to resin cement (Soares et al., 2005). However, HF etching does not produce adequate roughness on zirconia surface to improve the bonding between zirconia coping and veneering porcelain (Della Bona et al., 2007). The insignificant effect of the acid etching treatment on the zirconia surface is due to the absence of glassy component resulting in low bond strength values (Della Bona et al., 2007).

2.6.3 Surface coating of zirconia

The coating process is applying a thin film over the surface of a functional material of an object or substrate to improve surface properties such as surface roughness, wettability, thermal isolation, corrosion and wear resistance (Rad et al., 2014).

The ceramic liner is the common coating material used on zirconia coping that suggested by the dental ceramic manufacturers as an intermediate coating layer to mask the white colour and improve the wetting property of zirconia substrate to enhance the bond strength between the zirconia and the veneering porcelain (Aboushelib et al., 2005). The chemical composition of liner ceramic is the similar composition of veneering porcelain with some pigments and oxides according to manufacturer data.

According to several studies, the application of liner may reduce the bond strength between zirconia coping and veneering porcelain. These studies proposed that it should be combined with air abrasion to improve the bonding strength (Kim et al., 2011; Wang et al., 2014; Yoon et al., 2014).

Alternatively, different materials have been used as a surface coating on zirconia coping to increase bond adhesion with the veneering porcelain. One study proposed using a thin layer of zirconia powder (3 µm) mixed with glue over the zirconia surface to increase the mechanical interlocking of zirconia substrate to the veneering porcelain and enhance the bond strength between them. The study concluded that altering the zirconia surfaces significantly increased the bond strength (Teng et al., 2012). Furthermore, Zhang et al (2014), used a mesoporous zirconia coating after mixing with an aqueous solution as a surface conditioning to improve the zirconia-resin bond (Zhang et al., 2014).

Glaze porcelain is used to fill the pores formed during firing of veneering porcelain and provide an adequate polished surface simulate the natural tooth surface. The advantages of glazing are to allow a lower retention of bacterial plaque to the ceramic restoration that leads to avoidance of inflammation of the periodontal tissues, decrease wear of antagonist's teeth, more resistance to crack propagation and better esthetic for the restorations (da Silva et al., 2014).

Glaze porcelain was used as coating material with a so-called glaze-on technique which is composed of a thin layer of glaze porcelain applied on the fitting surface of the zirconia-based crown to create an intermediate etchable layer to improve the adhesive bond to the prepared tooth surface (Everson et al., 2012; Gowida & Aboushelib, 2016).

Fusion sputtering method is a simple technique used to increase the surface roughness of zirconia and to change surface architecture by the creation of round surface beads fused with the surface of the material. Green body zirconia, which is unsintered, sprayed with a solution rich in zirconia particles. Upon sintering, the particles become fused with the sprayed structure. Only short-term results are available about the performance of fusion sputtered zirconia implants (Salem et al., 2013).

Furthermore, another surface coating treatment method for zirconia was introduced by Aboushelib et al, in 2006s and tested with microtensile bond strength named selective infiltration etching (SIE). This method was used heat-induced development and grain diffusion on zirconia surface to transform the smooth non-retentive surface into a highly retentive surface. A low temperature melting glass is applied on selected zirconia surfaces and submitted to a heat-induced infiltration process and after that, the glass is removed with 5% hydrofluoric acid solution bath, leaving intergrain nanoporosities where low-viscosity resin materials may flow and interlock after polymerization (Aboushelib et al., 2006). This method mainly used as a surface treatment before cementation procedure to providing high and durable bond strength.

2.6.3.1 Airbrush spraying technique

A number of methods have been experimented over the last 25 years to produce bioceramic coatings, including gravity-controlled deposition (Bigi et al., 2005), sol-gel dipping (Fathi & Doostmohammadi, 2009), spin coating (Wang et al., 2010), electrophoretic deposition (Boccaccini et al., 2010) and sputtering (Yang et al., 2005).

Coating by the airbrush spraying technique is an innovative way introduced as an efficient deposition method used for coating ceramic slurries on the substrates that are having simple or complex forms with a sufficient control of the coating thickness. Airbrush spraying was applied instead of spreading a suspension with a wiper to achieve homogeneous thin layers (Waetjen et al., 2009; Baino & Vitale-Brovarone, 2015).

The important parameters to properly control spraying coating by an airbrush are includes; operating air pressure, the amount of material being released by the airbrush (concentration of material), spraying time and the distance of the airbrush nozzle to the surface of the substrate being sprayed (Scardaci et al., 2011). In order to optimise the quality of spray coating, these parameters were carefully selected according to preliminary experiments. It was noted that when a decrease of the coating dilution and air pressure leads to a higher number of defects such as pores or cracks in the coating, due to entrapment of air within the layer produced and increased the risk of an airbrush nozzle blocking because of thick coating material. Furthermore, when increased coating dilution and air pressure, obtained inhomogeneous coating thickness due to gravity force and high air pressure which tended the slurry to accumulate at the end of the material substrate thereby causing the thinning of the coating in the central region (Baino & Vitale-Brovarone, 2015).

2.7 Surface properties measurements

Various measurement techniques have been used for analysis surface properties including, surface roughness, surface morphology, elemental and microstructural identification after exposing to different kinds of surface treatments.

2.7.1 Surface roughness assessment

Surface roughness is often described as ‘uneven’, ‘irregular’ or ‘coarse in texture’ (Ezazshahabi et al., 2017) and may be counted by the vertical deviations of an actual surface from its original form. Roughness generally results from abrasion, etching, polishing and coating. Surface roughness can be measured with three different techniques or systems: a traditional mechanical stylus (contact) system, a non-contact laser scanning system, and the atomic force microscope.

One of the main disadvantages of the contact system is that a tip of measuring probe must be in a mechanical contact with a measured surface which leads to the possible risk of soft material damage. Their accuracy and sensitivity are low due to unwanted contact of the measuring tip during its movement over the rough surface. These can be mostly eliminated by using non-contact measuring devices which can be developed on the basis of optical principles (Valíček et al., 2012).

Nano and microroughness are measured with two dimensions and three dimensions of a non-contact laser scanning system and there is a number of standard parameters are used to describe surface roughness value either by surface profile roughness (R_a), or surface area roughness (S_a). The R_a is the arithmetic average of the absolute values of the profile height deviations from the mean line, recorded within the evaluation length.

The R_a is calculated by an algorithm that measures the average length between the peaks and valleys and the deviation from the mean line on the entire surface within the sampling length. R_a averages all peaks and valleys of the roughness profile and then neutralises the few outlying points so that the extreme points have no significant impact on the final results.

S_a considered as an extension of R_a (arithmetical mean height of a line) to a surface. It expresses, as an absolute value, the difference in height of each point compared to the arithmetical mean of the surface (Gadelmawla et al., 2002). The area roughness parameters (S_a) give more significant values because it measures all roughness area (Schuetz, 2013).

2.7.2 X-ray diffractometer (XRD)

The X-ray diffraction analysis has been used to study the two main parts; to evaluate the pattern of crystalline materials (structural phases) and to determine the changes in the chemical composition of composite material after processing. Each crystalline solid has its unique characteristic X-ray powder pattern which may be used as a "fingerprint" for its identification (Chipera & Bish, 2002).

X-ray diffraction is one of the most important description tools used to analyse the crystalline phase transformation from tetragonal to monoclinic phase (Allahkarami, 2012). The monoclinic and tetragonal phase is calculated by their diffraction patterns and compared to the standards patterns from software that are based on the International Center for Diffraction Data references (ICDD).

2.7.3 Surface morphology measurement

The scanning electron microscopy (SEM) has become a useful technical investigation that finds application in many areas of materials science (Goldstein et al., 2012). The SEM is an electro-optical instrument; essentially consists of a vacuum chamber and an electron gun that produces a thin beam of electrons of high energy (Reichelt, 2007).

The SEM principle is based on sending a beam of primary electrons of known intensity of a sample conductor and gathering, by appropriate scanning on the corresponding area is selected by the magnification operator, the image of two-dimensional and enlarged of the same surface, by converting the signal, by means of suitable detectors, the various phenomena resulting. These signals are then reproduced on a screen which cathode electron beam must be in phase with that of the SEM column, or sometimes are reprocessed using appropriate software packages to obtain chemical data quality or quantity (Beckhoff et al., 2007, Goldstein et al., 2012).

2.7.4 Elemental dispersive x-ray spectrometry

It is a chemical microanalysis technique used in conjunction with SEM using the characteristic of x-rays generated in a specimen by the electron beam, to determine the elemental composition of the specimen. There are two kinds of x-ray microanalysis, wavelength dispersive spectrometry (WDS) uses the wavelength of x-rays. The other kind is energy dispersive spectrometry (EDS or EDX) uses the energy of the x-rays (Wollman et al., 1997).

2.8 Mechanical properties measurement

2.8.1 Coefficient of thermal expansion (CTE)

It is a material property that gives the degree to which a material expands upon heating and it was measured by the thermomechanical analyser. Or it is the fractional increase in length per unit rise in temperature (James et al., 2001).

During the processing of ceramics restorations, residual tensile stress is produced as a result of the mismatch in CTE, which may lead to ceramic failure. Several studies suggested that the CTE of veneering porcelain should be lower than the ceramic coping. This recommendation will assist in establishing a strong bond between the zirconia coping and the veneering porcelain which could produce acceptable quantities of residual stresses (Isgrò et al., 2004; Fischer et al., 2009).

2.8.2 Shear bond strength (SBS) test

Different bond strength measurement methods for all-ceramic bi-layered systems have been suggested because a standardised method has not yet been identified. Several methods have been applied, each with advantages and disadvantages. These includes biaxial flexure strength (Yilmaz et al., 2007), three/four point flexure (White et al., 2005), Schwickerath test (Alsulami, 2014), Schmitz Schulmayer test (Guess et al., 2008), microtensile bond strength, (Aboushelib et al., 2005), and shear bond strength (SBS) (Al-Dohan et al., 2004; Mosharraf et al., 2011).

Mosharraf et al, (Mosharraf et al., 2011) used SBS test to assess the effect of different surface treatments and zirconia types on the bond strength between zirconia and veneering porcelain. Fischer et al, (Fischer et al., 2009) applied the shear bond strength test to evaluate the effect of coefficient thermal expansion misfit on shear strength between zirconia and veneering porcelain.

2.8.3 Fracture strength (FS)

The fracture resistance considered as one of the important mechanical properties through which the clinical performance of the restoration can be evaluated and improved (Quinn et al., 2005). The zirconia-ceramic crown consists of a multi-layered structure including one or two layers of ceramic. This complex structure could not be simulated by disc or bar shaped to measure their properties with standard test methods (Kelly, 1999).

Therefore, *in vitro* tests should simulate a clinical shape of restoration which used inside the patient mouth, in order to assess the restoration performance when applied load through their ceramic layers. The fracture strength test used to measure the bonding strength of veneering porcelain to zirconia coping by simulating all test component including zirconia crown within entire restoration layers include (coping, veneering porcelain and luting cement) to resemble the clinical condition. The clinical uses were contrasted by the traditional loading applied by testing machine until failure occurs to restoration (Kelly, 1999; AL-Makramani et al., 2009).

2.8.4 Fractographic analysis

A study of the fracture surfaces of the tested specimens to analyse and predicting the fracture behaviour which including the crack initiation and propagation in the brittle restorative ceramic materials as a result of the mechanical loading or clinical trials to assist researchers in identifying the subsequent treatment that may minimise and manage the factors caused failure of ceramic restorations (Scherrer et al., 2007; Anusavice, 2012).

The initial fractographic examination is commonly carried out on a macro scale using low power optical microscopy and SEM is often sufficient to identify the extent of cracking, failure modes and likely origins. The main fractographic features are the wake hackle (Figure 2.6), arrest fracture lines and compression curl (Quinn et al., 2005; Scherrer et al., 2008).

According to the several previous fractographic studies which evaluated the bond strength between zirconia and veneering layer, three modes of fracture have been categories; adhesive mode which revealed to a complete debonding of veneering layer from zirconia substrate surface as a result of a low bond strength between two materials, cohesive mode which showed a fracture at the veneering layer without exposing the substrate because there are a good bond strength and mixed mode which indicated a combination between adhesive and cohesive modes (Al-Dohan et al., 2004; Guess et al., 2008; Fischer et al., 2009).

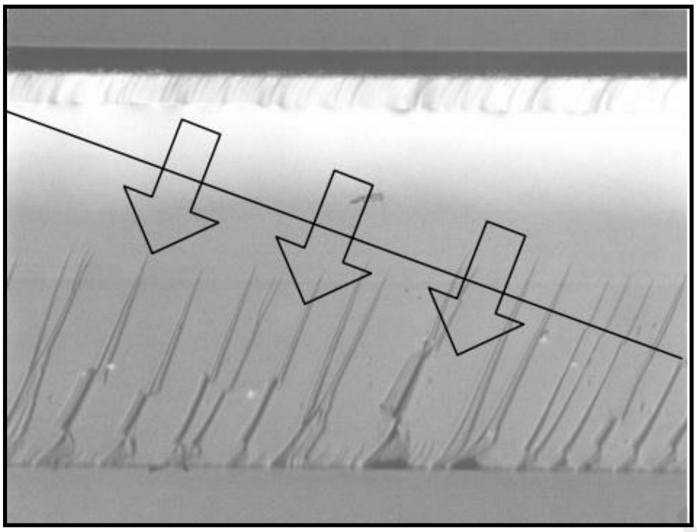

Figure 2.6: Hackle crack created by breaking process. The arrows represented the crack propagation direction (Ono & Allaire, 2000)

2.9 Image analysis

The scientific image analysis program was originated from US National Institutes of Health (NIH) by a programmer Wayne Rasband, who developed image J software at the National Institute of Mental Health, part of the intramural campus of the NIH in 1987 (Rasband, 1997; Schneider et al., 2012).

Image J can display, edit, analyse, process, save and print 8-bit, 16-bit and 32-bit images. It can read many image formats including TIFF, GIF, JPEG, BMP, DICOM, FITS and “raw”(Collins, 2007). The program supports a series of images that share a single window and it can calculate the area and pixel value statistics of user defined selections. Density histograms and line profile plots can be created with image J. Finally, this software has standard image processing functions such as contrast manipulation, sharpening, smoothing, edge detection and median filtering (Bailer, 2006).

2.10 Finite element analysis (FEA)

Finite element analysis used to expect the results of *in vivo* trials for a new materials or technique service because the clinical investigation needs a long period to collect data, the cost of using a lot of materials is high and a large number of volunteers is required to obtain adequate statistical results (Rosentritt et al., 2009).

FEA is sequences of computational procedures were used to calculate the stress and strain within a digital structural model, caused by external force, pressure, thermal changes and is useful for analysing the mechanical aspect of biomaterials characteristics and human tissue that difficulty measured *in vivo* (Wakabayashi et al., 2008).

In the area of dentistry, FEA has been used to simulate the bone remodelling process, to study internal stresses in teeth and different dental materials, and to optimise the shape of restorations. Because of the large inherent variations in biological material properties and anatomy, mechanical testing involving biomaterials usually require a large number of samples. With FEA the necessity of traditional specimens can be avoided, and by using a mathematical model it also eliminates the need for a large number of experimental teeth. It has been used to represent simulated tooth mechanical behaviour under occlusal loads in details (Li et al., 2011).

CHAPTER 3: MATERIALS AND METHODS

3.1 Preparation of zirconia coating powders

3.1.1 Compaction zirconia powder

Unsintered yttria stabilised zirconia powder contains 3 mol yttrium oxide (Y_2O_3) as a stabiliser (SIGMA-ALDRICH Co., Saint Louis, USA) with an average particle size ≤5 μm according to the product description by the manufacturer. The zirconia powder was pressed using a uniaxial hydraulic press (SIRIO DENTAL, di Zaccaelli Antonio, Italy) and a custom made stainless steel mould which composed of a base, cylindrical body with a central cavity and two sizes of plungers (short and long). The internal surface of mould cavity was painted with a thin film of isolator liquid (Picosep, Renfert, Germany) to avoid powder sticking to the mould. The powder (2 g) was inserted into the mould cavity and a short plunger placed over the powder inside the cavity. The long plunger was placed over the short one and pressed by a hydraulic press at 10 psi (68947.6 Pascal) for 15 minutes as shown in Figure 3.1a. After compressing the powder, the mould was removed from the press and the mould base was separated to push down the compacted powder in tablet shape using the long plunger. The dimensions of the produced zirconia tablet were 12 mm diameter and 4 mm thickness. The tablets were compressed by the cold isostatic press (CIP) (Riken Seiki Co. Ltd., Japan) at a pressure of 2050 kgf/cm^2 (≈ 200 MPa) for 15 minutes to produce uniformly compacted tablets as shown in Figure 3.1b.

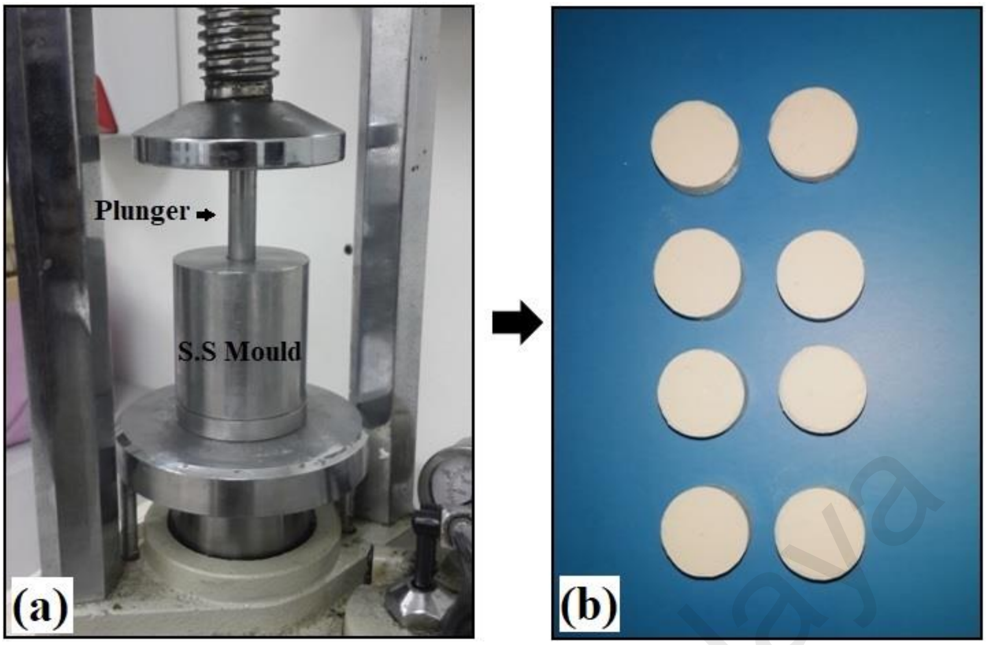

Figure 3.1: (a) Uniaxial press and stainless steel mould and (b) Pressed zirconia tablets by cold isostatic press

The tablets were partially sintered at 1100 °C for 2 hours using a hot air furnace (Xinyu-1700, Henan, China) according to a heating cycle suggested by the furnace manufacturer to produce partially-sintered zirconia tablets (9 mm in diameter and 3 mm thickness) with a harder form and regular density as shown in Figure 3.2.

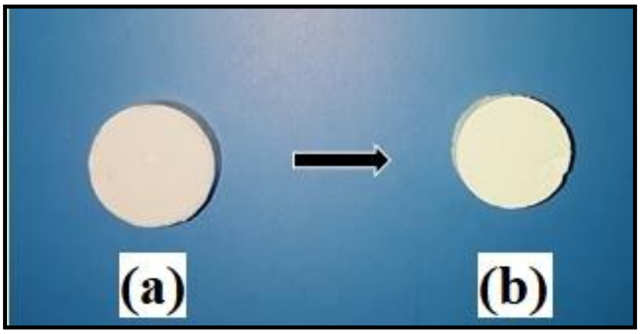

Figure 3.2: (a) Compacted unsintered zirconia tablets and (b) Partially-sintered tablets

Density (ρ) of the unsintered and partially-sintered tablets were measured to compare the densification of zirconia powder after compaction by using a densitometer (Sartorius AX224, Sartorius AG, Göttingen, Germany) based on the Archimedes' principle (equation 1):

$$\rho = \frac{Wa \times \rho w}{Wa - Ww} \tag{1}$$

Where (W_a), and (W_w) are the weight of the specimens in air and water, respectively. (ρ_w) is the water density = 0.99 g/cm^3.

3.1.2 Grinding of zirconia tablets and powders separation

The partially-sintered zirconia tablets were ground by using a zirconia ball milling machine (XQM Planetary ball mill, China) (Figure 3.3) for 7 hours at 200 rpm for each ground cycle to produce powders with different particle sizes. The number of the cycle was determined according to the pilot study that produced fine and coarse particle sizes. The resulted powder was sieved by vibratory sieve shaker (Retsch GmbH-Allee Haan, Germany) with mesh sizes 25, 30, 35, 40, 45 and 50 µm. The meshes were arranged in the shaker machine from coarse to fine size and sieved with amplitude 40 decibels (dB) for 60 minutes.

Figure 3.3: Planetary Ball milling machine

3.1.3 A pilot study to select the zirconia particle sizes of the coatings powders

A study was prepared to assess different particle sizes of partially sintered zirconia powder which were to be mixed with glaze porcelain and liner ceramic and measure their effect on surface area roughness (S_a). Table 3.1 shows the different particle sizes and each selected powder was coated over the zirconia substrate and sintered at 1350 °C to measure the surface roughness. S_a value of the powder collected from meshes 45-50 µm was higher than other powders. In order to compare the effect of the particle sizes on the surface and mechanical properties, the smaller particle size powder was selected from meshes 25-30 µm because the roughness value of the powder collected from mesh 15-20 µm was close to the roughness value produced by airborne particle abrasion surface treatment.

Table 3.1: Surface area roughness of selected particle sizes

Mesh sizes in µm	Average particle size in µm collected between two meshes	Surface area roughness (Sa) in µm
15	15.5-16.5	1.953
20		
25	27-28	4.220
30		
35	36.5-39	5.277
40		
45	46-48	7.629
50		

Based on the pilot study, two ranges of powder sets were found appropriate for this study (Appendix A). The first powder set (size A) was collected between sieve meshes 25 and 30 µm while the second powder set (size B) was collected between meshes 45 and 50 µm as shown in Figure 3.4. The zirconia powders collected from the selected meshes were dried in an incubator at 90 °C.

Each collected powder was analysed by scanning electronic microscope (SEM) (FEI Quanta 250, Eindhoven, Netherlands) to assess the average particle size as shown in Figure 3.5. Two SEM images were used for each particle size measurement.

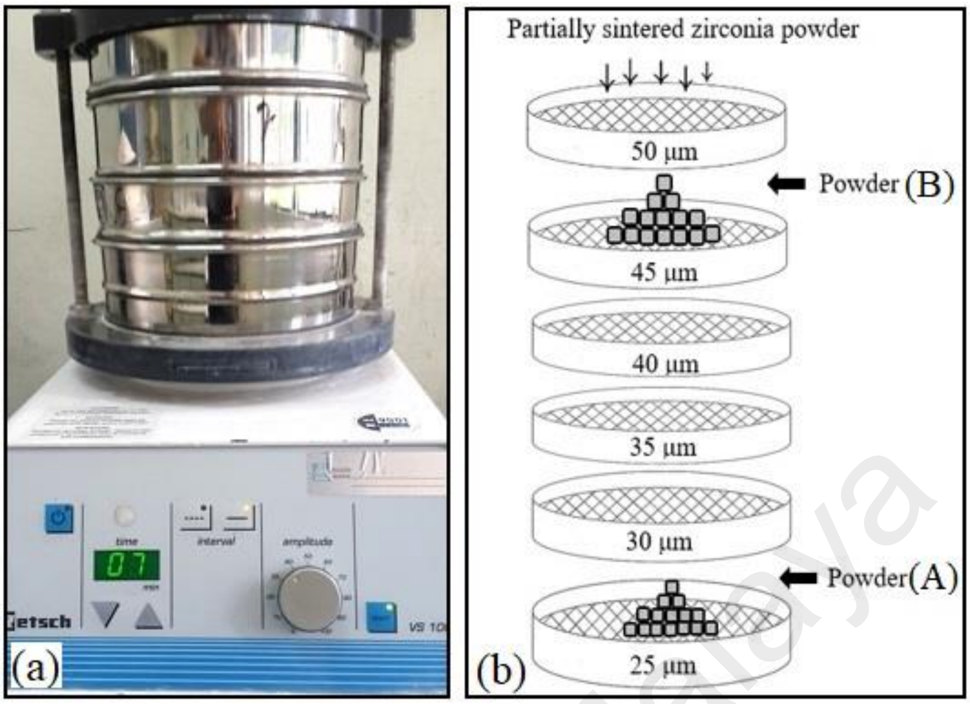

Figure 3.4: (a) Sieve shaker machine and (b) Diagram shows the collection of the selected powders A: for the powder collected between meshes 25-30 µm, B: between meshes 45-50 µm

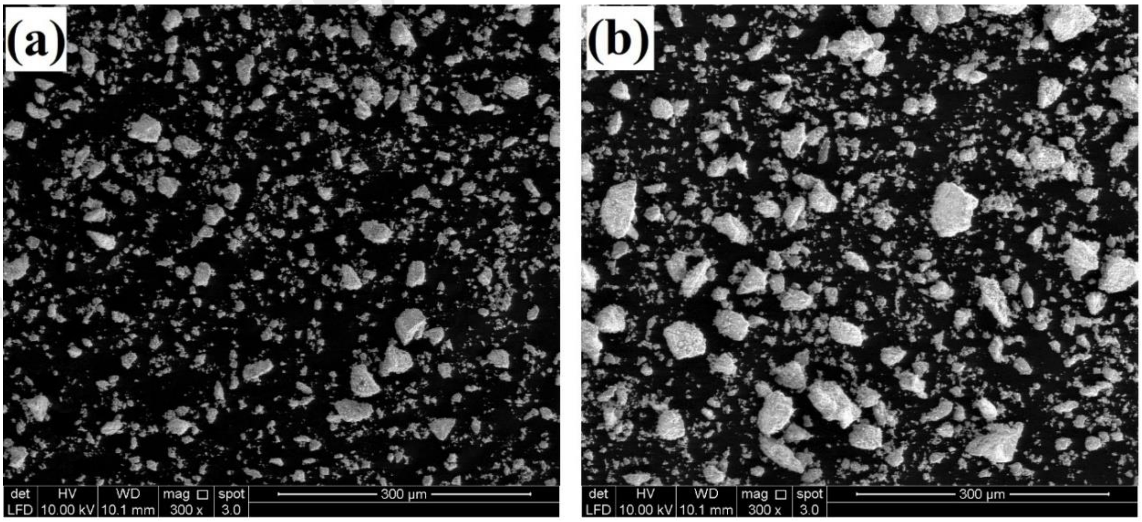

Figure 3.5: SEM images of two powders of zirconia powders to assess average particle sizes. (a) For powder size A and (b) For powder size B

3.1.4 Particle size assessment of coating powders

The average particle sizes were estimated using the SEM images and Image analyser (Image J Software Java 1.6.0) developed by Wayne Rasband of the National Institutes of Health (NIH) (Rasband, 1997). The Image J was used with two SEM images for each powder set to calculate the outline of the powder particles displayed in SEM image as shown in Figure 3.6.

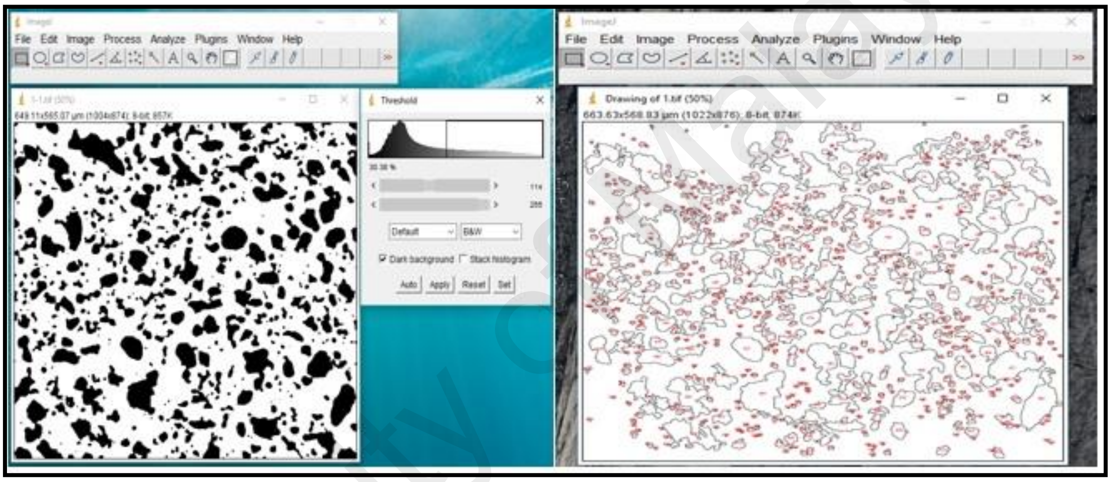

Figure 3.6: Image J software used to assess the particle outlines of zirconia coating powders

3.2 Preparation of specimens

3.2.1 Specimens used for surface properties and shear bond test

Unsintered cylindrical zirconia blocks (Cercon Base 38; DeguDent GmbH, Hanau-Wolfgang, Germany) were sectioned into 50 discs measuring 25 mm in diameter and 2.5 mm in thickness using a high-speed cutting machine (MICRACUT$^{@}$ 176, Metkon, Turkey) as shown in Figure 3.7. All zirconia discs were ground finished with 600, 800 and 1000 grit silicon carbide paper under water coolant at 200 rpm for 10 seconds by using a polishing platform machine (Beta, BUEHER, USA) to standardise the specimen surface texture and morphology as shown in Figure 3.8. The disc specimens were used to measure surface area roughness (S_a), surface morphology, energy dispersive X-ray spectrometry (EDX), X-ray diffraction (XRD) and shear bond strength (SBS).

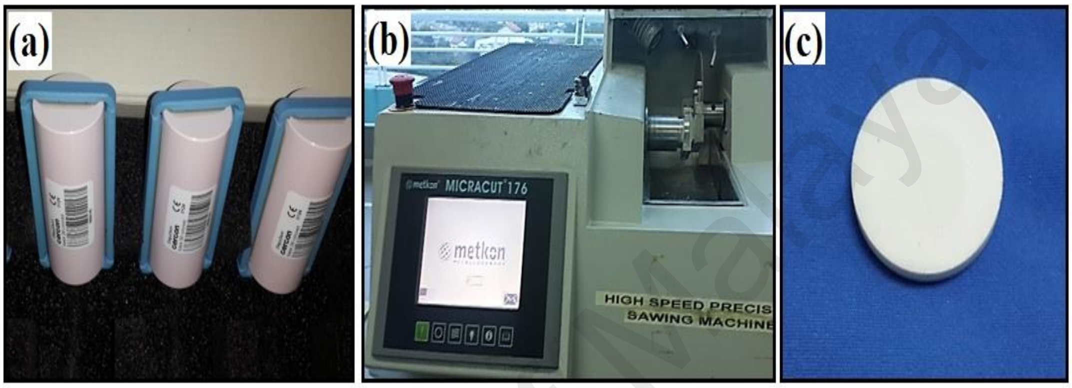

Figure 3.7: (a) Cercon zirconia base blocks, (b) Cutting machine and (c) Unsintered zirconia disc

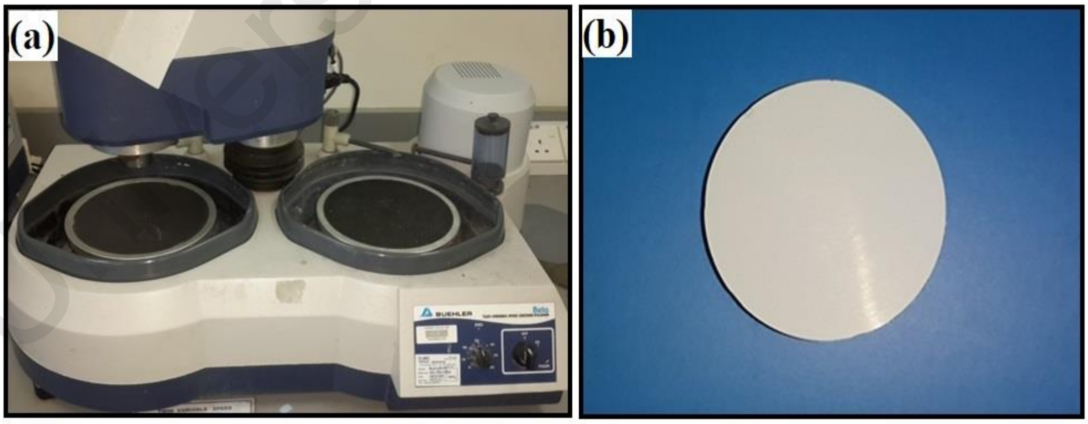

Figure 3.8: (a) Polishing machine and (b) Unsintered zirconia specimen with standardising surface

3.2.2 Specimens used for coefficient of thermal expansion (CTE) test

Fifty rods with a diameter of 5 mm and a length of 10 mm were prepared by pressing the zirconia powder in a custom made stainless steel mould as shown in Figure 3.9a. The final compaction of the powder was achieved by using a cold isostatic press with 3000 kgf/cm^2 (≈ 294 MPa) to produce zirconia rod specimens as shown in Figure 3.9b. The rod specimen shape was prepared according to the requirement of the CTE test.

Figure 3.9: (a) Stainless steel mould used to produce CTE specimen and (b) Final shape of rod specimen

3.2.3 Preparation crowns for fracture strength (FS) test

An artificial maxillary first premolar was positioned in a full mouth dental model (Nissin dental model, Kyoto, Japan) and manually prepared by using a dental high-speed air handpiece (Kavo, Smart Torque, Charlotte, USA). The tooth was prepared according to the clinical instructions proposed for zirconia-ceramic restorations. The limitation of tooth reduction was calculated by using depth orientation groove (Figure 3.10a) by a bur placed on the tooth surface. The preparation involved a 1.2 mm circumferential chamfer finish line at the gingival margin using a tapered flat-ended diamond bur (ISO No. 169-010, REF 6856P314021, Komet dental, Brasseler GmbH & Co., Germany) and the axial wall reduction was 1.5 mm using the same bur reference. The occlusal surface was prepared at 2.0 mm by a barrel bur (ISO No. 13036, REF 8372P314023, Komet dental, Brasseler GmbH & Co., Germany). The angle of convergence was approximately 6°, and all of the sharp angles and undercuts were rounded and smoothed by finishing bur as shown in Figure 3.10 b and 3.10c.

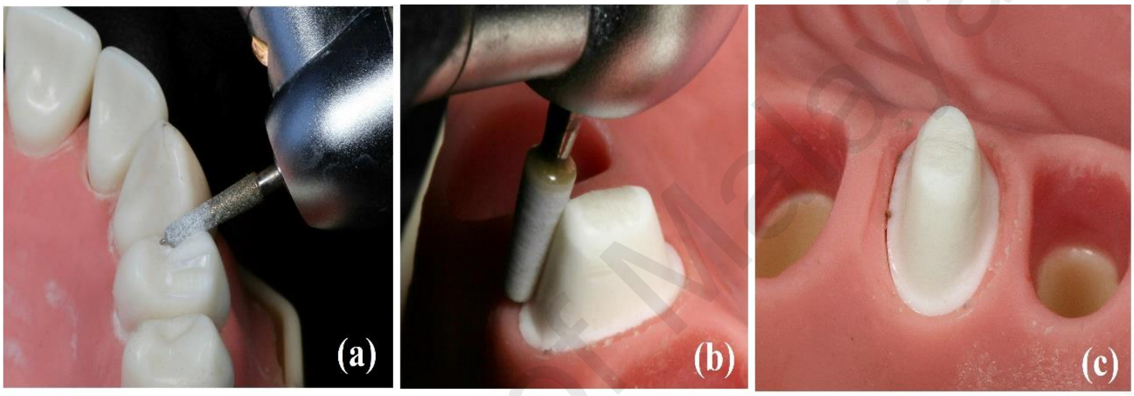

Figure 3.10: Tooth preparation procedure. (a) Using orientation depth groove as preparation index, (b) Tooth smoothening and (c) Final tooth preparation

The prepared tooth (crown with its root) was duplicated with a Vinyl Polysiloxane impression (Reprosil®, DENTSPLY, USA) to create a mould that was filled with molten wax to form a wax pattern. The wax pattern was invested and casted with Co/Cr alloy (Remanium® - Dentaurum, Germany) to construct 5 metal master dies as shown in Figure 3.11a. Each metal die was trimmed and polished. The metal die was perpendicularly embedded in the epoxy resin (Ultrathin resin, PACE Technologies, USA) by positioning the metal die 2 mm apical to the finishing line using a cubic silicone mould with dimension 30 × 30 × 30 mm length, width and height respectively as shown in Figure 3.11b. An impression was made of each metal die and poured with the type IV dental die stone material (Elite Rock, Zermack, Italy) to produce stone die as shown in Figure 3.11c.

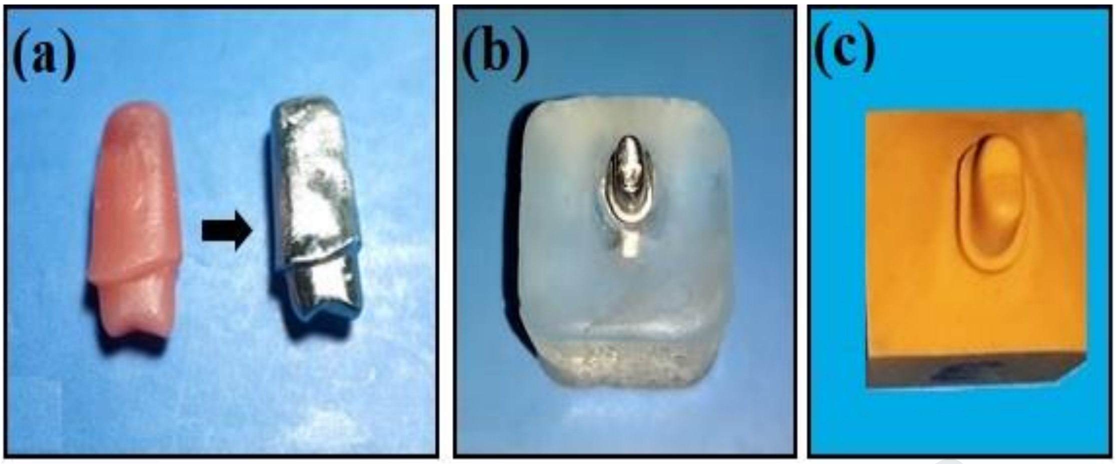

Figure 3.11: (a) Converted wax pattern to the metal die, (b) Metal master die fixed in epoxy resin and (c) Stone die

3.2.3.1 Modelling and designing of CAD/CAM copings

Fifty zirconia copings were fabricated by Cercon CAD/CAM technology (Cercon-Smart Ceramic System, DeguDent GmbH, Germany). The stone dies were scanned by a laser scanner (Cercon eye) to digitise the stone model data that can be read by the CAD software. The stone die was positioned on the scanning platform and the cross lines were positioned in the middle of the stone tooth preparation by using the Cercon art PC software as shown in Figure 3.12a.

The dimensions were calculated by Cercon art PC software and display the resulting points cloud for tooth preparation. The points should be distributed evenly up to the preparation margin of tooth preparation as shown in Figure 3.12b. The next step was to define the tooth preparation parameters including cementing gap, finishing line and correction of the surface line angles as shown in Figure 3.12c. The final step was designed the coping configurations to give its individual anatomic shape and wall skeleton thickness as shown in Figure 3.12d.

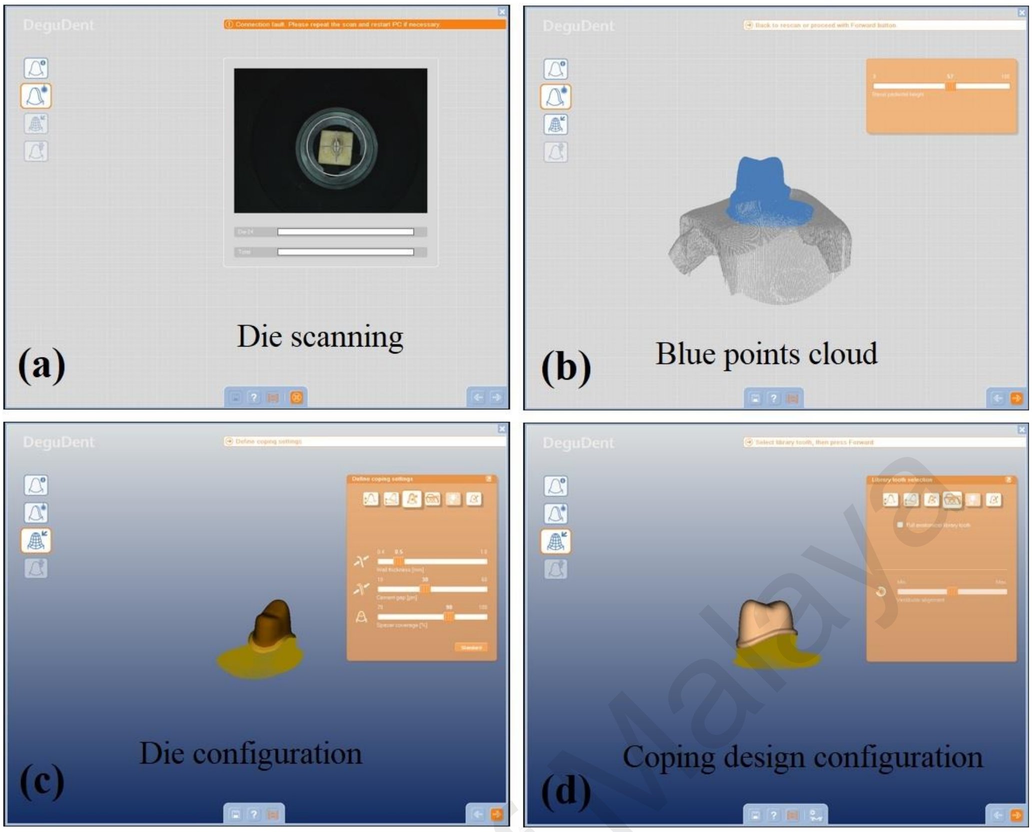

Figure 3.12: (a) The die scanning, (b) Die geometry construction, (c) Die configuration and (d) Designing zirconia coping by Cercon art PC to produce model data

3.2.3.2 Milling of zirconia copings

The data of the coping designed by Cercon art PC was transferred to the milling machine (Cercon brain) to produce the zirconia copings. The unsintered zirconia block (Cercon Base 47, DeguDent, Germany) was mounted by special metal holder called milling frame and placed in the right holder of the rotary and turning unit of the milling machine. Scanning of the zirconia block and milling were carried out automatically and without interruption. Depending on the designated data, the copings were produced by milling machine with 0.4 mm skeleton wall thickness as shown in Figure 3.13.

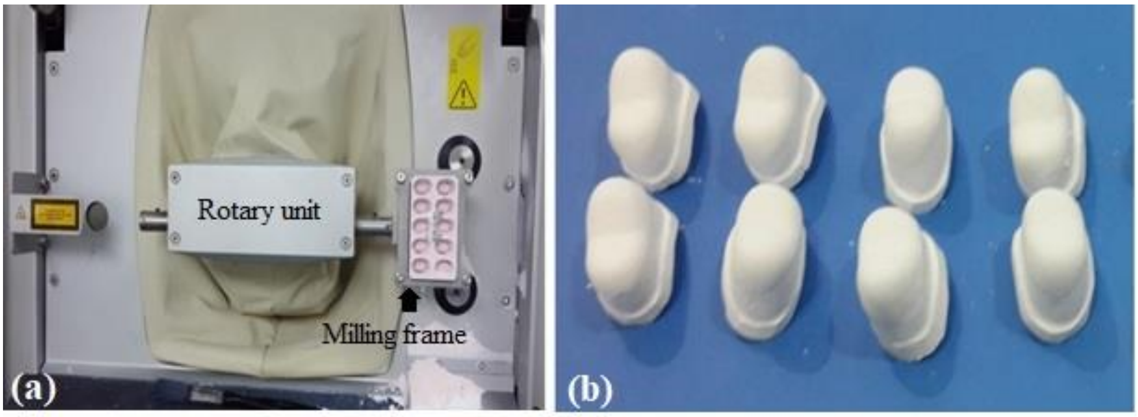

Figure 3.13: (a) Milling process and (b) Unsintered zirconia copings

3.3 Specimens grouping

One hundred and fifty specimens (discs, rods and crowns) were randomly divided according to the type of surface treatments into three main groups; airborne particle abrasion (APA), glaze zirconia mixture (M1) and liner zirconia mixture (M2). The details of grouping are summarized in Appendix B.

Group APA: 30 zirconia specimens (10 discs, 10 rods and 10 copings) were sintered in an atmospheric air furnace (Cercon heat, DeguDent GmbH, Hanau, Germany) at 1350 ºC according to the manufacturer’s instructions and treated with airborne-particle abrasion as a control group. The sintered zirconia specimen was blasted with 50 µm aluminium oxide powder (Korox®, Bego, Germany) using an air-abrasion machine (Basic Quattro, Renfert GmbH, Hilzingen, Germany) its nozzle fixed perpendicularly to the specimen by a special metal holder (Figure 3.14a) at a constant pressure of 4 bars (= 0.4 MPa) and 10 mm distance for 10 seconds (Nishigori et al., 2014). For the rods and copings specimens, the APA treatment was applied to all their surfaces as shown in Figure 3.14b.

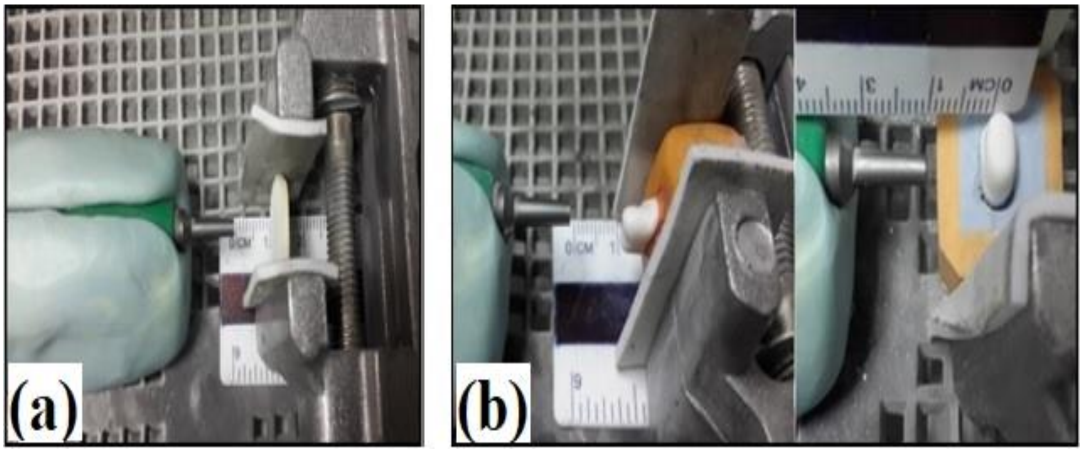

Figure 3.14: Airborne particle abrasion surface treatment. (a) For zirconia disc specimens and (b) For all surfaces of coping and rod specimens

Group M1: zirconia powder and glaze ceramic powder mixture group, 60 unsintered zirconia specimens (20 discs, 20 rods and 20 copings) were coated with the mixture prepared by mixing 50 wt% glaze ceramic powder (Cercon® Ceram Kiss, DeguDent, Germany) with 50 wt% of partially-sintered zirconia powder.

Group M2: zirconia powder and liner ceramic paste mixture, 60 unsintered zirconia specimens (20 discs, 20 rods and 20 copings) were coated with a mixture of zirconia powder with a ceramic liner paste (Cercon® Ceram Kiss, DeguDent, Germany) with the same mixing ratio in the group M1.

The coated groups were subdivided according to the particle sizes of zirconia coating powder particle sizes (A=26 µm and B=47 µm) into M1A, M1B, M2A, and M2B respectively (for each group10 specimens).

The coated specimens were sintered at 1350 °C in the Cercon furnace (Cercon Heat; DeguDent, Hanau, Germany) according to the manufacturer instructions. Each group was evaluated for its surface, physical and mechanical properties. The grouping of tested specimens is shown in Figure 3.15.

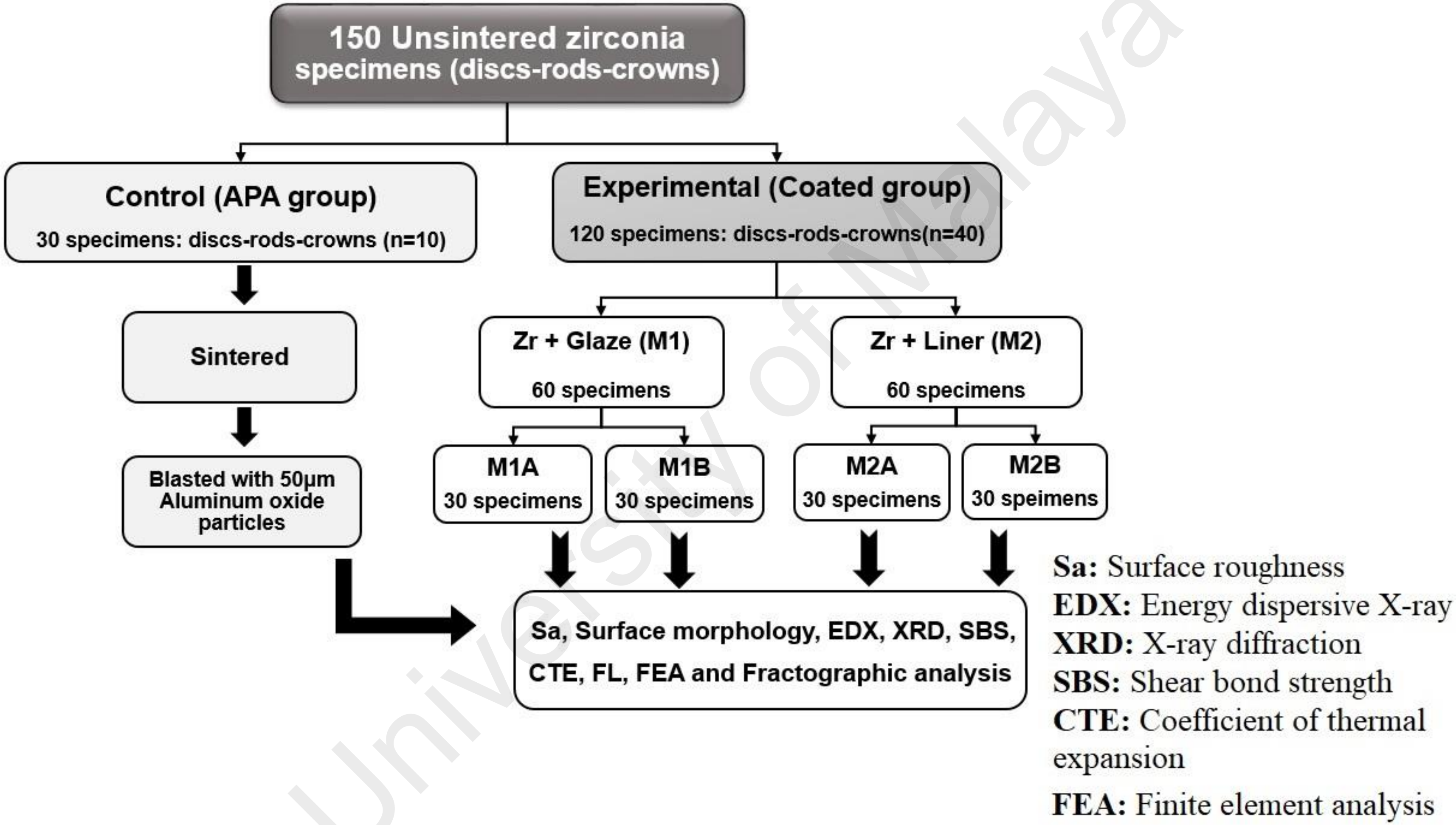

Sa: Surface roughness
EDX: Energy dispersive X-ray
XRD: X-ray diffraction
SBS: Shear bond strength
CTE: Coefficient of thermal expansion
FEA: Finite element analysis

Figure 3.15: Diagram showed the grouping of tested specimens. M1A and M1B for groups of zirconia glaze mixture size A and size B. M2A and M2B for groups of zirconia liner mixture size A and size B.

3.4 Coating procedure

The coating material was prepared by mixing each selected average particle sizes of zirconia powder 50 wt% with 50 wt% of the ceramic liner or glaze ceramic (the chemical components of materials are listed in Table 3.2) and diluted with 1.5 mL of pure ethanol of 99.7% (Systerm, ChemAR, Germany) to form a homogeneous slurry using a magnetic stirrer (RCT Basic, IKA® Werke Staufen/Germany) at 500 rpm for 15 minutes. The coating was performed by a mini airbrush gun (model 130-dual action airbrush kit, Taiwan) with a 50 μm nozzle diameter that was fixed vertically to the zirconia specimens using a laboratory clamp holder.

Prior to coating, each specimen was washed with ethanol for five minutes in the ultrasonic bath and dried with a piece of cotton. The spraying quantity of the slurry was standardized by controlling the air pressure with 2.5 bars and the spray total time of 2 seconds with 13 cm distance as shown in Figure 3.16. These parameters were designated on the basis of the pilot experiment (Appendix C). For the rod and coping specimens, the coating procedure was accomplished by dividing specimen into two halves using a silicone separator over the specimen to ensure uniform coating thickness as shown in Figure 3.17.

All coated copings (Figure 3.18) were sintered at 1350 °C according to manufacturer's instructions in the furnace with atmospheric air (Cercon Heat; DeguDent GmbH, Germany) (Appendix D). Each coated coping was checked for their marginal fit with the own metal master die before veneering with ceramic.

Table 3.2: Shows the chemical composition of zirconia substrate, powder, ceramic liner glaze ceramic and veneering ceramic according to manufacturer data

Materials	Chemical Composition
Cercon zirconia substrate and powder	ZrO_2; Y_2O_3 (3 mol) ; Hf_2O_3 and Al_2O_3
Glaze ceramic powder (M1)	SiO_2; Al_2O_3; K_2O; ZnO; Na_2O; Ba, Pigment and Other Oxide
Ceramic liner paste (M2)	SiO_2; Al_2O_3; K_2O; Na_2O; CaO, P_2O_5, F and other oxides
Cercon Ceram Kiss (veneering porcelain)	SiO_2, Al_2O_3, K_2O, CaO, BaO, B_2O_3, Na_2O, CeO_2, P_2O_3, Li_2O, ZnO, SnO_2 and pigments

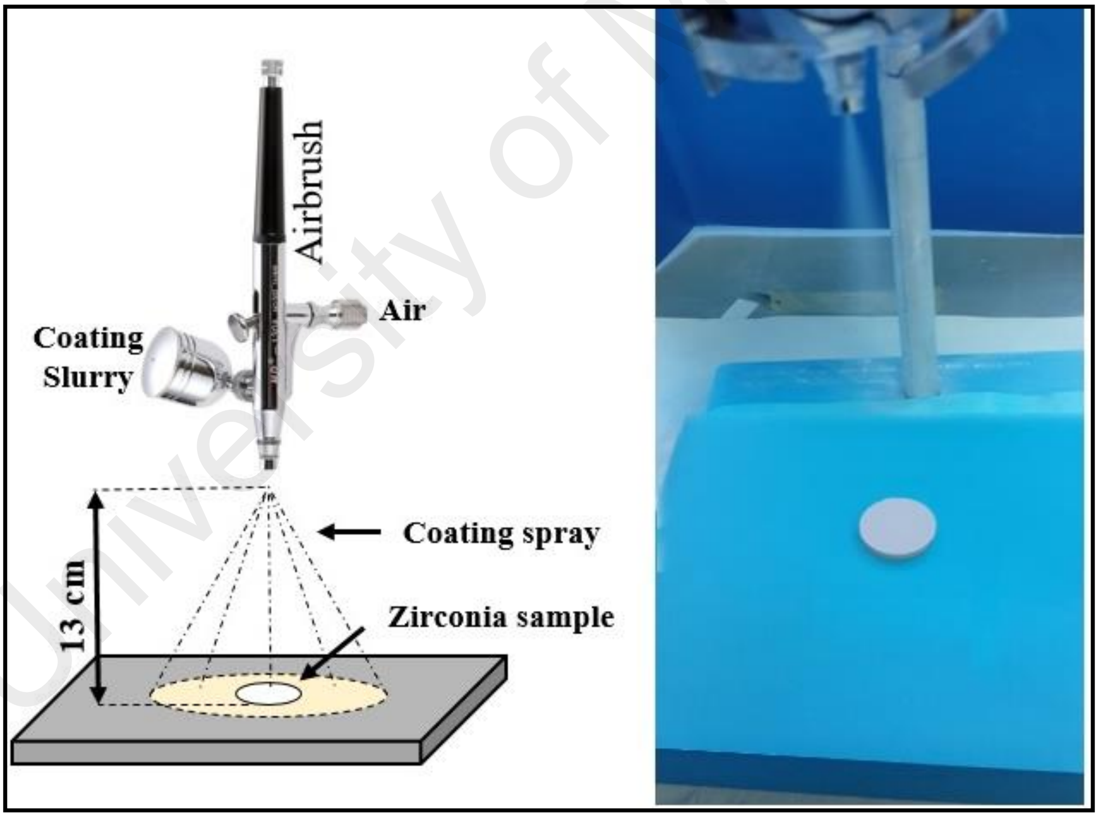

Figure 3.16: Airbrush spraying coating method of unsintered zirconia disc

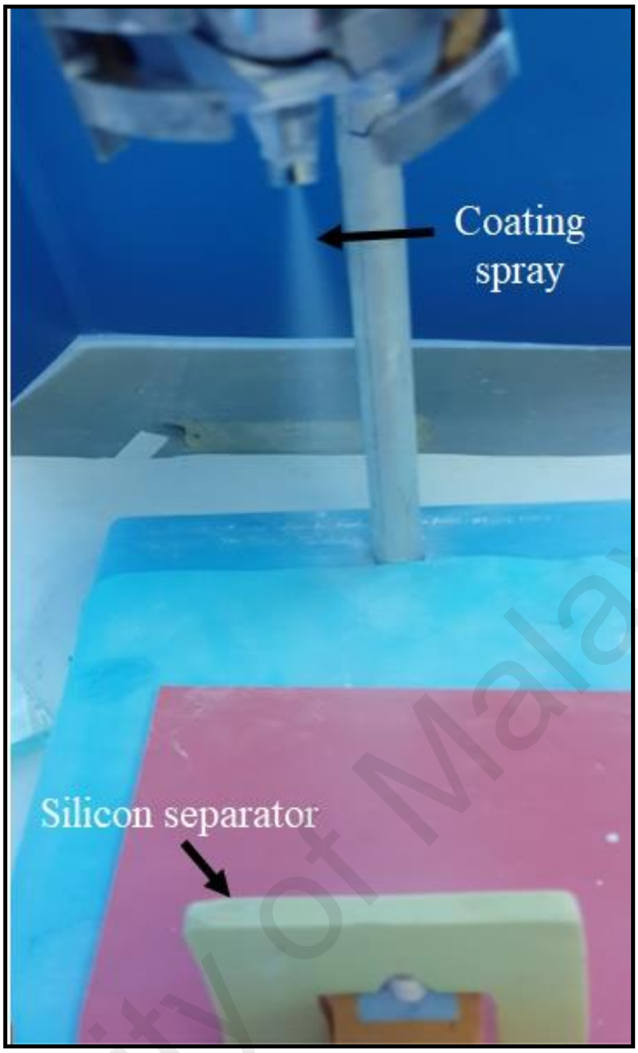

Figure 3.17: Coating procedure of unsintered zirconia coping

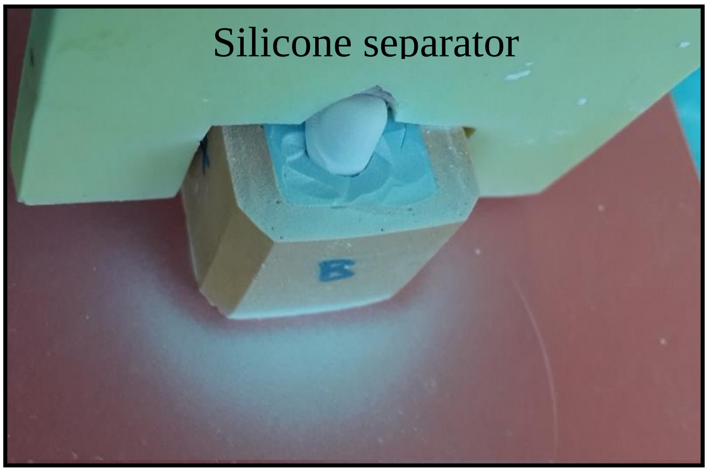

Figure 3.18: Final coated coping

3.5 Surface properties evaluation

3.5.1 Surface roughness measurement

The surface area roughness (S_a) value for the coated and APA discs in each group was measured by three-dimensional (3D) optical surface analyser microscope (Infinity focus, Alicona, Germany) as shown in Figure 3.19. S_a measurements were performed according to the ISO 25178 (ISO, 2010) as a numeric value in micrometre (µm) of total area roughness. The 3D digital image was captured at 20 X magnification for each disc and then analysed with a software included in the device. In order to standardise the roughness measurement, five different locations were chosen in each disc by drawing two cross lines and divided into four quarters (one point in the centre of the meeting point of the two lines and four in the margins at quarters). The S_a result was attained by calculating the mean of the five readings (Chang et al., 2005; Yasuno et al., 2014).

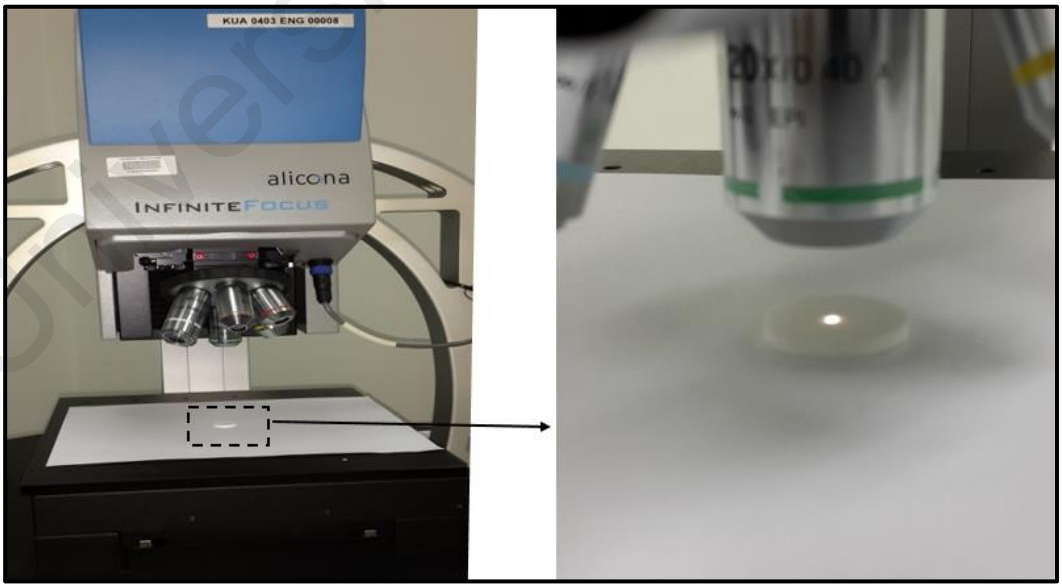

Figure 3.19: Surface texture analyser and disc specimen to measure surface roughness

3.5.2 Surface morphology and elemental composition examination

The surface morphology of all zirconia discs and copings with different surface treatments was evaluated using SEM (FEI Quanta 250, Eindhoven, Netherlands) as shown in Figure 3.20. The elemental composition of the zirconia surfaces was investigated and analysed using the energy dispersive X-ray spectrometry (EDX) (Inca software, Oxford Instruments, Bucks, UK) mounted on the SEM machine. The coating thickness measurement was conducted by cross-sectional observation after embedding the coated disc with epoxy resin and then sectioned with a high-speed cutting machine into two halves. The cross-sectional part was investigated with SEM to analyse the morphology and profile of the coated specimens.

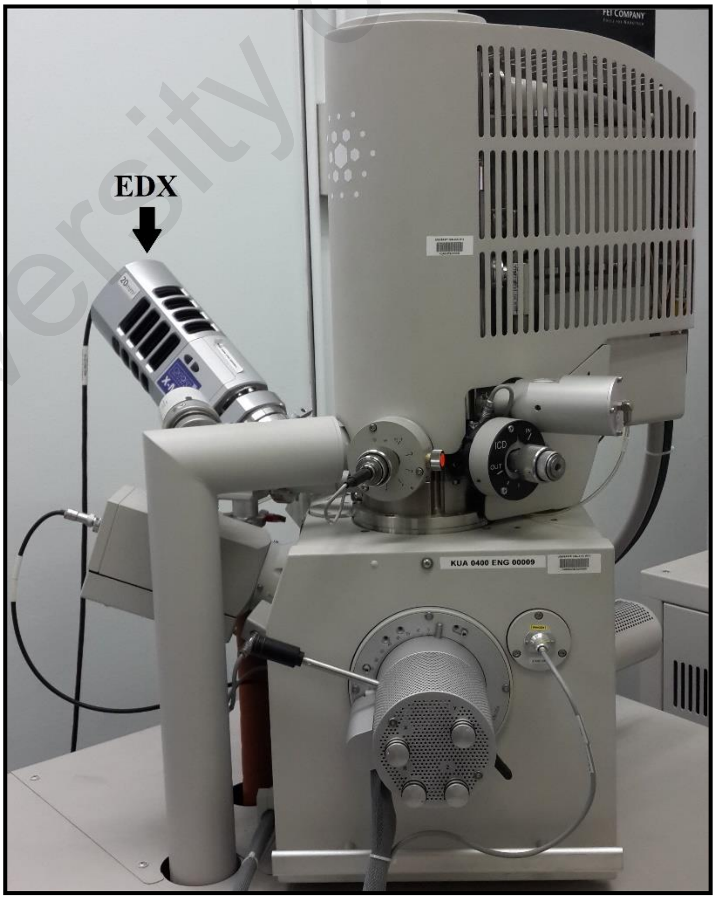

Figure 3.20: SEM machine and EDX device

3.5.3 Crystallographic analysis

The X-ray diffraction machine (XRD) (BRUKER-AXS, GmbH, Germany) (Figure 3.21) was used to determine the structural changes in the crystalline phases of the coated and air abraded zirconia discs by identifying the monoclinic and tetragonal phases. The diffraction patterns were analysed by using the X’Pert HighScore program (X’Pert Pro, Panalytical, Netherlands) in conjunction with the International Center for Diffraction Data references (ICDD).

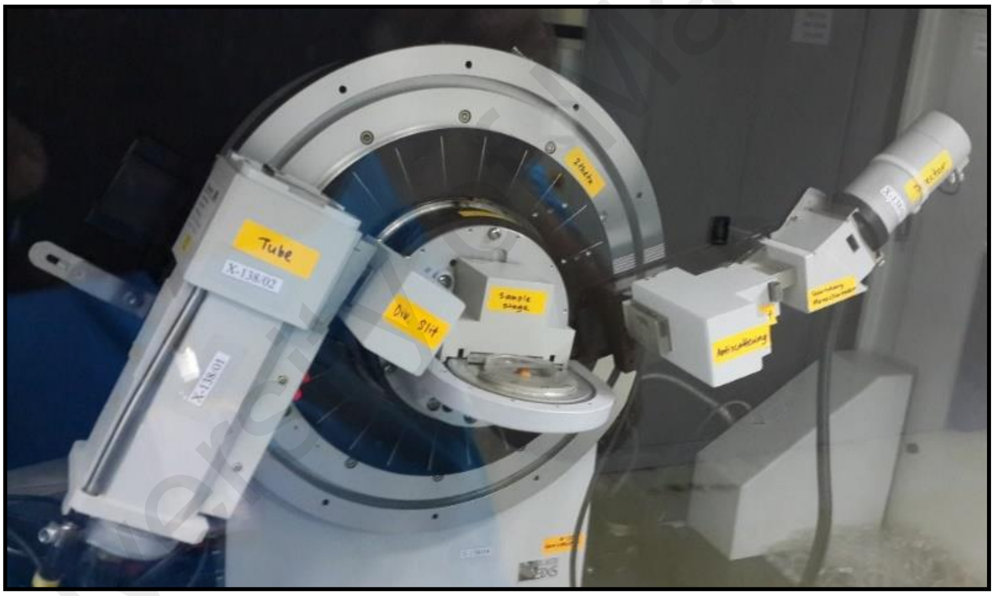

Figure 3.21: XRD machine

3.6 Mechanical properties measurements

3.6.1 Coefficient of thermal expansion (CTE) measurement

Thermomechanical analyser machine (TMA-60, Shimadzu, Japan) was used according to ASTM-E 831, which describes the standard test method for linear thermal expansion of solid materials (ASTM, 2003). Fifty rod specimens with a diameter of 5 mm and a length of 10 mm (10 for each group) were prepared. A standard fused quartz rod with similar dimensions to the test specimens was used as a reference material for measuring CTE as manufacturer's instructions as shown in Figure 3.22a. The zirconia and quartz rods were mounted vertically parallel to each other using sample holders as shown in Figure 3.22b. They were heated from 25 to 1000 ºC at a rate of 10 ºC/min and kept at this temperature for 10 minutes to ensure homogeneous heat distribution, followed by slow cooling. The average expansion analysis was assessed using 'TA60' software.

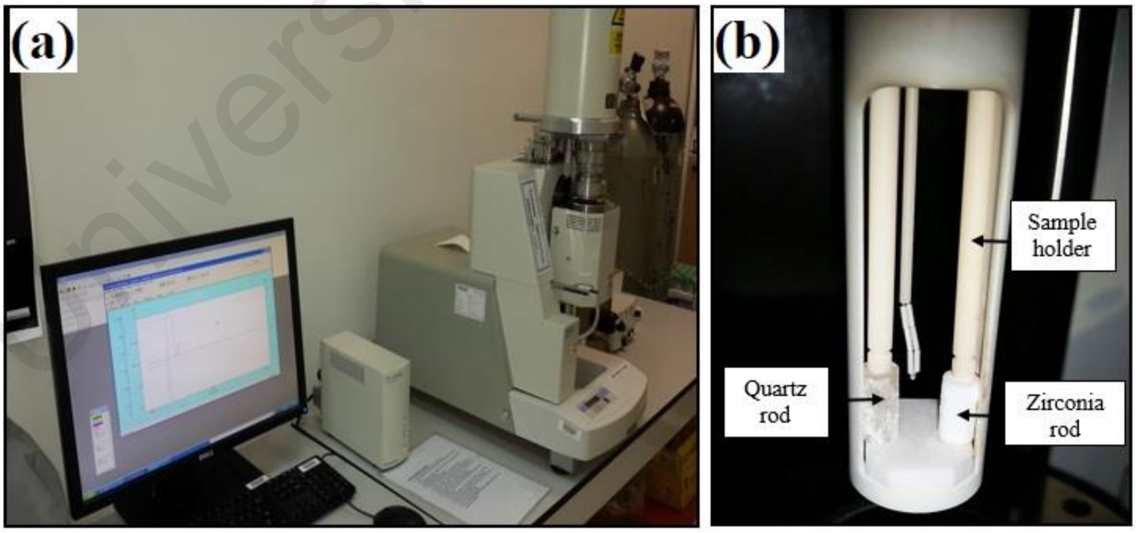

Figure 3.22: (a) Thermomechanical analyser with TA software and (b) Zirconia and quartz rods positioned in the thermal analysis portion of the analyser

3.6.2 Shear bond strength (SBS) test

The method used for this multilayer ceramic system was according to the ISO 9693 (ISO 2012). Fifty zirconia discs were treated with different surface treatments (M1, M2 and APA) and veneered with a cylindrical shape with dimension of 3 mm height and 3 mm diameter of veneering porcelain layer (Cercon Ceram Kiss, DeguDent, Germany) in the centre of the disc using a separable custom-made silicone mould as shown in Figure 3.23a. The ceramic powder was mixed with an appropriate amount of build up liquid to form a ceramic slurry, which was applied with light condensing and vibration on a silicone mould that was lubricated with a porcelain isolating agent (Renfert Picosep, Hilizingen/Germany) to prevent adhesion of the ceramic slurry to the mould as shown in Figure 3.23b and 3.23c.

The veneered discs were sintered in a porcelain furnace (Programat® EP 5000, Ivoclar Vivadent, Schaan/Liechtenstein) according to the manufacturer's recommendations. Each sintered disc was embedded in a cylindrical epoxy resin using the plastic ring (30 mm diameter and 30 mm height) (Figure 3.23d) to place on a stainless steel holder of the universal testing machine (UTM Shimadzu, Tokyo, Japan). A semi-circular metal jig was loaded on a cylindrical ceramic 0.5 mm to the interface area as shown in Figure 3.24 at a crosshead speed of 0.5 mm/min until fracture of veneering porcelain occurred. The SBS was measured in megapascals (MPa) by dividing the load force at fracture in Newton (N) over the area of the bonded veneering porcelain in square millimetre (mm^2).

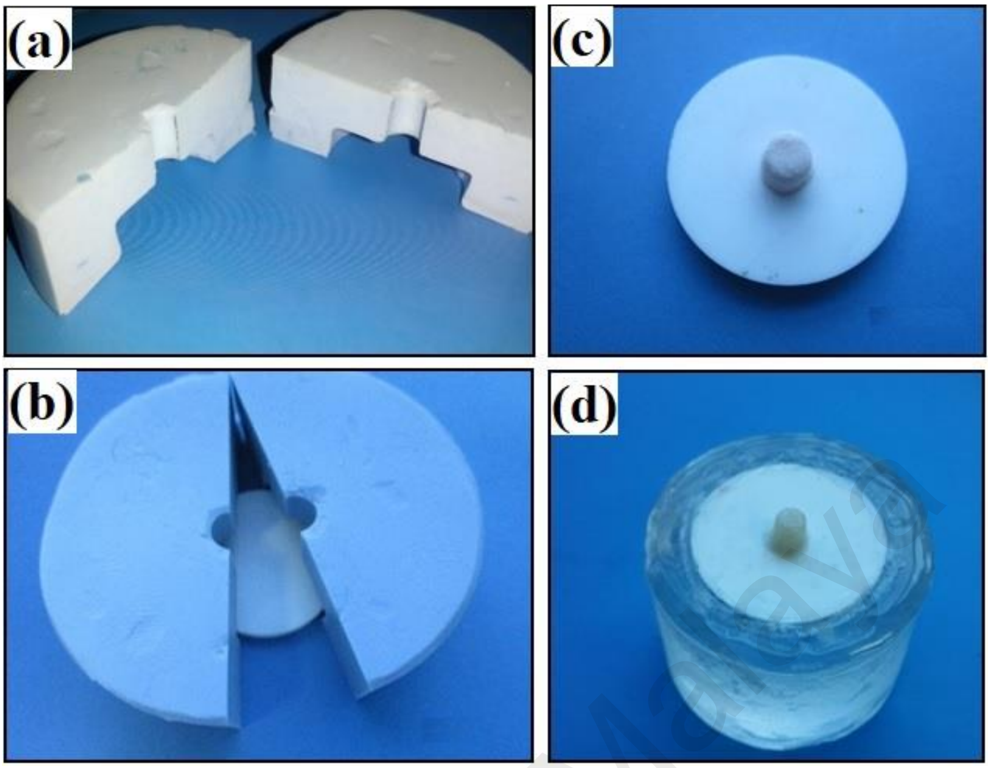

Figure 3.23: (a) Separable silicone mould, (b) Zirconia disc adjusted in the mould, (c) Ceramic slurry build-up over the treated disc and (d) Veneered zirconia discs ready for SBS test

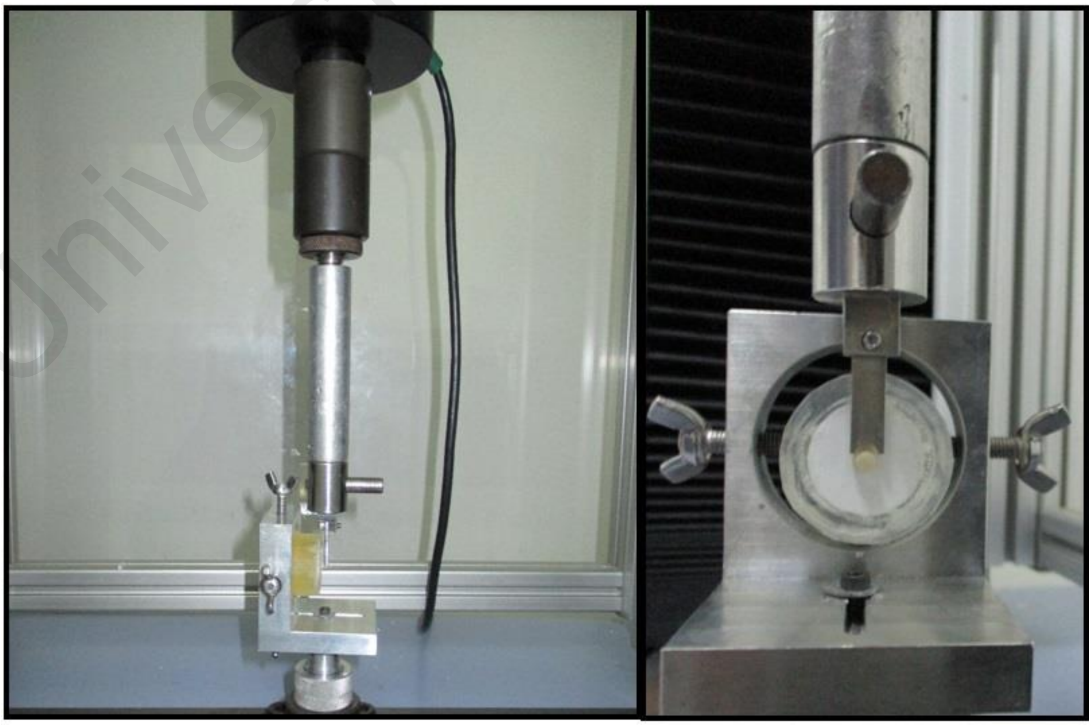

Figure 3.24: SBS Specimen tested by a universal testing machine

3.6.3 Fracture strength test for zirconia-ceramic crowns

Each treated coping was ultrasonically washed in 70% ethanol solution for 15 minutes and then rinsed with deionized water. The standardisation of the crown shape and veneering layer thickness was accomplished by a separable silicone index mould with the desired anatomy (occlusal inclination was 45°) manufactured by duplication of the CAD/CAM lithium disilicate crown designed and milled with the Cerec system (In LAB, Sirona Dental Systems, Germany).

Porcelain powder (Cercon Ceram Kiss, DeguDent, Germany) was mixed with the appropriate amount of a special ceramic liquid to produce a ceramic slurry which was then added and condensed to a silicone mould after lubricating with a porcelain isolating agent (Renfert Picosep, Hilizingen/Germany) as shown in Figure 3.25. Porcelain firing was performed in a porcelain furnace (Programat® EP 5000, Ivoclar Vivadent, Schaan/Liechtenstein) as instructed by the manufacturer. The final crown was checked with their specific metal die.

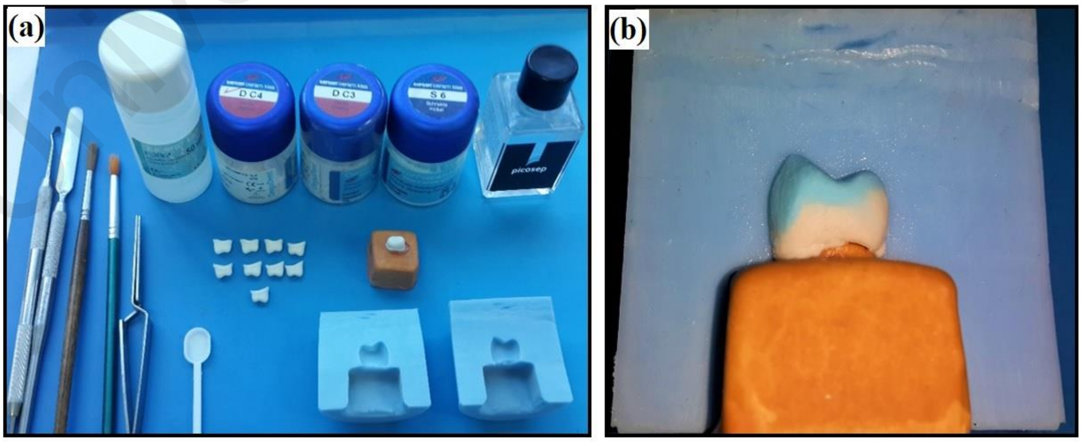

Figure 3.25: (a) Porcelain materials and instruments and (b) Silicone mould used as a reference for build-up crown

All tested crowns for five groups were cemented on their respective metal die by conditioning the inner surface of the crown with hydrofluoric (HF) acid to clean any contaminated debris. The metal die was first cleaned with acetone and dried by compressed air, then mixing the RelyX U200 self-adhesive resin cement (RelyX U200, 3M ESPE, Neuss-Germany) according to the manufacturer's instructions and applied to the inner surface of the zirconia crown. The cemented crowns were placed in a vertical loading device (hydraulic press) with a 5 kg load for 10 minutes after covering the occlusal surface with a custom-made silicone plate to avoid any damage to the crown. Any excess cement was removed from the crown and die margin as shown in Figure 3.26.

After completion of the cementation process, the cemented crown was placed in a specially designed stainless steel holder for testing on the universal testing machine (Shimadzu, Tokyo, Japan). A 3 mm stainless steel knife edge jig was mounted in the testing machine to apply a compressive load obliquely at an angle of 45^{o} to the occlusal surface of the crown and 135^{o} angle to the long axis of the tooth as shown in Figure 3.27. The knife edge bar was applied on the palatal cusp 2 mm away from the central occlusal groove at a crosshead speed of 0.5 mm/min until fracture occurred. The maximum force value to produce fracture was calculated in Newton. After testing of the first crown, any cement remnants on the metal die were removed ultrasonically, then the dies were steam cleaned and air dried before cementation of the following crown.

Figure 3.26: Cemented zirconia crown on the metal die

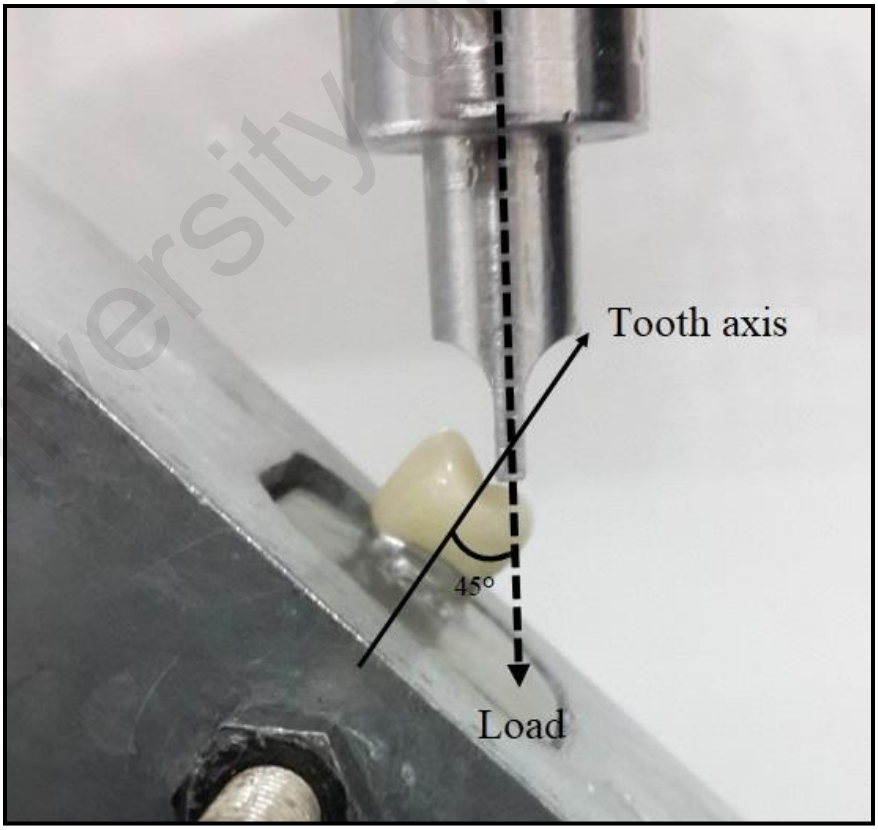

Figure 3.27: Fracture strength test of zirconia crown in the universal testing machine

3.7 Fractographic examination

3.7.1 Fracture modes for shear bond strength test

All fractured specimens retrieved from the shear bond strength test were visually classified and in order to support the visual results, the remaining veneered layer of detected specimens was examined under a stereomicroscope (SZ X7, Olympus, Japan) at 20 X magnification to approve the fracture mode classification as shown in Figure 3.28. Different fracture modes were defined; an adhesive mode which occurred at the coping/veneer interface, cohesive mode located in the veneering porcelain and mixed mode which included both modes. In order to support the visual findings, the remaining veneered layer of classified specimens was examined under a stereomicroscope and SEM.

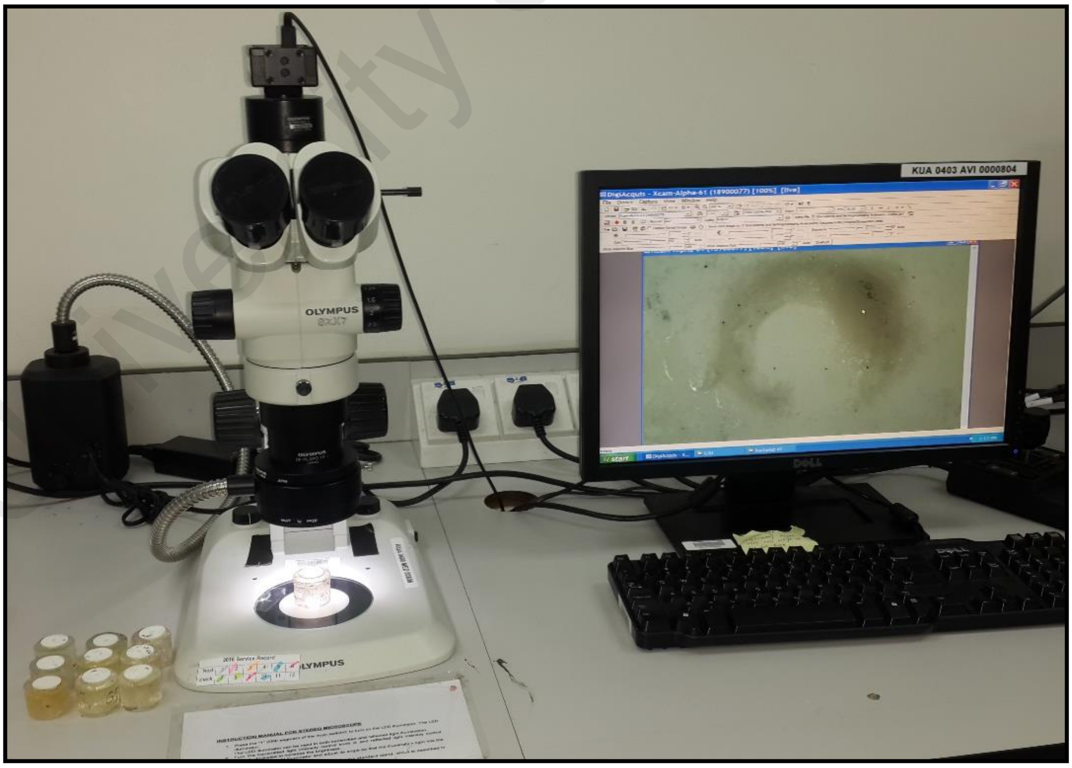

Figure 3.28: Tested SBS specimens examined under a stereomicroscope

The fracture modes were classified according to the percentage of remaining ceramic in the fractured interface by determining and calculating the outline colour of remaining ceramic area by using the colour profiler tool in Image J software (Collins, 2007) and was divided over the total area of the zirconia disc. The percentage was classified into the cohesive fracture (more than 80%), mixed fracture (20-80%) and adhesive fracture (less than 20%) (Alsulami, 2014). Figure 3.29 shows an example of the tested SBS specimen assessed by this method.

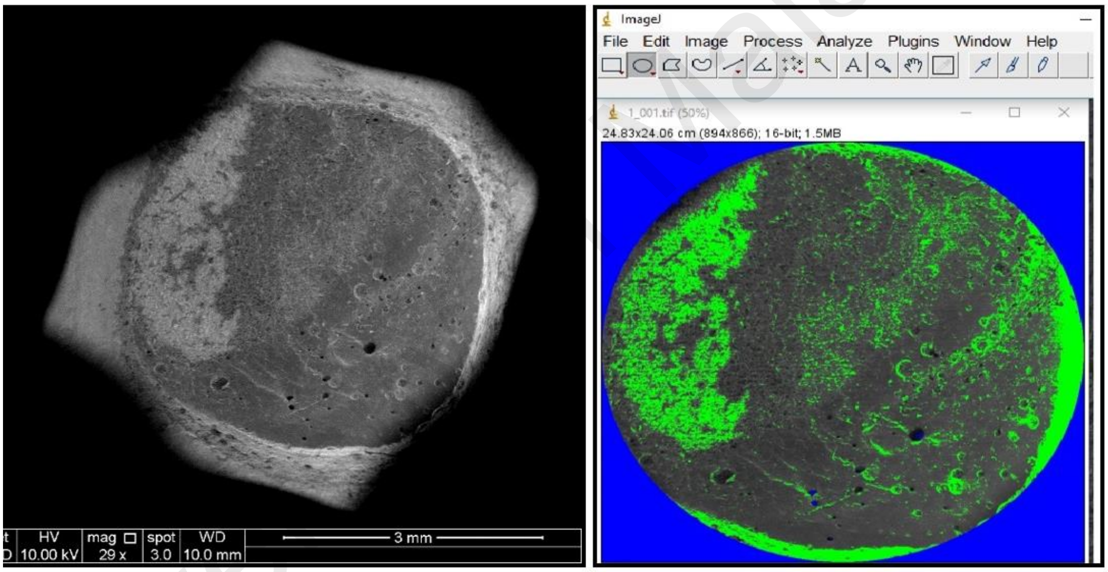

Figure 3.29: Fracture mode classification for tested SBS specimen assessed by SEM image and Image J software

3.7.2 Fracture modes for fracture strength test

All fractured crowns tested with fracture strength test were visually detected to separate fracture modes. In order to approve the visual results, the remaining veneered area of differentiated specimens was examined under a stereomicroscope (SZ X7, Olympus, Japan) at 0.8 X magnification to settle the classification of the crown fracture modes. Three specimens were selected with the highest, middle and lowest FS values in every group to study their fractured modes with SEM. The three fracture modes were defined include; an adhesive mode which occurs at the zirconia coping/veneer interface and the zirconia coping was mostly exposed, cohesive mode located in the bulk of veneering porcelain and the mixed mode includes both adhesive and cohesive modes (Campos et al., 2015).

3.8 Finite element analysis (FEA)

To simulate and predict the stress distributions by fracture strength test for coated and non-coated zirconia based crowns modelling by using FEA.

3.8.1 Construction of geometric models

An extracted human maxillary premolar tooth collected from oral and maxillofacial department clinics of University of Malaya (Ethics No.: DF RD1201/1007(P), Dental Committee, Faculty of Dentistry, University of Malaya) was used for the geometrical model. The tooth was intact with fully formed root without any caries lesion and all surfaces were smooth to scan by 3D dental laser scanner system (Maestro 3D Dental Scanner - MDS400, Italy) to produce a group of Stereolithography (STL**)** file as shown in Figure 3.30.

The STL files of the prepared tooth (dentin), veneering porcelain, coating layers, zirconia coping and cement layer was assembled to the final solid model by using the SolidWorks CAD system (Dassault Systems Corp, USA). A digital model of the prepared tooth was designed according to clinical recommendations for zirconia-ceramic restoration. Following this preparation, a digital crown model of bilayer zirconia-ceramic crowns was created.

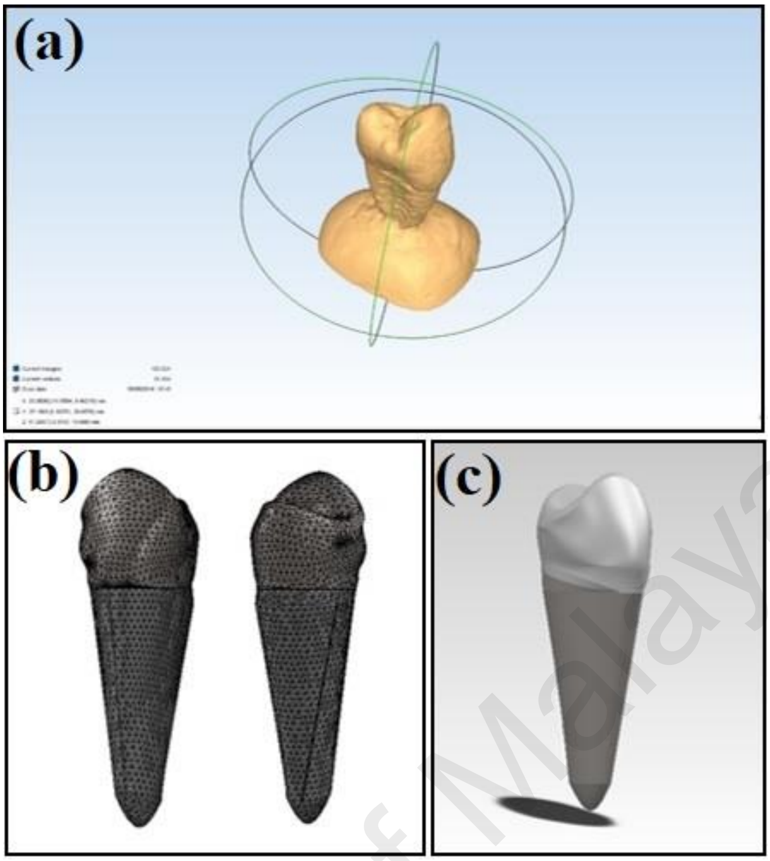

Figure 3.30: (a) 3D Scanning for maxillary premolar tooth, (b) Meshing of tooth model and (c) Final tooth model

Three geometric models with different coping coating surface treatments were established, the first crown model was ZG model (zirconia glaze mixture coated crown), and the second model was ZL model (zirconia liner mixture coated crown). Both models have coating layer thickness of 0.055 mm. The third model was NC model for the non-coated crown as shown in Figure 3.31. All models were designed with a coping thickness of 0.4 mm and full coverage with veneering porcelain varied from 1 mm for the axial region to 1.5 mm for the occlusal area of the crown model. Furthermore, these models were cemented with a uniform cement layer thickness, which was 0.045 mm for each model. These parameters were selected according to the clinical instructions used for zirconia-ceramic restoration.

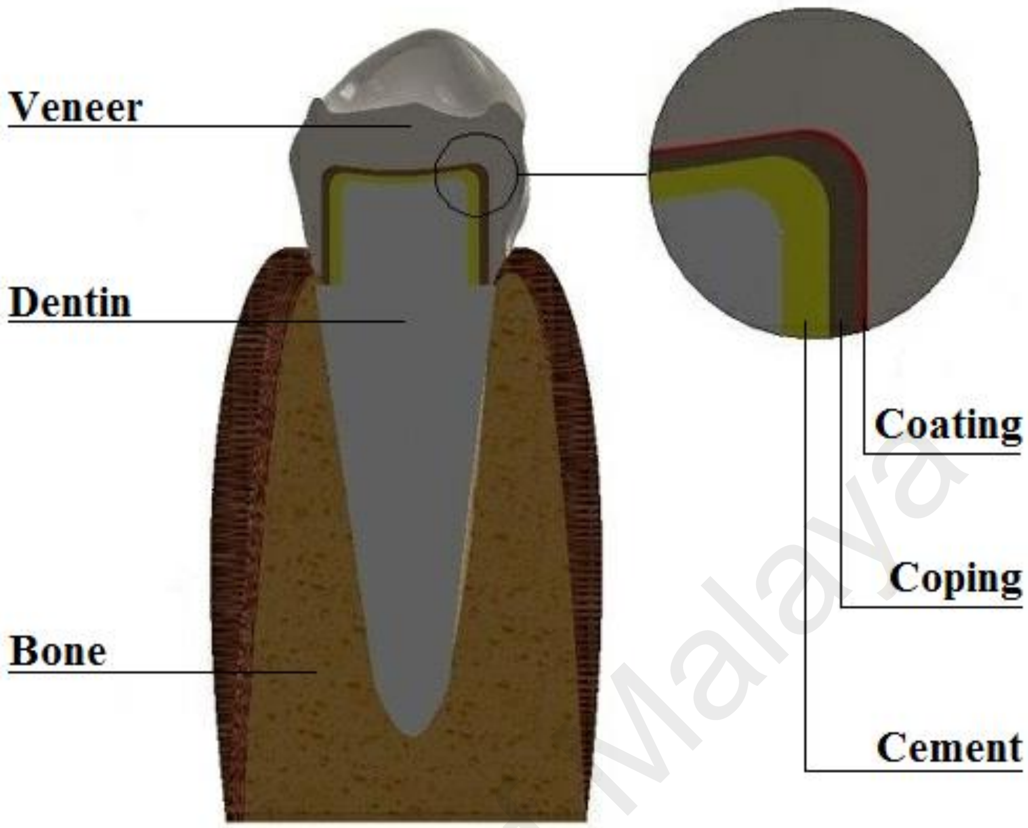

Figure 3.31: The compartments of the models used in the finite element analysis. The coating layer was only used in the zirconia glaze (ZG) and zirconia liner (ZL) models

3.8.2 Meshing of geometric models

The generated models (tooth and crowns) were imported into a finite element software package (SolidWorks/surface modelling Version premium 2015, Dassault Systèmes, USA) in order to convert into finite element model. Linear tetrahedral solid elements (C3D3) with four nodes were used for stress analysis to meshing all component of geometry models as shown in Figure 3.32. A standard convergence study was conducted by running FEA for the mesh grids with the size of 0.5 mm using different mesh refinement levels because constant tetrahedral elements exhibited slow convergence. The convergence was considered acceptable when relative errors were less than 1%.

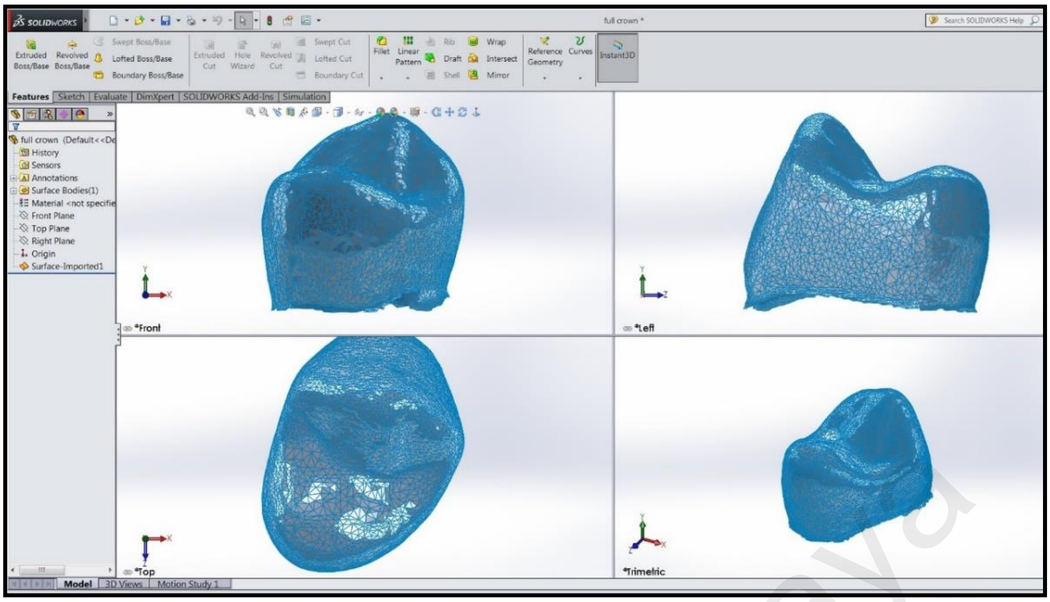

Figure 3.32: Crown model constructing and meshing by SolidWork software

The meshing nodes and elements quantity for different models are listed in Table 3.3. The mechanical properties Young's modulus (*E*) and Poisson's ratio (*v*) used for each component in this study were obtained from the literature as listed in Table 3.4 (De Jager et al., 2006; Dejak et al., 2007; Ausiello Pietro et al., 2011; Dejak et al., 2012). The Young's modulus and Poisson's ratio values for each coating layer with various compositions were estimated by the "rule of mixture" (ROM), which used the theoretical properties and percentage of each composite material to calculate mechanical properties (Al-Maqtari et al., 2013). All solid components were assumed homogeneous, linear elastic and isotropic through the entire distortion.

Table 3.3: Quantity of meshing nodes and elements for tooth and crown models

Models	Number of Nodes	Number of Elements
Tooth model	142958	91517
Dentin	47094	32303
Veneer	43741	27478
Coping	9371	4792
Cement	10911	6099
Coating layer	11809	5853

Table 3.4: Material properties data used in the FEA

Material	Young's modulus (GPa)	Poisson's ratio	References
Veneer ceramic	69	0.28	(Ausiello P. et al., 2011)
Coating layer ZG	9.75	0.26	ROM
Coating layer ZL	5.64	0.26	ROM
Zirconia coping	210	0.22	(De Jager et al., 2006)
Dentin	18.6	0.30	(Dejak et al., 2012)
Enamel	84.1	0.30	(Ausiello P. et al., 2011)
Resin cement	16	0.24	(Dejak et al., 2012)
Alveolar bone	11.5	0.30	(Dejak et al., 2007)

A static load simulation of 200 N (Hu et al., 2013) was applied on an area of 2.5 mm^2 on the palatal cusp of the crown at an oblique angle of 45° to the tooth axis (Figure 3.33) to simulate the mastication load (Hu et al., 2013; Abdulmunem et al., 2016). Stress patterns were obtained from the centrally located nodes on the surfaces of the veneer ceramic, zirconia coping, cement, and dentin which spanned from the cervical line of the buccal surface to the cervical line of the palatal surface.

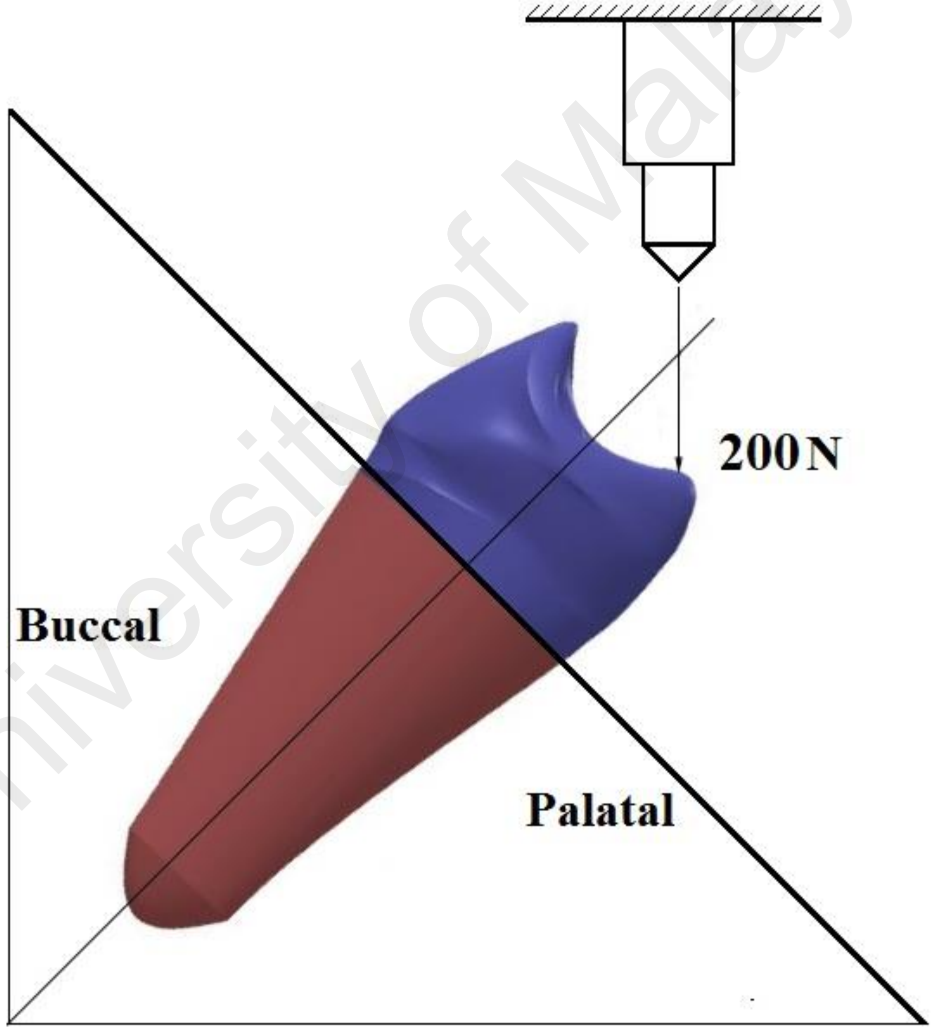

Figure 3.33: Application of static load on FEA model in the oblique direction

3.8.3 Defining the boundary condition

The nodes of all models were fixed at the bottom surface of the tooth root. The components of a tooth restored with zirconia-ceramic crown were assumed to be perfectly bonded without any gap between them.

3.8.4 Finite element analysis output

Calculation of the stress distribution was carried out using (SolidWorks/surface modelling Version premium 2015, Dassault Systèmes, USA). The von Mises criterion was used to evaluate the model coherence and to measure the possible flow of the stress of load through the different model components. The stresses were evaluated along the veneering porcelain and interface area.

3.9 Statistical analysis

Descriptive statistical values (mean and standard deviation) for particle sizes assessment, S_a, CTE, SBS and FS were calculated. All results were analysed with one-way analysis of variance (ANOVA) and post hoc multiple comparisons by Tukey HSD test between groups at a significance level of $P<0.05$ using Statistical Package for Social Sciences (SPSS 22, SPSS Inc., Chicago, USA).

CHAPTER 4: RESULTS

4.1 Coating powder particle sizes

The Image J software and SEM images were used to assess average particle sizes of the zirconia coating powders showed averages of 26.0 ± 0.3 µm for the powder A with a median of 25.55 µm and 47.0 ± 0.5 µm for the powder B with a median of 46.9 µm as shown in Figure 4.1. These results indicated that the two particle sizes were agreed with the planned target by preliminary experiments which produced particle sizes with different surface roughness values.

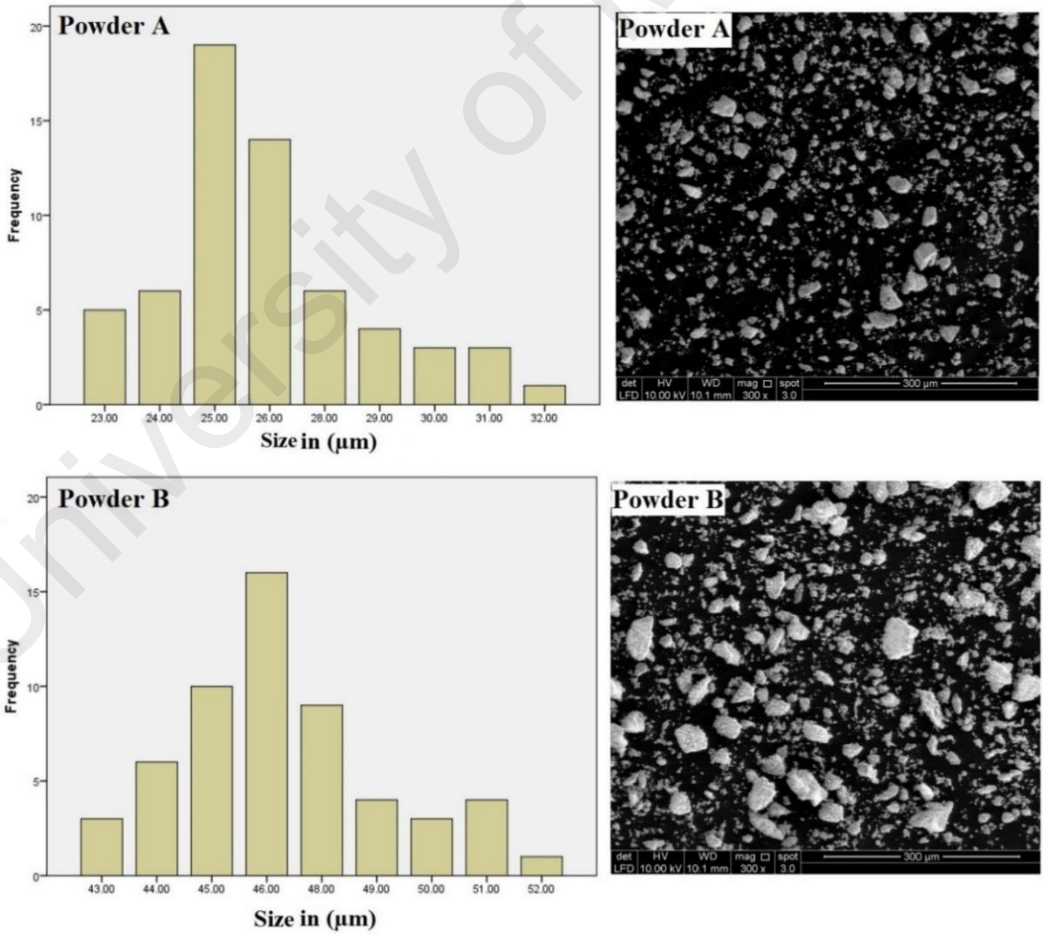

Figure 4.1: Distribution graphs for particle sizes averages in micrometre (µm) of two zirconia coating powder sets (A and B) calculated by Image J software and SEM images

4.2 Surface roughness

The mean and standard deviation (SD) for surface area roughness (S_a) values of zirconia disc specimens were significantly affected by the type of surface treatment. The surface roughness results of coated zirconia disc specimens showed a higher value than the APA group. Statistical analysis by One-way ANOVA showed that there was a significant difference (*P*<0.05) between all groups as shown in Figure 4.2. The Multiple comparisons by the Tukey HSD test revealed that M1B and M2A groups had a significant difference compared to other coated groups as shown in Table 4.1.

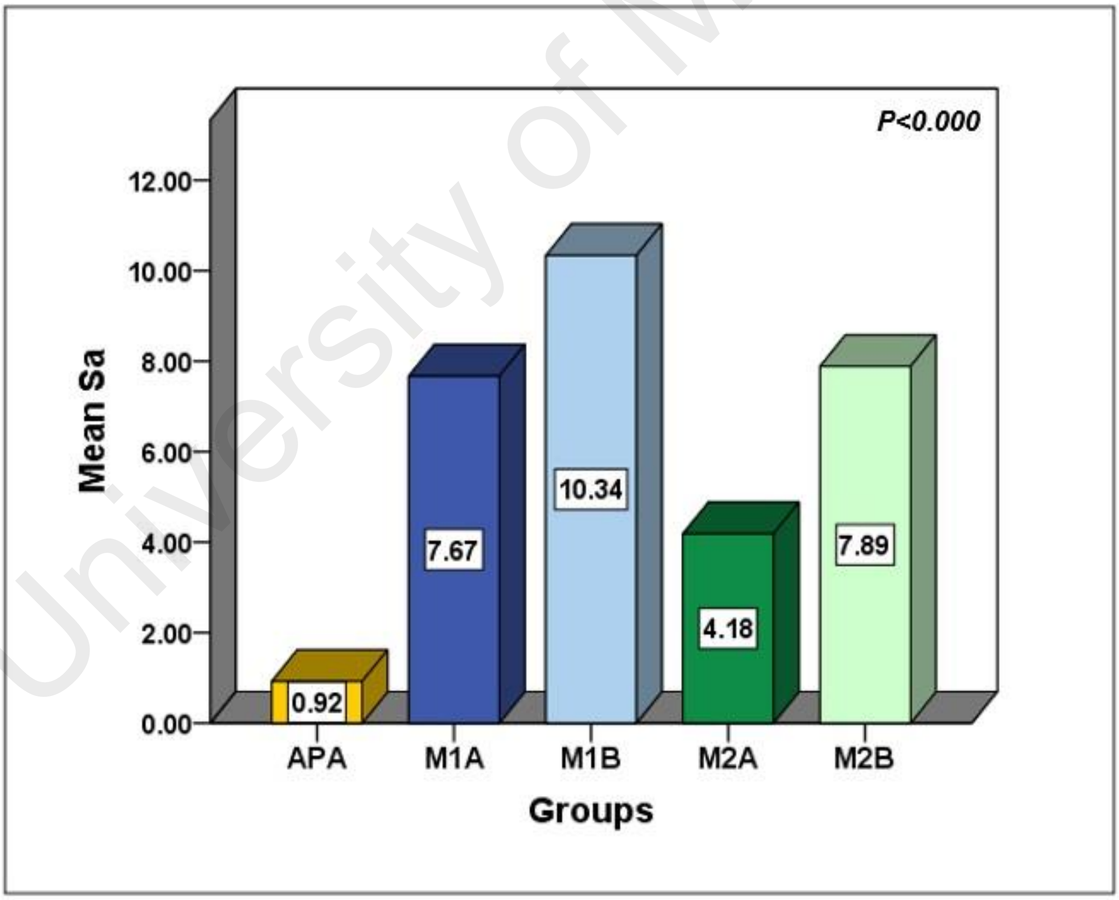

Figure 4.2: Surface roughness means in micrometre (µm) for all tested groups. M1A and M1B for coated specimens by zirconia glaze mixture with sizes A and B. M2A and M2B for coated specimens with zirconia liner mixture with sizes A and B. APA for airborne particle abrasion

Table 4.1: Multiple comparisons of the surface roughness values between the zirconia specimens with different surface treatments by Tukey HSD test. M1A and M1B for coated specimens by zirconia glaze mixture with sizes A and B. M2A and M2B for coated specimens with zirconia liner mixture with sizes A and B. APA for airborne particle abrasion specimens

Group (I)	Group (J)	Mean Difference (I-J) (μm)	Sig.
APA	M1A*	-6.478	0.000
	M1B*	-9.413	0.000
	M2A*	-3.261	0.000
	M2B*	-6.691	0.000
M1A	M1B	-2.665	0.861
	M2A*	3.487	0.000
	M2B*	-0.213	0.000
M1B	M2A*	6.152	0.000
	M2B*	2.452	0.000
M2A	M2B*	3.700	0.000
*Significance level at *P*<0.05			

The surface profile analysis for tested discs showed different irregular surface profiles depending on the type of surface treatments. Coated groups seemed to have more prominent irregularities than APA (uncoated) group as shown in Figure 4.3.

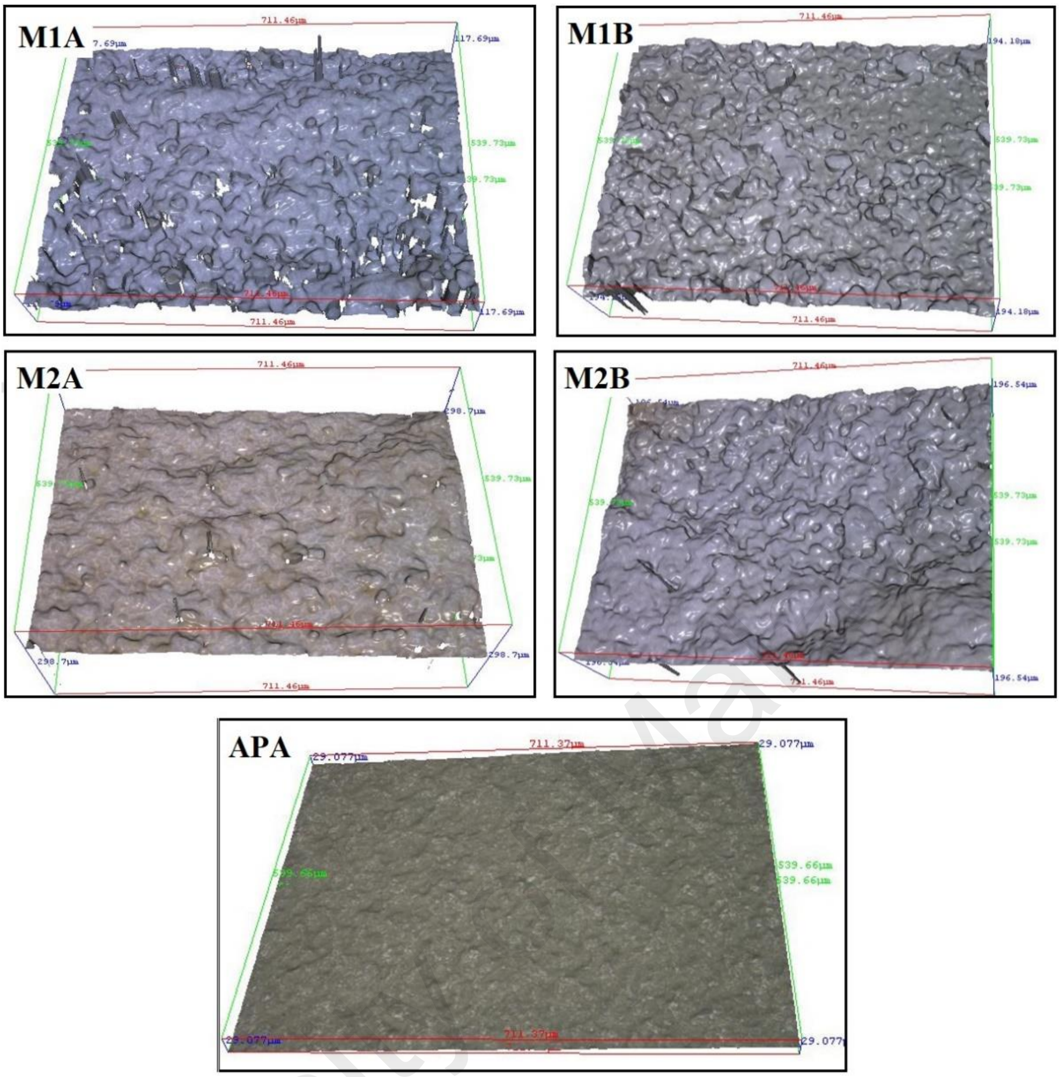

Figure 4.3: Surface profile Images of treated zirconia specimens. (M1A and M1B) zirconia glazing coating mixture, (M2A and M2B) zirconia liner coating mixture and (APA) airborne particle abrasion

4.3 Surface morphology

The morphology of the discs and copings of tested groups examined with SEM exhibited different surface roughness values. The coated groups M1A, M1B and M2B showed higher surface irregularities and deep undercuts produced by coating projections while group M2A showed fewer surface irregularities. In the APA group showed less formation of surface irregularities without principal undercuts which was easily differentiated when compared with the coated groups as shown in Figure 4.4 and 4.5.

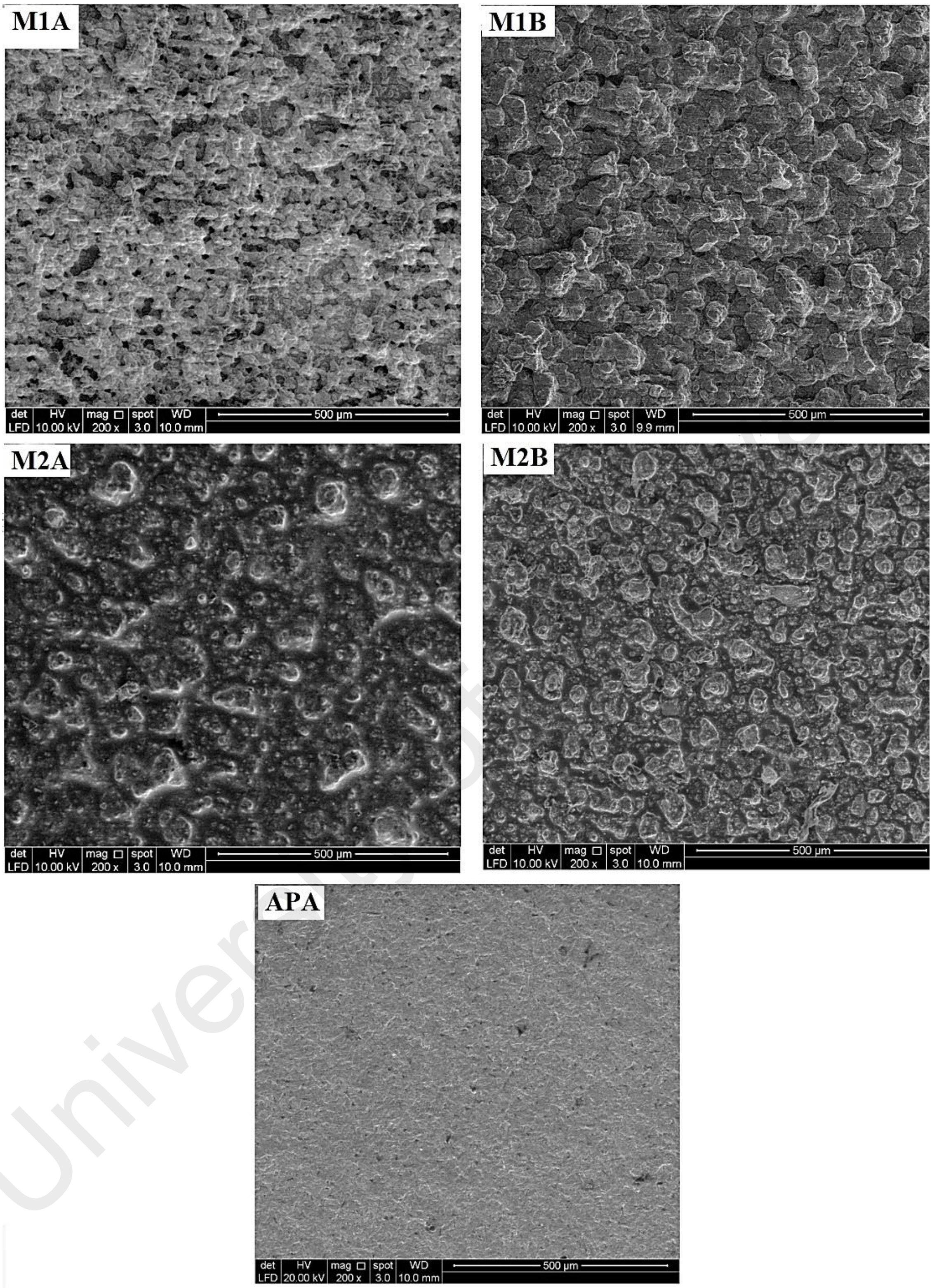

Figure 4.4: SEM images of the treated zirconia disc specimens. M1A and M1B coated with zirconia glaze mixture with sizes A and B. M2A and M2B coated with zirconia liner mixture with sizes A and B. APA for airborne particle abrasion surface treatment

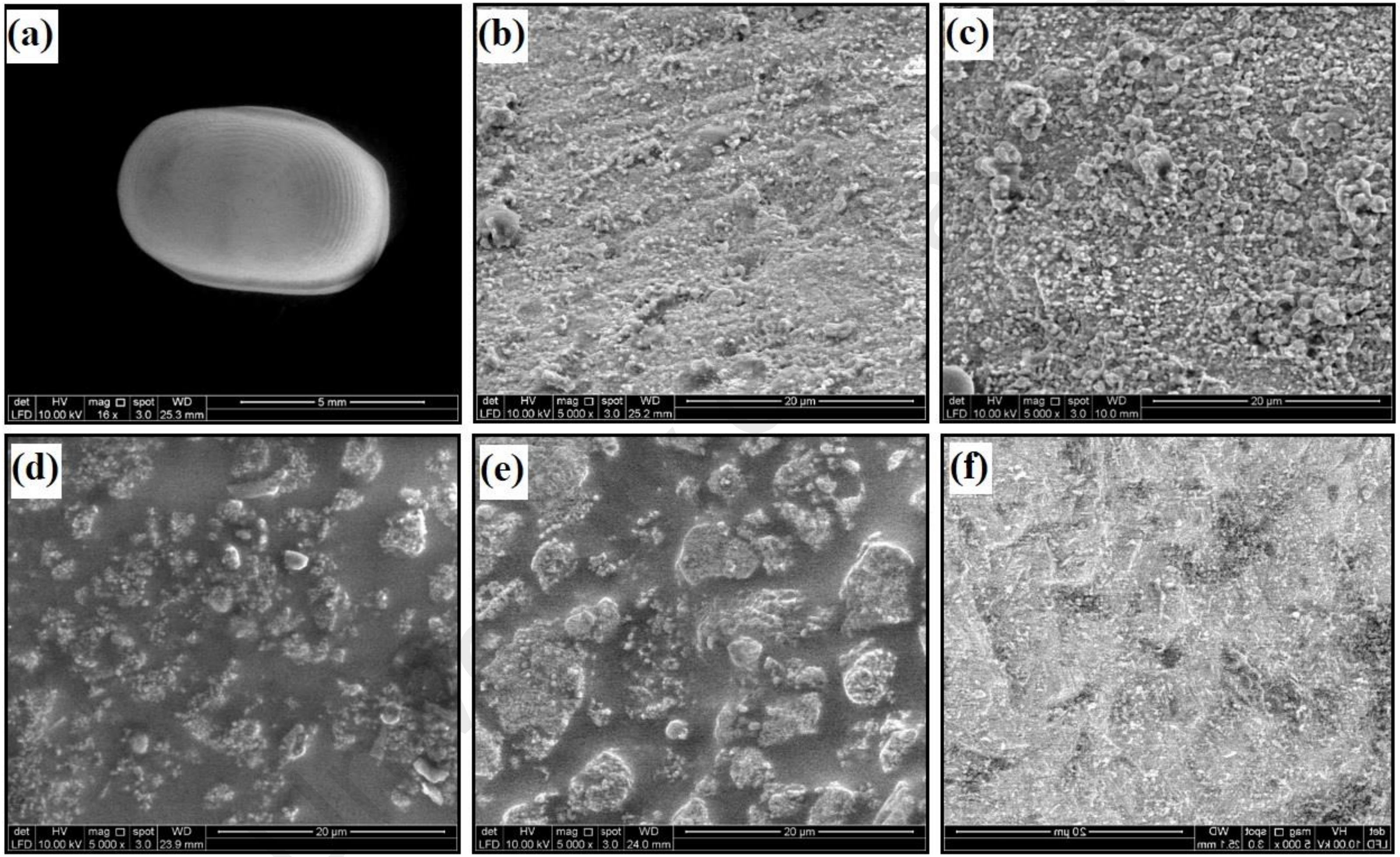

Figure 4.5: SEM images to analyse surface morphology. (a) Treated coping, (b) Coping coated with M1A, (c) Coping coated with M1B, (d) Coping coated with M2A, (e) Coping coated with M2B and (f) Coping treated with APA

A cross-section view of the coated specimens with M1 and M2 showed the homogeneity and uniform thickness as shown in Figure 4.6.

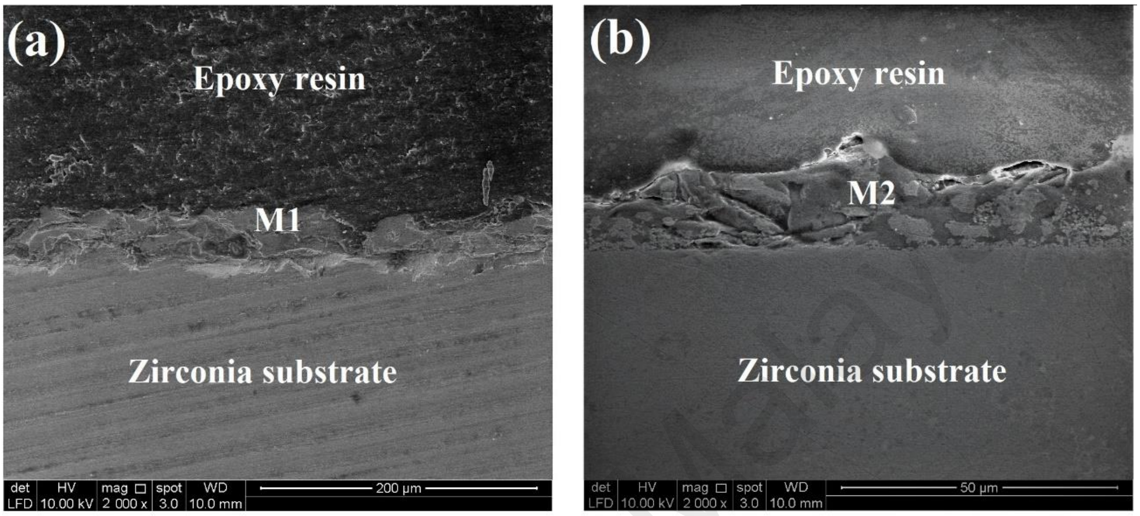

Figure 4.6: Cross-section SEM image of the coated zirconia specimens showed the homogeneity of the coating layer. (a) Coated with glaze zirconia mixture (M1) and (b) Coated with liner zirconia mixture (M2)

4.4 Surface elemental analysis

The results of the EDX analysis for tested zirconia discs and copings with various treatments are shown in Figure 4.7. The APA group showed the zirconium and aluminium elements which derived from alumina powder of the abrasion method and zirconia substrate. For the M1 groups; in addition to zirconium, the glaze porcelain elements were present as silicon, potassium, aluminium and barium while for the M2 groups, the zirconium element was seen with the liner ceramic elements including silicon, sodium, potassium and aluminium as showed in Table 4.2. These results revealed that the coating mixture components did not change after zirconia sintering at 1350 °C.

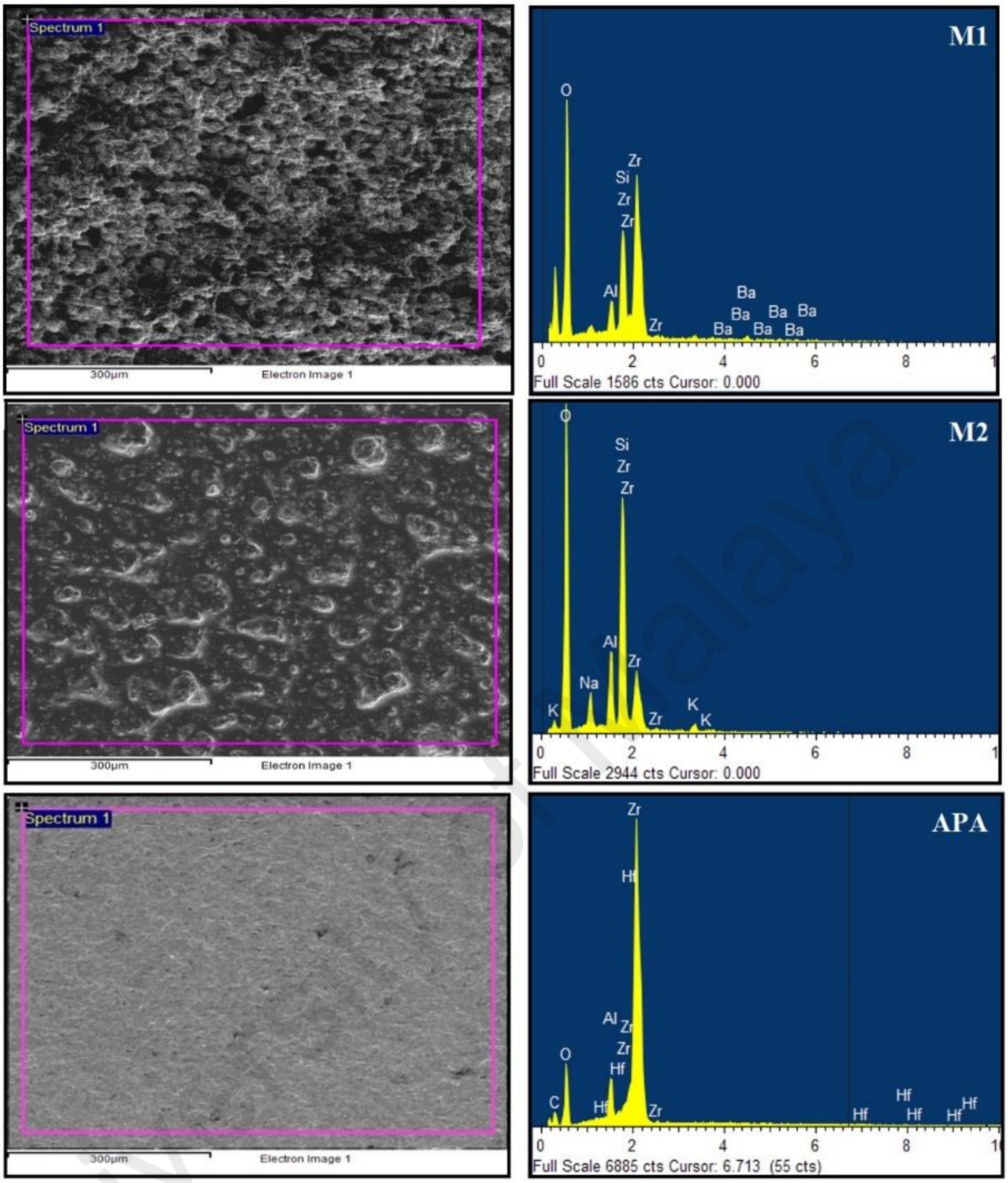

Figure 4.7: EDX results of zirconia disc specimens with different surface treatments; M1-zirconia glaze mixture; M2-zirconia liner mixture and APA-airborne particle abrasion

Table 4.2: Elements atomic percentage of different surface treatments. M1-zirconia glaze mixture; M2-zirconia liner mixture and APA-airborne particle abrasion

Elements	Atomic %		
	APA	M1	M2
Zr	90.83	54.67	50.29
Si	-	9.08	13.51
Al	9.17	7.86	3.86
Na	-	4.42	2.44
K	-	-	1.11
Ba	-	3.50	-

4.5 Phase change identification

The XRD patterns of the tested groups showed that the major peak of the *tetragonal* phase was seen at 30.57° corresponding to the crystallographic ICDD reference 014-0534. The *monoclinic* phase peaks were present at 28.47° corresponding to the crystallographic ICDD reference 002-0343. All coated specimens showed the presence of only the *tetragonal* phase in comparison to the APA specimens which exhibited both *monoclinic* and *tetragonal* phases as shown in Figure 4.8.

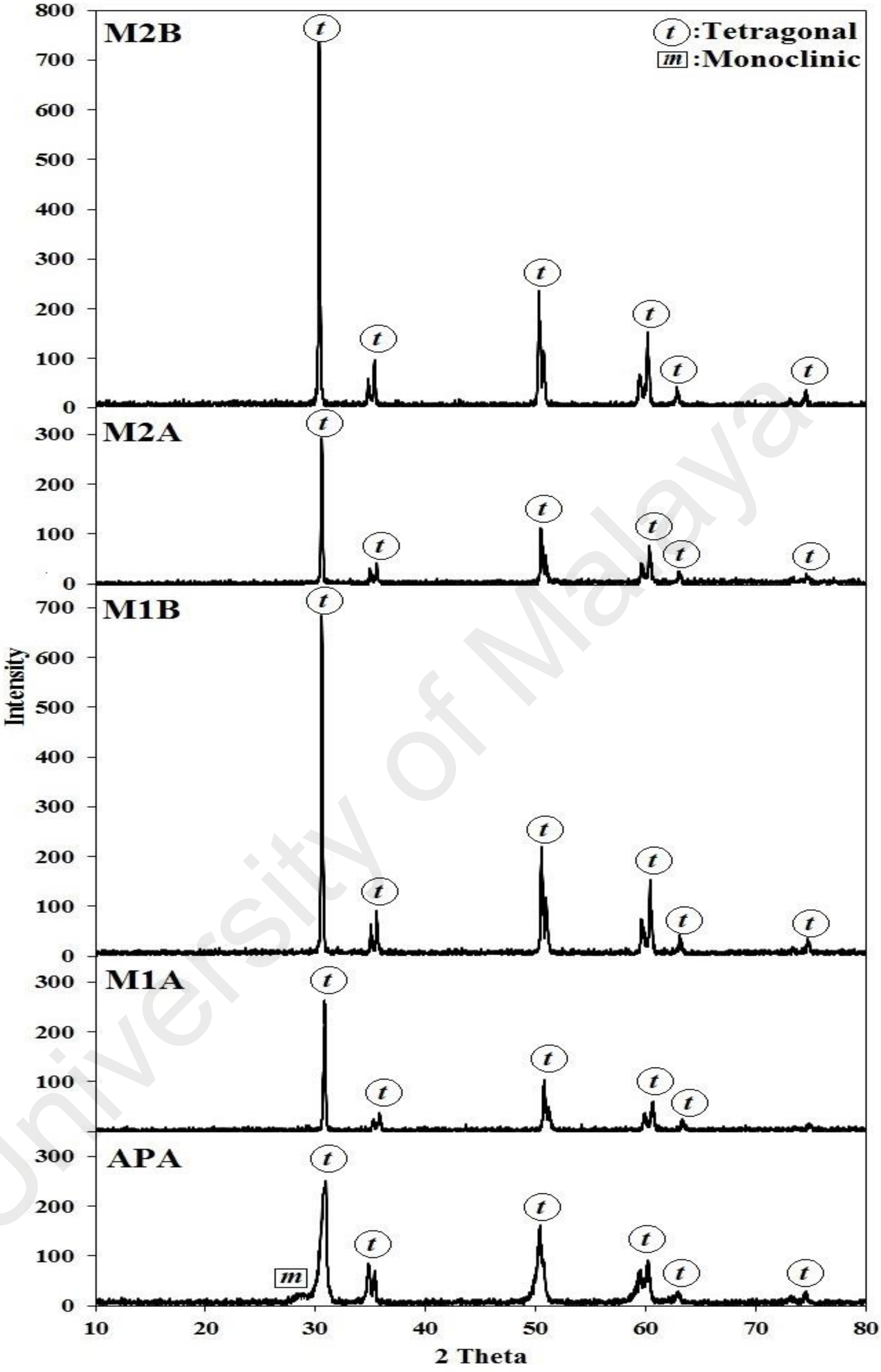

Figure 4.8: XRD analyses of all tested groups. M1A and M1B for specimens coated with two powder sizes of zirconia glaze mixture, M2A and M2B for specimens coated with two powder sizes of zirconia liner mixture and APA for specimens treated by airborne particle abrasion treatment

4.6 Coefficient of thermal expansion

The mean coefficient of thermal expansion values of coated and abraded surface treatment groups is listed Figure 4.9. The highest CTE values were seen in group M1A while the lowest value was observed in group APA. According to One-way ANOVA test, there was a significant difference between the tested groups (*P*<0.05). For coated groups, the Tukey HSD test showed there was a significant difference between groups M1A and other coated groups, except for M2A group that showed a non-significant difference as shown in Table 4.3.

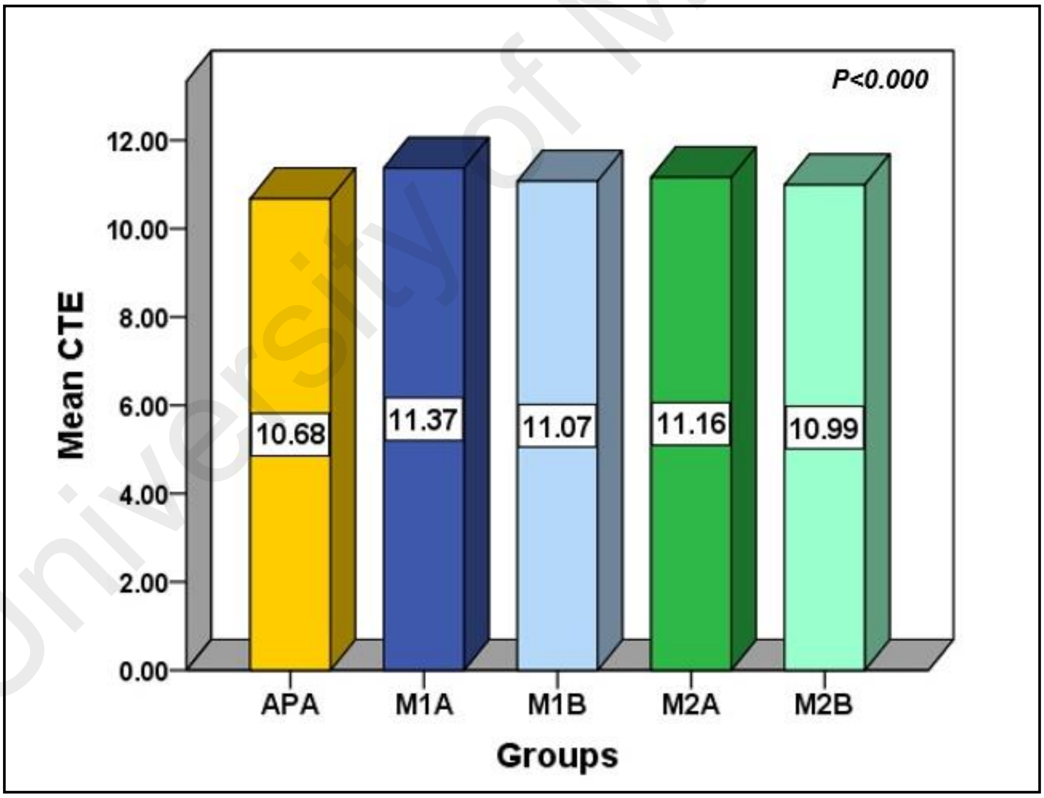

Figure 4.9: Coefficient of thermal expansion values in (×10^{-6} K^{-1}) for all tested groups. M1A and M1B for coated specimens by zirconia glaze mixture with sizes A and B. M2A and M2B for coated specimens with zirconia liner mixture with sizes A and B. APA for airborne particle abrasion specimens

Table 4.3: Multiple comparisons of the CTE values between the zirconia rod specimens with different surface treatments by Tukey HSD test. M1A and M1B for coated specimens by zirconia glaze mixture with sizes A and B. M2A and M2B for coated specimens with zirconia liner mixture with sizes A and B. APA for airborne particle abrasion specimens

(I) Group	(J) Group	Mean Difference (I-J) ($\times 10^{-6}$ K^{-1})	Sig.
APA	M1A*	-0.683	0.000
	M1B*	-0.396	0.002
	M2A*	-0.481	0.000
	M2B*	-0.313	0.024
M1A	M1B*	0.297	0.012
	M2A	0.212	0.230
	M2B*	0.380	0.004
M1B	M2A	-0.085	0.914
	M2B	0.083	0.920
M2A	M2B	-0.168	0.457
*Significance level at *P*<0.05			

4.7 Shear bond strength

The SBS results of the coated specimens showed higher values than the APA specimens. Statistically, the M1B group showed a significant difference than the other tested groups (*P*<0.05) as shown in Figure 4.10. The multiple comparisons by Tukey HSD test showed there was a significant difference of the M1B group compared with other groups. In addition, all coated groups, except the M1B group, showed a non significant difference between them as shown in Table 4.4.

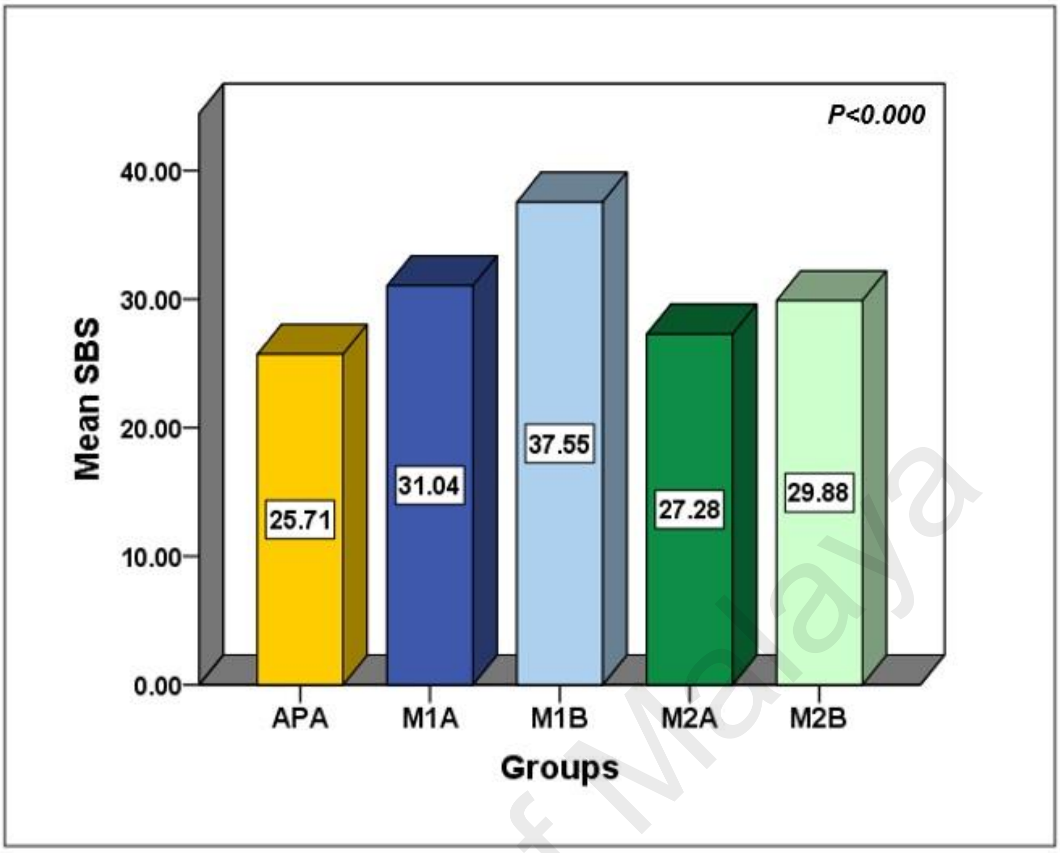

Figure 4.10: SBS mean in Megapascal (MPa) for all tested groups. M1A and M1B for coated specimens by zirconia glaze mixture with sizes A and B. M2A and M2B for coated specimens with zirconia liner mixture with sizes A and B. APA for airborne particle abrasion specimen

Table 4.4: Multiple comparisons of the SBS values between the zirconia specimens with different surface treatments by Tukey HSD test. M1A and M1B for coated specimens by zirconia glaze mixture with sizes A and B. M2A and M2B for coated specimens with zirconia liner mixture with sizes A and B. APA for airborne particle abrasion specimen

(I) Group	(J) Group	Mean Difference (I-J) (MPa)	Sig.
APA	M1A	-5.330	0.151
	M1B*	-11.836	0.000
	M2A	-1.568	0.958
	M2B	-4.171	0.368
M1A	M1B*	-6.506	0.048
	M2A	3.762	0.473
	M2B	1.159	0.986
M1B	M2A*	10.268	0.000
	M2B*	7.665	0.013
M2A	M2B	2.603	0.783
*Significance level at *P*<0.05			

4.8 Fractographic analysis for tested SBS

The fracture modes after the SBS test revealed that all tested groups showed a high percentage of mixed fracture mode. The cohesive fracture with high percentage was seen in group M1B 40%, while 20% for group M1A and 10% for M2B. APA group showed a higher percentage of adhesive fracture mode at 60%. All fracture modes ratios are displayed in Table 4.5 and Figure 4.11. The fracture mode morphologies were assessed by a stereomicroscope as shown in Figure 4.12. The EDX at the interface area of fracture specimens showed a higher percentage of elemental compositions of silicon (Si) which is the main element in the structure of veneering porcelain that was presented on the surface of the coated groups than APA group. This is an indication that there is good mechanical interlocking between the coated zirconia discs and the veneering porcelain as shown in Figure 4.13.

Table 4.5: Fracture modes percentage of SBS test for the specimens with different surface treatments. M1A and M1B for coated specimens by zirconia glaze mixture with sizes A and B. M2A and M2B for coated specimens with zirconia liner mixture with sizes A and B. APA for airborne particle abrasion specimens

Groups	N	Cohesive %	Mixed %	Adhesive %
APA	10	0	40	60
M1A	10	20	70	10
M1B	10	40	60	0
M2A	10	0	50	50
M2B	10	10	60	30

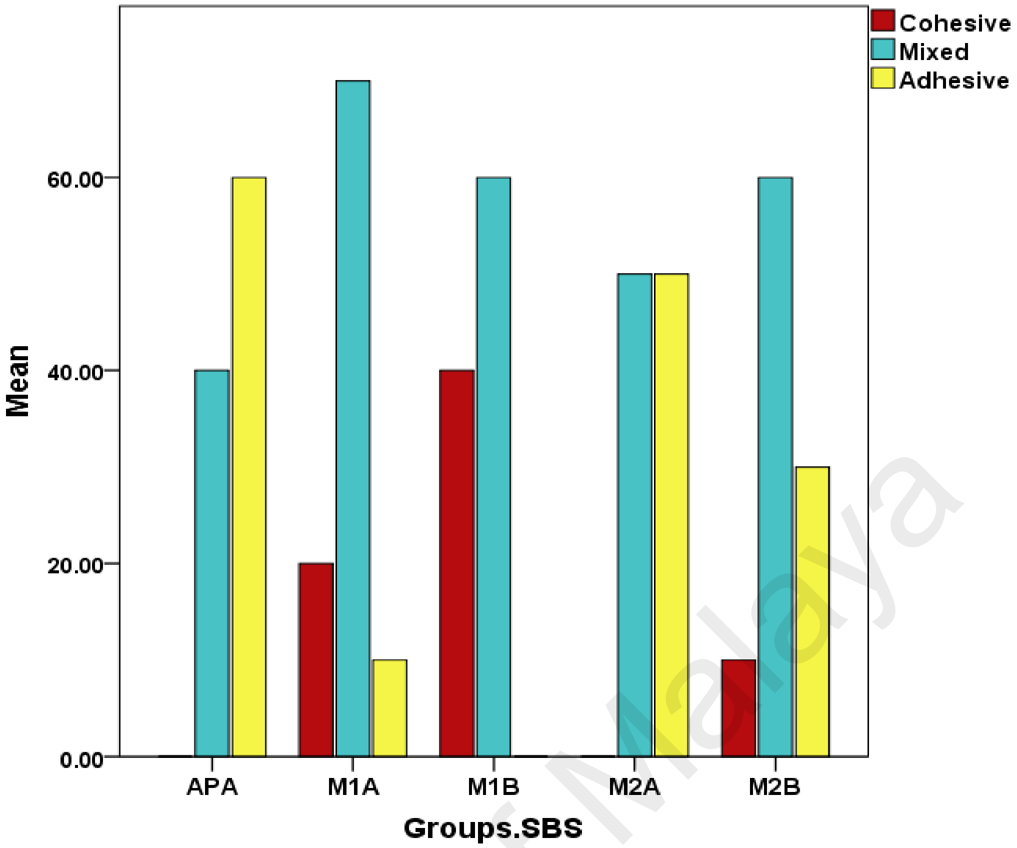

Figure 4.11: Fracture mode distribution of all tested groups with the shear bond test. M1A and M1B for coated specimens by zirconia glaze mixture with sizes A and B. M2A and M2B for coated specimens with zirconia liner mixture with sizes A and B. APA for airborne particle abrasion specimens

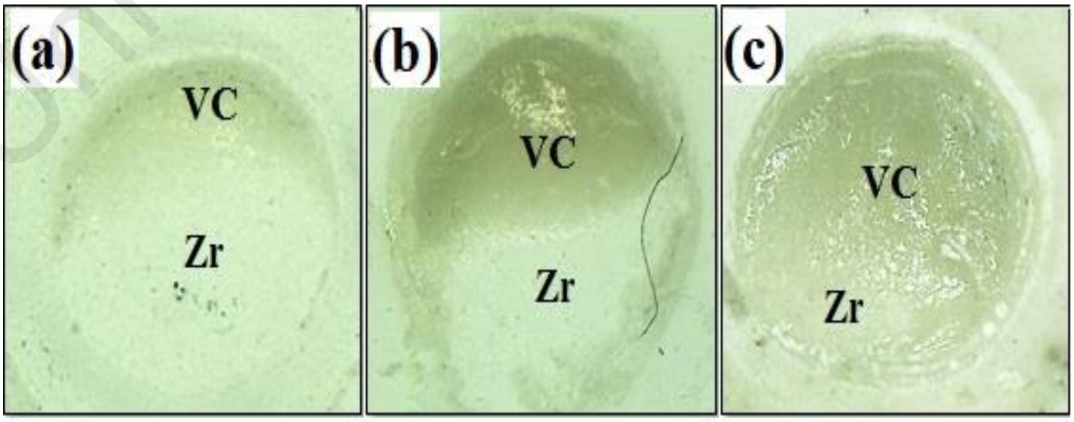

Figure 4.12: Fracture modes examined by a stereomicroscope of zirconia disc (Zr) and veneering ceramic (VC). (a) Adhesive mode, (b) Mixed mode and (c) Cohesive mode

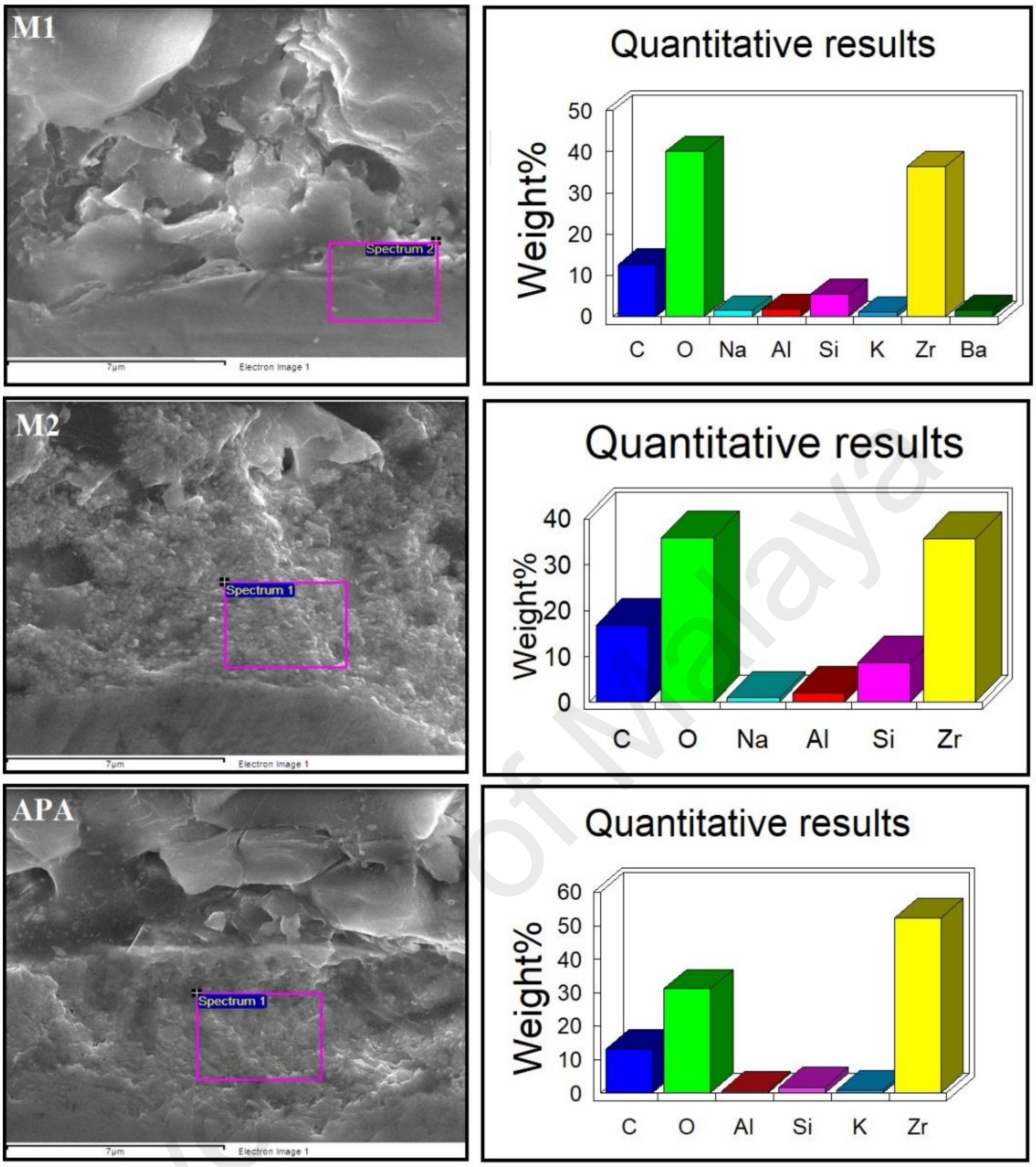

Figure 4.13: The EDX for interface areas after SBS test of different surface treatments. M1-for zirconia disc coated with zirconia glaze mixture, M2-for zirconia disc coated with zirconia liner mixture and APA-for zirconia disc treated with airborne particle abrasion

4.9 Fracture strength test assessment

The mean fracture strength values for the tested crowns revealed that the results significantly affected by the type of surface treatment, whereby the coated groups showed greater fracture strength than the APA group with significant difference ($P<0.05$) as shown in Figure 4.14. Moreover, the M1B group showed a significant difference with other tested groups except for M1A group as listed in Table 4.6.

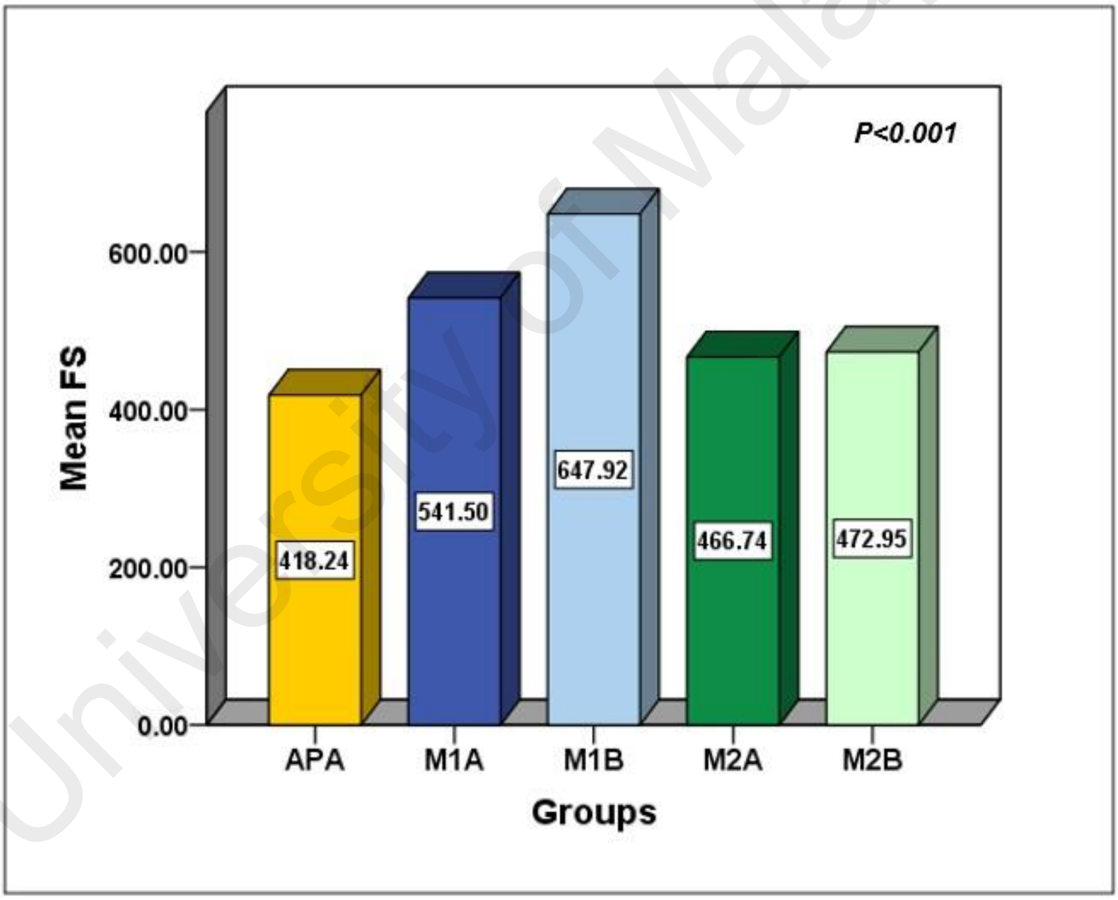

Figure 4.14: Fracture strength means in Newton (N) for all tested groups. M1A and M1B for coated specimens by zirconia glaze mixture with sizes A and B. M2A and M2B for coated specimens with zirconia liner mixture with sizes A and B. APA for airborne particle abrasion specimens

Table 4.6: Multiple comparisons of the fracture strength values between the zirconia specimens with different surface treatments by Tukey HSD test. M1A and M1B for coated specimens by zirconia glaze mixture with sizes A and B. M2A and M2B for coated specimens with zirconia liner mixture with sizes A and B. APA for airborne particle abrasion specimens

(I) Group	(J) Group	Mean Difference (I-J) N	Sig.
APA	M1A	-123.252	0.161
	M1B*	-229.678	0.001
	M2A	-48.499	0.892
	M2B	-54.708	0.843
M1A	M1B	-106.425	0.286
	M2A	74.752	0.631
	M2B	68.54	0.703
M1B	M2A*	181.178	0.012
	M2B*	174.969	0.017
M2A	M2B	-6.208	1.000
*Significance level at $P<0.05$			

4.10 Fracture modes for fracture strength test

The fracture modes observed under the stereomicroscope classified the tested specimens to adhesive, mixed and cohesive modes as shown in Figure 4.15. In the coated groups, the mixed mode was the most frequent failure observed while the adhesive mode was prominent in the APA crowns, as listed in Table 4.7 and Figure 4.16.

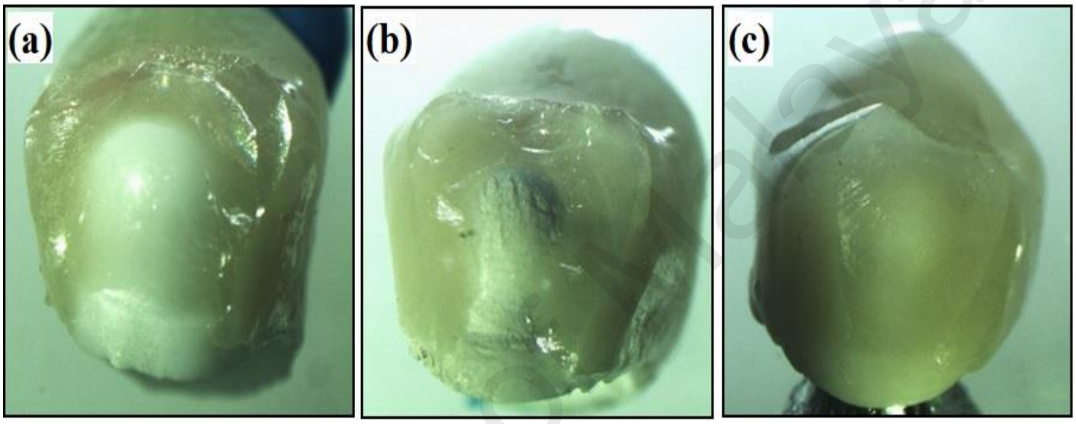

Figure 4.15: Stereomicroscope images showed fracture modes of tested zirconia crowns; (a) Adhesive mode, (b) Mixed mode and (c) Cohesive mode

Table 4.7: Fracture modes classification of the specimens tested by fracture strength test. M1A and M1B for coated specimens by zirconia glaze mixture with sizes A and B. M2A and M2B for coated specimens with zirconia liner mixture with sizes A and B. APA for airborne particle abrasion specimens

Groups	N	Cohesive	Mixed	Adhesive
APA	10	0	3	7
M1A	10	0	7	3
M1B	10	2	7	1
M2A	10	0	5	5
M2B	10	0	6	4

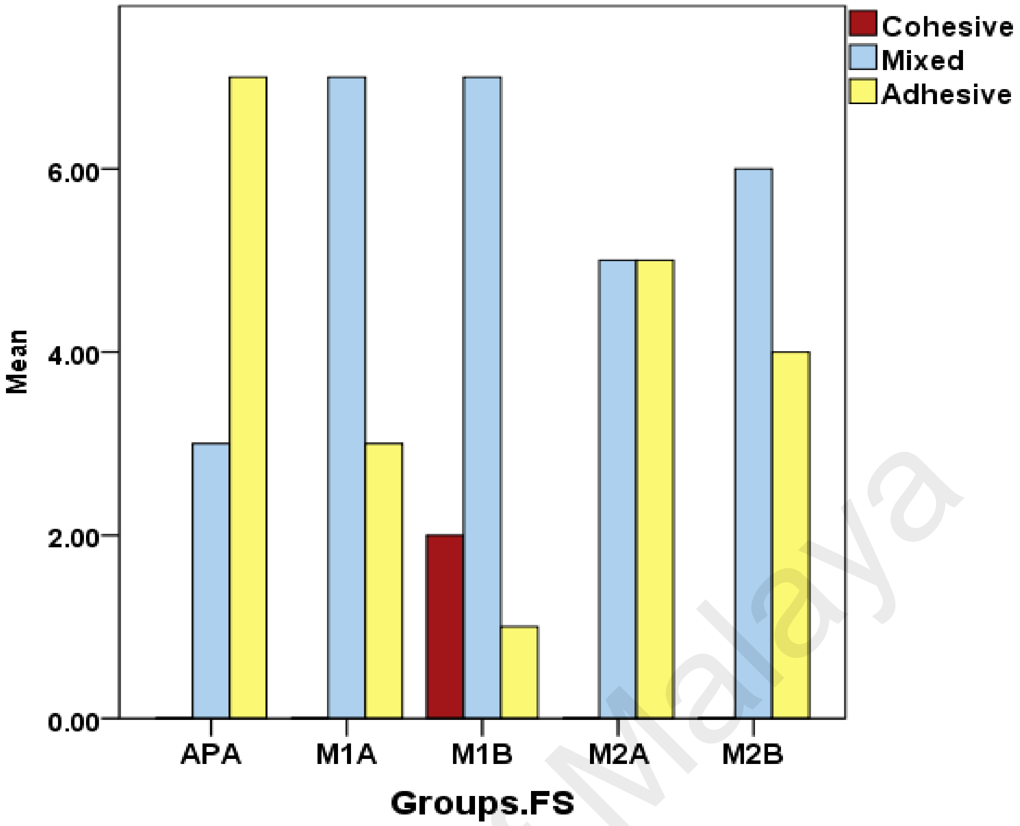

Figure 4.16: Fracture mode distribution of all tested groups with fracture strength test. M1A and M1B for coated specimens by zirconia glaze mixture with sizes A and B. M2A and M2B for coated specimens with zirconia liner mixture with sizes A and B. APA for airborne particle abrasion specimen

SEM images of the tested crowns with mixed fracture mode showed the site of the fracture initiation was the point of contact with loading device as shown in Figure 4.17. The high stress under the loading point probably lead to the crack initiation and propagating toward the cervical area and formed Hertzian cone crack which depends on the bonding of veneering porcelain to the zirconia coping. Wake hackle and arrested lines were detected around the pores in the veneering porcelain of all crowns, which could be utilised to determine the direction of the fracture path.

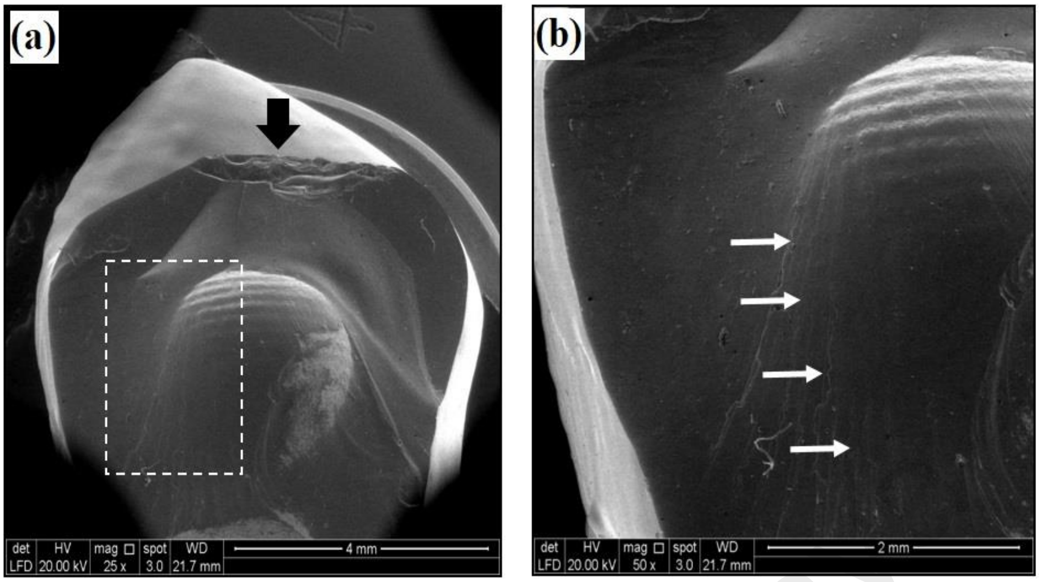

Figure 4.17: SEM image of fractured crowns with mixed fracture mode. (a) Black arrow represents the loading area and exposed coated coping and (b) White arrows represent a series of the arrested lines

4.11 FEA evaluation

4.11.1 Maximum stresses assessment

The FEA results showed that the high stress levels of oblique force on the veneering layer was at the area beneath the loading point in all models. The highest stress level was at the area below the force application point on the palatal side of the crown model and slightly decreased towards the inner parts (interface area, coping and prepared tooth model) and the lowest stress was at the root apex. The maximum von Mises stress value for ZG model was 580 MPa, while for the ZL model the value was 650 MPa and for the NC model was 832 MPa as shown in Figure 4.18, 4.19 and 4.20. According to these results, the ZG model showed the lowest value when compared with the ZL model and NC model.

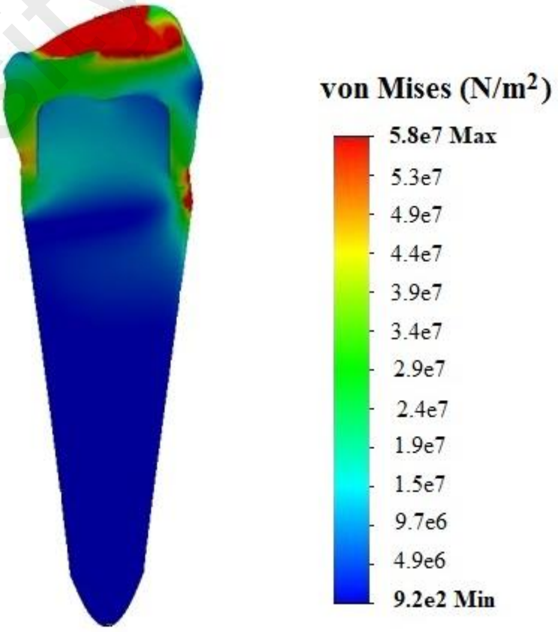

Figure 4.18: Von Mises stress level under the oblique load of zirconia glaze (ZG) model

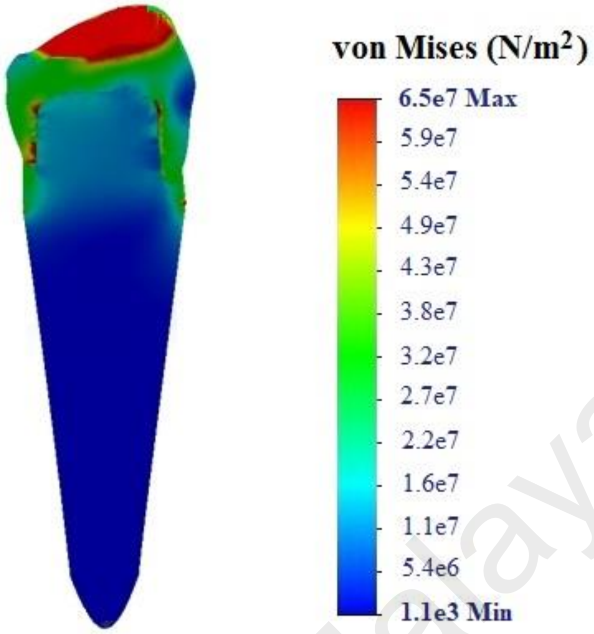

Figure 4.19: Von Mises stress level under the oblique load of zirconia liner (ZL) model

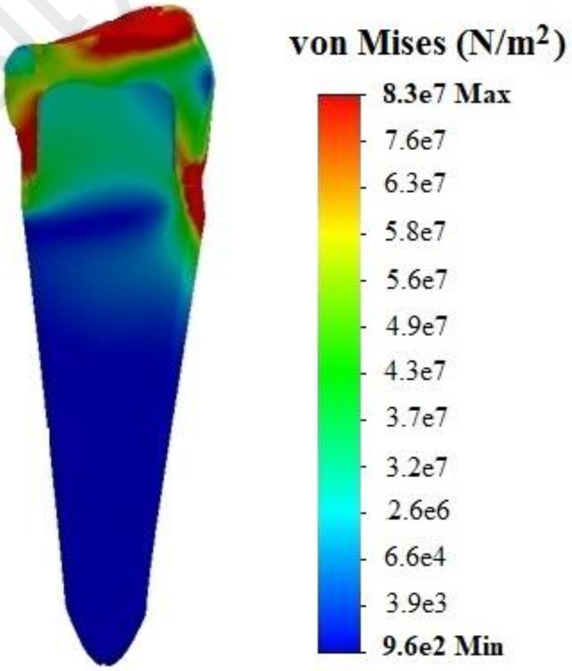

Figure 4.20: Von Mises stress level under the oblique load of non-coated model

4.11.2 Stress distribution analysis

The stress distribution patterns of the different crown models showed the propagation of maximum stress level from the location of oblique loading site on the occlusal surface of the veneering porcelain to the veneer/coping interface area, which then ends at the cervical area and inner side of crown toward the prepared tooth. The stresses were distributed evenly in the ZG model along the interface area as shown in Figure 4.21.

Furthermore, the propagation of stresses in ZL and NC models were localised in different degree at veneer/coping interface area as showed in Figure 4.22 and 4.23.

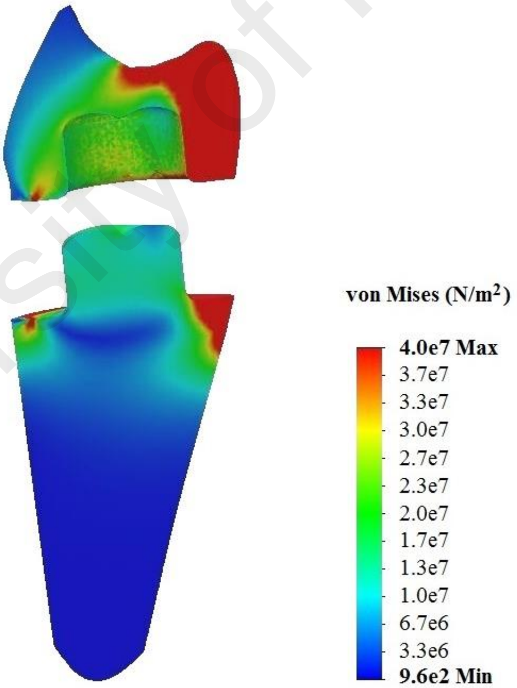

Figure 4.21: Stress distribution at interface area under the oblique load of treated zirconia glaze (ZG) model

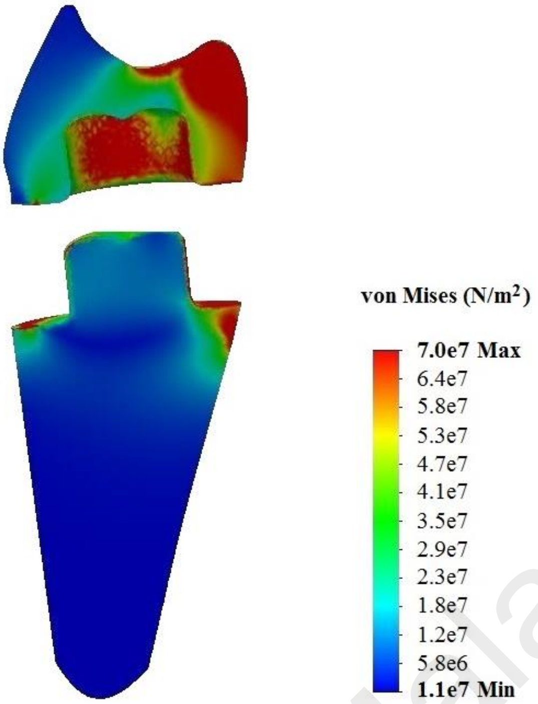

Figure 4.22: Stress distribution at interface area under the oblique load of treated zirconia liner (ZL) model

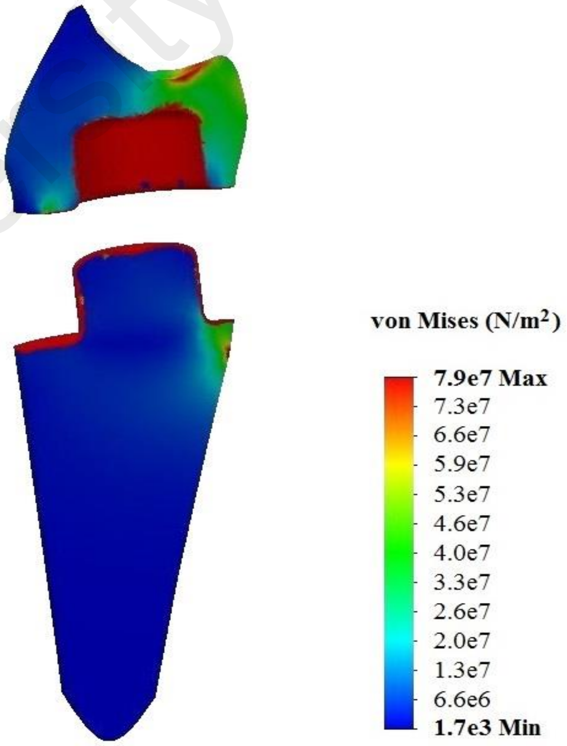

Figure 4.23: Stress distribution at interface area under the oblique load of model non-coated (NC) model

The distribution of the oblique stresses inside the coping of the crown models showed different values. For the ZG model, the stress value ranged from 200 to 260 MPa (Figure 4.21) while the stress values in ZL model ranged from 466 to 641 MPa (Figure 4.22) and for the NC stress level was recorded above 790 MPa (Figure 4.23) which is higher than both the ZG and ZL models.

On the other hand, the stresses subjected to the tooth preparation model was higher in the NC model compared to those of the other models (ZG and ZL), which caused damage to the tooth preparation.

CHAPTER 5: DISCUSSION

5.1 Preparation of zirconia coating powders

In the current study, partially sintered zirconia powder was prepared at 1100 ℃ from unsintered zirconia powder to produce coating powder with harder consistency and a stable tetragonal phase. The partially sintered zirconia powder created a higher surface roughness than the unsintered powder when applied on zirconia surface substrate. The partially sintered zirconia powder with two average particle sizes of 26 ± 0.3 µm and 47 ± 0.5 µm was selected according to a preliminary experiment. The size of less than 50 µm was selected because when using zirconia coating powder with particle sizes more than 50 µm will block the airbrush nozzle used in this study which was 50 µm in diameter and produced coating layer with greater thickness.

The smaller size powder (26 µm) was used as a fine particle size to compare with the coarser size powder (47 µm) because the use of particle size less than 20 µm leads to the production of a thin slurry which tended to accumulate at the end of the zirconia substrate border due to gravity force and air pressure, thereby forming a thin layer of coating at the central region. In addition, the finest particle size was assumed to create lower surface roughness and less affects on the mechanical properties such as shear bond and fracture strength tests when compared with the coarse and fine particle sizes. High surface roughness and its morphology are required for sufficient mechanical interlocking between zirconia substrate and veneering porcelain.

Moreover, the use of these two different particle sizes were to differentiate the current study from the previous study that used 3 µm zirconia coating powder which produces nanometer surface roughness (Teng et al., 2012), while in this study the particle sizes were increased to evaluate the effect of micrometre sizes on the surface roughness and the bonding strength between veneering porcelain and zirconia substrate.

The current study aimed to develop a new zirconia coating surface treatment with different particle sizes and evaluate their effects on the physical and mechanical properties of the various coated zirconia specimens (discs, rods and crowns) depending on the requirement of each test and compare them with the specimens treated by airborne particle abrasion (APA) as the control specimen.

The tested unsintered zirconia disc specimens were finished by platform polishing machine with grit silicon carbide paper to produce specimens with a standard surface form to apply different surface treatments. In order to control the standardised surface form, fixed parameters were used during polishing including; time, polishing plate speed and pressure.

5.2 Preparation of new zirconia coatings on the zirconia substrate

In order to avoid undesirable phase transition generated by APA, a thin layer of zirconia coating was applied using an airbrush spraying system. A mini airbrush instrument was used as a new spraying technique on the zirconia surface substrate. The advantages of these methods are it is easier to apply, simple and efficient to control the coating thickness. These advantages of airbrush spraying method were in agreement with several studies using the same method (Matyas & Caputo, 1982; Waetjen et al., 2009; Baino & Vitale-Brovarone, 2015) when compared with other techniques such as fine hand brush coating or magnetron sputtering deposition (Window, 1996; Kelly & Arnell, 2000).

The coating by hand brush has several problems, including difficulty to control coating thickness because of difficulty to standardise the amount of coating material carried by the brush and the pressure applied by the operator on the brush during coating procedure over zirconia surface substrate. The magnetron sputtering technique used on zirconia substrate coating needed a special complex equipment with an expensive target which was used as the coating material. It produced nano coating thickness and cannot coat the substrate with a complex shape (Kelly & Arnell, 2000).

The coating mixtures used in the present study included preparation of two micron-sized partially sintered zirconia powders (26 and 47 µm) that were mixed with glaze porcelain powder (M1) and ceramic liner paste (M2). The selected powders were mixed separately with two ceramic materials (glaze and liner) because these materials have already used as coating material for the zirconia-ceramic crown construction and their chemical compositions are similar to the composition of veneer ceramic as shown in Table 3.1, which may enhance the chemical bonding of zirconia substrate to the veneering porcelain (Wang et al., 2014).

The coating parameters used in the current study were selected according to the pilot study (Appendix B) which include mixing ratio, spraying pressure, dilution of the mixture, the distance of airbrush nozzle to the zirconia specimens and the total spray time. Based on this study, the coating thickness was easily controlled and provided a uniform surface roughness. The aim of the coating constituted three elements:

1. Zirconia substrate that used as core material for zirconia crown was in an unsintered state.
2. The coating mixtures were composed of partially sintered zirconia powders with two particle sizes which were mixed with glaze porcelain (M1) or ceramic liner (M2) that have the same chemical composition of veneering porcelain.

3. Coating procedure by airbrush spraying was used to precipitate the coating mixture on to the zirconia specimens (discs, rods and crowns) with uniform thickness and sufficient roughness.

The mixing ratio of the coating materials and dilution with pure ethanol have significant effect on the formation of coating slurry which was used in an airbrush. The mixing ratio with high dilution leads to the creation of a thin coating slurry with an inhomogeneous thickness on the zirconia substrate due to the gravity effect and air pressure of spraying made the slurry to collect at the end of the zirconia substrate and decrease the coating layer thickness at the central region. On the other hand, by decreasing the dilution of the high solid powder content of coating mixture was produced irregular and an uneven coating layer with elongated pores due to agglomeration of the mixed powders. Furthermore, this high solid agglomeration increases the risk of obstructive the nozzle of the spraying system.

The coated specimens after sintering at 1350 °C in a zirconia vacuum furnace which leads to the compact of zirconia powder to the zirconia substrate. Furthermore, the glass component of glaze and liner materials were overlapped on coated zirconia substrate as showed in the EDX results as shown in Figure 4.7 and this result agreed with Fouquier study (Fouquier, 2010).

The surface area roughness (S_a) of coated and control disc specimens were measured by a three-dimensional non-contact optical surface analyser microscope to avoid the possible risk of coating damage by analyser probe if contact surface method was used which, effects a final S_a result (Valíček et al., 2012). The specimens coated with zirconia glaze mixture (M1) and zirconia liner mixture (M2) showed higher S_a value than the APA specimens. The M1B group showed the highest roughness value than the other coated groups as shown in Figure 4.2. This is due to the presence of zirconia powder which depending on the particle size and the consistency of other mixture material (glaze and liner) which produce micro projections with various sizes over the coated surface that created microporosities and undercuts in different degrees as shown in Figure 4.4 and 4.5.

Even though the M1 group with size A and M2 with size A used a similar particle size (47 µm) of zirconia coating powder, but the results showed M1A group had higher roughness value (7.67 µm) than M2A (4.18 µm). This was probably attributed to the fact that the zirconia glaze mixture (M1A) is made up of a combination of two powders compared to the zirconia liner mixture (M2A) which is a powder and a paste. Moreover, the consistency of the ceramic liner paste may disturb the surface roughness by filling a portion of the micropores (valleys) and undercuts created by the coating mixture as stated by Kim et al. study (Kim et al., 2011).

The surface roughness value of the APA specimens is highly dependent on the increases of the abrasion parameters which include the size of the alumina particles, the duration of abrasion and air pressure (Kim et al., 2011; Nishigori et al., 2014). Nonetheless, the change of the abrasion parameters generates stress on zirconia surfaces and accelerates phase transformation from tetragonal (*t*) to monoclinic (*m*) due to an increase of collision forces applied by grit particles on the zirconia surface (Kosmac et al., 2000; Juy & Anglada, 2007). Subsequently, the phase change from *t* to *m* lead to volume expansion of zirconia substrate, which produced tensile stress on the veneering porcelain.

The surface morphology of coated specimens examined with SEM exhibited different surface roughness values. The specimens in M1A, M1B, M2A and M2B groups showed higher surface irregularities and deep undercuts formed from coating projections compared with the specimens of the APA group, which showed shallow irregularities without principal undercuts. Furthermore, a cross-sectional view of coated specimens by airbrush spray method showed a uniform thickness and homogeneity which was persistent with the regular surface roughness as shown in Figure 4.6.

Microscopic observations revealed that the partially sintered zirconia particle and glass particles from both liner and glaze materials may infiltrate to the zirconia surface (Yoon et al., 2014). The elemental analysis showed a diffusion of some components of the glaze and liner materials into the surface of the zirconia during sintering, as shown in Figure 4.7 and Table 4.2, which is in agreement with previous studies proposed by Aboushelib et al, 2006 and Fischer et al, 2008 (Aboushelib et al., 2006; Fischer et al., 2008). For the APA group, there is a small amount of aluminium oxide over the zirconia surface resulting from blasting procedure.

The structural phase changes analysed by x-ray diffraction (XRD), indicated only the *tetragonal* phase in all coated groups (M1A, M1B, M2A and M2B) compared to the APA specimens which exhibited both *monoclinic* and *tetragonal* phases as shown in Figure 4.8. This may be due to the presence of zirconia coated powder with *tetragonal* phase. The XRD results of the current study agree with the previously mentioned studies related to the presence of the *monoclinic* phase in the APA group.

According to Kim et al., (2011) and Kosmač et al., (2008) studies, the APA was unfavourable for achieving effective bond strength because of the mechanical stresses generated on zirconia surface produced by the shooting force of the APA treatment which leads to the phase transition from *tetragonal* to *monoclinic* (Kosmač et al., 2008; Kim et al., 2011). This phase transition accompanied by a volume expansion of about 3–5% results in compressive stress on the veneer ceramic and induces crack propagation at core/veneer interface (Moon et al., 2011).

5.3 Mechanical properties of coated and APA specimens

The coated groups in this study showed a higher coefficient of thermal expansion (CTE) than the APA group as shown in Figure 4.9. This might be due to the stability of the tetragonal phase (Hallmann et al., 2014) which has been identified by the XRD analysis as showed in Figure 4.8. The increase in CTE in the coated zirconia specimens caused the veneering porcelain to be in a beneficial state of residual compressive stress and this was in agreement with the studies by Hallman et al, (2014) and Craig et al, (2004) which proposed that the difference in the coefficients of thermal expansion between the ceramic framework and the veneer ceramic was significantly influenced the stability of the tetragonal phase of zirconia-ceramic and a slightly higher CTE (Craig et al., 2004; Hallmann et al., 2014).

There are several tests used to measure the bond strength of all-ceramic restoration and there is no standardised method because the zirconia restoration is composed of a multilayer system. In general, it is important to evaluate the actual bonding strength of the interface area between the core material and veneering porcelain. This should be done under stress to record the real results of debonding between materials during the test (Komine et al., 2012). These tests include; the biaxial flexure strength (Yilmaz et al., 2007), three/four point flexure strength (White et al., 2005), microtensile bond strength (Aboushelib et al., 2005), and shear bond strength (Al-Dohan et al., 2004).

Mosharraf et al., (2011) utilised the shear bond test to evaluate the effect of surface treatments and zirconia types on the bond strength between zirconia and veneering porcelain (Mosharraf et al., 2011). Fischer et al., (2009) used the SBS test to evaluate the effect of coefficient of thermal expansion misfit on the shear strength between zirconia and veneering porcelain (Fischer et al., 2009).

The shear bond strength values in the current study showed that all the coated groups had higher strength values than the APA group and there was a significant difference ($P<0.05$) between all the groups. This can be attributed to the increase in the surface roughness of the coated specimens compared to the APA specimens, which enhanced micromechanical interlocking and improved bonding strength between zirconia substrate and veneer ceramic (Farhan et al., 2017). The M1B specimens had the highest strength value (37.05 ± 3.34 MPa) because it has the highest S_a value than the other tested groups as shown in Figure 4.10. Furthermore, the absence of residual stresses on the veneering porcelain of coated specimens leads to decrease in susceptibility to crack and fracture.

EDX analysis indicated that there were no elemental changes in the coating mixture after the sintering process. As shown in Table 3.1, the chemical composition of the glaze porcelain and ceramic liner were similar to the chemical composition of veneering porcelain. Wang et al (2014), proposed that when the chemical compositions of the liner material are similar to the veneering porcelain, consequently the mechanical properties are similar too. This may be the reason for a stronger chemical bond with the veneer ceramic compared to its bond with the zirconia core (Wang et al., 2014). Consequently, this chemical bond of zirconia coatings with the veneering porcelain may be the reason for the increase in bond strength values of the coated specimens.

The fracture strength results of the present study revealed that the coated groups possessed a higher value than the APA group and the M1B group showed the highest strength value among coated groups as shown in Figure 4.14. Although its fracture strength value was not statistically different from that M1A group as showed in Table 4.6. This is probably due to a high mechanical interlocking at coping/veneer interface as a result of increased surface roughness produced by coarse particles of the zirconia powder in the M1B group. Moreover, the M1 coating was made of a combination of two ceramic powders rather than a powder/paste mixture in M2 coating.

5.4 Fractographic study

Fracture analysis by light microscopy and SEM is a useful method for determining the fracture mechanism of tested fractured specimens (Moeser, 2007; Øilo & Gjerdet, 2013). The current study presents a fracture analysis of both shear bond strength and fracture strength tests which composed of the multilayer system. The fracture analysis of these *in vitro* tests revealed that the fractures initiated at the load applied point of the device, for SBS specimens at the zirconia disc/veneer interface while for crown specimens at the occlusal surface.

Fracture mode classifications into cohesive, adhesive and mixed were consistent with previous studies using the SBS test (Everson et al., 2012; Naji et al., 2017). In the present study, the failure mode percentages of the SBS tested specimens were categorized by using a stereomicroscope and SEM, which exhibited different percentages as shown in Table 4.5. The cohesive mode represented a strong bond between core and veneer ceramic. The M1B group revealed a higher percentage (40%) than the other tested groups. For other coated groups, the cohesive mode was exhibited in the M1A group (20%) and in the M2B group (10%), and this can be supported by the fact that when the surface becomes rougher, the bond strength increased (Fischer Jens et al., 2008). The higher surface roughness could also increase the number of surface defects. This defects could be points for stress concentration which could lead to crack initiation. Interestingly, a high percentage of the adhesive mode of fracture obtained for both APA and M2A groups were 60% and 50% respectively, due to the lower roughness values. The mixed mode of fracture was presented in a high percentage of all tested groups, as a main fractographic result.

The fractographic classification of fractured crowns of all tested groups (Figure 4.13) showed the dominance of mixed failure mode (70%) in the M1B group, followed by cohesive (20%) and adhesive (10%) modes as shown in Table 4.7. The cohesive mode referred to the fractures that occurred in the bulk of the veneering porcelain layer, which indicates a high interlocking between zirconia coping and the veneering porcelain. When a finer particle size was used, the cohesive failure was not observed even though the mixed failure was still the most frequent failure mode (70%). On the other hand, the mixed and adhesive modes were the most observed failures in the M1A and M1B groups with almost similar frequencies, and independent of the coating particle size. In contrast, adhesive (70%) and mixed modes were the prominent failures found in the specimens with APA surface treatment.

The high stress at the loading point in fracture strength test probably lead to initiation and propagating of Hertzian cone crack that represents the expanding path of a fracture in a cone shape from point of contact which depends on the degree of bonding between the veneering porcelain and the zirconia coping. Wake hackle and arrested lines were detected around the pores in the veneering porcelain of all the crowns (Figure 4.17), which could be utilised to determine the direction of the fracture path.

5.5 Finite element analysis (FEA)

Stresses on the dental restoration structures are generated when bite force is applied during the masticatory function. In order to understand the performance of the restoration, especially when stresses become extreme and exceed the elastic limit of restoration materials, failure may occur (Raposo et al., 2012). These stresses cannot be directly measured and it is not easy to understand why and when a failure process is initiated in the structures of the restoration. Therefore, the application of engineering information in dentistry by using computational techniques such as finite element analysis (FEA) has assisted in understanding dental restoration biomechanics features (Li et al., 2011). The main advantage of FEA is to expect the biomechanical problems which are exhibited throughout the structure of the restoration by calculating stresses at every point and predict possible failure causes of future restorations constructed by FEA modelling.

In this study, three copings FEA models of the zirconia-ceramic crown with different surface treatments were constructed; non-coated (model NC), zirconia glaze coated (model ZG), and zirconia liner coated (model ZL). The existing FEA study used a static load simulation of 200 N (Hu et al., 2013) which applied on an area of 2.5 mm^2 of the occlusal surface on the palatal cusp of the crown model at an oblique angle of 45° to the tooth axis because this angle simulate a mastication load (Hu et al., 2013; Abdulmunem et al., 2016). The fracture possibility of the zirconia-ceramic restorations with the coating and the non-coating layer was determined by computing the maximum stress level and distributions through the layers of the crown model. The force applied to a node or an element upon the area of the occlusal surface of the crown is predicted to resemble the occlusal stress during mastication.

According to several studies, the high rate failures of fixed dental restorations used zirconia-ceramic restoration is caused by tensile stress which is produced at this angle. In general, the stress distributions pattern on all FEA models were easily distinguished with this angle (Imanishi et al., 2003; Rezaei et al., 2011; Abduljabbar et al., 2012; Al-Maqtari et al., 2013; Abdulmunem et al., 2016).

Finite element analyses have shown higher tensile stress in the area underneath the loading device than in the cervical areas, and this is consistent with the current fracture strength findings. The maximum von Mises stress value for the ZG model was 580 MPa, while for the ZL model the value was 650 MPa and for the NC model was 832 MPa as shown in Figure 4.18, 4.19 and 4.20. According to these results, the ZG model showed the lowest value when compared with the ZL model and the NC model.

According to the results of the three FEA models in the current study, a higher stress level showed in the NC model may lead to increased veneering layer chipping due to lower bonding strength between zirconia coping and veneering porcelain. On the other hand, the low stress level on the ZG model and the ZL model resulted in high bond strength between the zirconia coping and the veneering porcelain. According to previous *in vitro* findings, decrease in the incidence of veneering layer chipping related to decreased stress on veneering layer (Lin et al., 2012).

The tensile stresses occurred at the outer surface of the loading site and on the inner surface of the veneer/core interface. The stress distribution patterns propagated from the location of oblique loading site on the occlusal surface of the veneering porcelain to the veneer/coping interface area, which then ends at the cervical area and inner side of crown toward the prepared tooth. The stress at the interface area in the model ZG was evenly distributed (Figure 4.21) while the ZL and NC models showed an unevenly stress accumulated at different parts of the interface as shown in Figure 4.22 and 4.23. This localised stress may facilitate crack initiation at coping/veneer interface area during mastication and propagate towards the veneering layer, resulting in catastrophic failure or fracture.

The distribution of the oblique stresses level at the inner side of the zirconia coping of the crown models showed a different stress level, which indicated the growth of tensile stresses at an interface area. For the ZG model, the stress value ranged from 200 to 260 MPa (Figure 4.18) while values increased in ZL model from 466 to 641 MPa (Figure 4.19) and for the NC, the level was higher than in the ZL model to record above 790 MPa (Figure 4.20). According to these results, the location of the high stress at the zirconia coping could affect the tooth preparation supported crown and may cause further trauma to the restored tooth. This finding agreed with the numerous studies on dental crown fractures conducted by other investigators (Al-Maqtari et al., 2013; Hu et al., 2013).

5.6 Clinical significant of zirconia coatings

The normal chewing force applied on the human teeth ranged from 300 N in premolar region and 350 N in the molar region (Julien et al., 1996; Al-Makramani et al., 2010). Zirconia-ceramic restorations fabricated from multilayer structures comprised of an aesthetic veneering porcelain over a high strength coping which tolerate the chewing force. The coping/veneer bond strength generally is essential to improve the clinical performance of zirconia crown by providing sufficient strength to withstand cyclic loading applied in the oral environment during food mastication (Aboushelib et al., 2005). According to the clinical follow-up studies, the veneering porcelain chipping over zirconia coping become one of the main causes of failure of zirconia-ceramic restorations compared with the metal-ceramic restorations (Sailer et al., 2009a; Raigrodski et al., 2012).

In general, the bonding between the zirconia substrate and veneering porcelain was affected by two main factors; (1) the interfacial bonding between the coping and veneer materials at the interface area. The lack of chemical bond, poor wettability and insufficient mechanical interlocking due to insufficient surface roughness may cause lower core/veneer bond strength (Guazzato et al., 2004; Aboushelib et al., 2006) and (2) zirconia core and veneering porcelain physical properties mismatch. The coefficient of thermal expansion (CTE) mismatch induces thermal residual stresses after cooling from the preparation temperature of two materials which may generate excessive stresses on veneering porcelain (Komine et al., 2010). In addition, the phase changes from *t* to *m* generates residual stresses on the veneering layer which induces fracture possibility.

However, the weakest characteristics of the zirconia-ceramic restorations are the bonding between the zirconia core and veneering porcelain at an interface area. Consequently, improvement of the bonding in this area is essential to increase the clinical success rate of zirconia restorations (Özkurt & Kazazoğlu, 2010). Surface treatments on the zirconia substrate prior to veneering, play an important role in enhancing the bond strength and durability by converting a non-retentive surface to a retentive one. Surface preparation is considered as one of the important parameters which are directly related to the material properties and surface elements to bond to other materials (Ghumatkar et al., 2016).

The new zirconia surface coating using airbrush technique is a promising surface treatment to obtain a rougher surface which subsequently improves the bond strength of the veneer ceramic without phase changes. Furthermore, this treatment is applicable for zirconia copings for zirconia-ceramic crowns and fixed bridges which enhances the clinical performance and increases the success rate.

CHAPTER 6: CONCLUSION

6.1 Conclusion

With the limitation of the study the following conclusion was drawn:

1. A new zirconia surface coatings with two particle sizes (fine and coarse) were successfully treating the zirconia surface without causing flaws and any phase transformation using spraying technique to control the coating thickness and homogeneity.

2. The surface area roughness of coated specimens with coarse particle was higher than air born particle abrasion (APA) with prominent irregularities and undercuts. Phase identification showed only tetragonal phase in coated specimens while both tetragonal and monoclinic in APA specimens.

3. All coated zirconia specimens showed the higher coefficient of thermal expansion values than APA specimens due to phase stability.

4. The coated specimens with M1B mixture showed a significant increase in shear bond strength (SBS) values than other coated mixture and APA specimens.

5. The fracture strength (FS) values of coated crowns with M1B mixture was significantly higher than other tested crowns.

6. The fractographic analysis of tested SBS specimens indicated that the cohesive mode with a high percentage (40%) was in group M1B and adhesive mode with a high percentage (60%) in group APA. For tested FS specimens, all coated showed a mixed mode with cohesive mode only in group M1B. The adhesive mode was prominent in the APA group.

7. FEA showed the maximum stress level of model ZG was less and distributed evenly at interface area compared to localized stresses in ZL and NC models.

6.2 Limitations of the study

1. Using different CAD/CAM systems to compare the effect of new zirconia coatings on the veneering bonding because it is costly and not all systems used unsintered zirconia substrate.

2. The effects of thermomechanical conditions on the bond quality of coated zirconia substrate to the veneering porcelain were not evaluated because the sample sizes will increase and need more time.

6.3 Recommendations for further studies

1. The effect of zirconia coatings on the bonding strength between zirconia substrate and different veneering porcelain materials.
2. The influence of using different sintering temperature of veneering porcelain on the bonding strength with the coated zirconia substrate.
3. The fatigue failure under cyclic loading to simulate the clinical performance of the coated zirconia-ceramic crown.
4. The effect of the surface and mechanical properties by the airbrush spray technique and compare with another technique.
5. The clinical trial study of coated zirconia-ceramic crowns.

REFERENCES

Abduljabbar, T., Sherfudhin, H., AlSaleh, S., Al-Helal, A. A., Al-Orini, S. S., Al-Aql, N. A. (2012). Fracture resistance of three post and core systems in endodontically treated teeth restored with all-ceramic crowns. *King Saudi University Journal of Dental Sciences, 3*(1), 33-38.

Abdulmunem, M., Dabbagh, A., Naderi, S., Zadeh, M. T., Halim, N. F. A., Khan, S., Abdullah, H., Kasim, N. H. A. (2016). Evaluation of the effect of dental cements on fracture resistance and fracture mode of teeth restored with various dental posts: A finite element analysis. *Journal of the European Ceramic Society, 36*(9), 2213-2221.

Aboushelib, M. N., De Jager, N., Kleverlaan, C. J., Feilzer, A. J. (2005). Microtensile bond strength of different components of core veneered all-ceramic restorations. *Dental Materials, 21*(10), 984-991.

Aboushelib, M. N., Kleverlaan, C. J., Feilzer, A. J. (2006). Microtensile bond strength of different components of core veneered all-ceramic restorations: Part II: Zirconia veneering ceramics. *Dental Materials, 22*(9), 857-863.

Aboushelib, M. N., Kleverlaan, C. J., Feilzer, A. J. (2007). Selective infiltration-etching technique for a strong and durable bond of resin cements to zirconia-based materials. *Journal of Prosthetic Dentistry, 98*(5), 379-388.

Aboushelib, M. N., Kleverlaan, C. J., Feilzer, A. J. (2008). Effect of zirconia type on its bond strength with different veneer ceramics. *Journal of Prosthodontics, 17*(5), 401-408.

Al-Dohan, H. M., Yaman, P., Dennison, J. B., Razzoog, M. E., Lang, B. R. (2004). Shear strength of core-veneer interface in bi-layered ceramics. *Journal of Prosthetic Dentistry, 91*(4), 349-355.

Al-Makramani, B. M. A., Razak, A. A. A., Abu-Hassan, M. I. (2010). Biaxial flexural strength of Turkom-Cera core compared to two other all-ceramic systems. *Journal of Applied Oral Science, 18*(6), 607-612.

Al-Maqtari, A. A., Razak, A. A. A., Hamdi, M. (2013). 3D Finite element analysis of functionally graded multilayered dental ceramic cores. *Dental Materials Journal, 33*(4), 458-465.

Al-Sanabani, F. A., Madfa, A. A., Al-Qudaimi, N. H. (2014). Alumina ceramic for dental applications: a review article. *American Journal of Material Research, 1*(1), 26-34.

AL-Makramani, B., Razak, A. A., Abu-Hassan, M. I. (2009). Comparison of the Load at Fracture of Turkom-Cera to Procera AllCeram and In-Ceram All-Ceramic Restorations. *Journal of Prosthodontics, 18*(6), 484-488.

Allahkarami, M. (2012). *X-ray diffraction analysis of residual stress in zirconia dental composites*: (Doctoral dissertation), Oklahoma State University.

Alsulami, U. E. N. (2014). *Influence of the coefficient of thermal expansion mismatch on the bond strength of bi-layered all ceramic system.* (Doctoral dissertation), Universität Tübingen.

Altamimi, A. M., Tripodakis, A. P. D., Eliades, G., Hirayama, H. (2014). Comparison of fracture resistance and fracture characterization of bilayered zirconia/fluorapatite and monolithic lithium disilicate all ceramic crowns. *International Journal of Esthetic Dentistry, 9*(1), 98-110.

Anderson, J., Leaver, K., Rawlings, R., Alexander, J. (1990). Mechanical properties. *In Materials Science* (pp. 181-244): Springer.

Andersson, M., Odén, A. (1993). A new all-ceramic crown: a dense-sintered, high-purity alumina coping with porcelain. *Acta Odontologica, 51*(1), 59-64.

Antonson, S. A., Anusavice, K. J. (2001). Contrast ratio of veneering and core ceramics as a function of thickness. *International Journal of Prosthodontics, 14*(4), 316-320.

Anusavice, K. J. (1996). Dental Ceramics. In: Anusavie KJ, ed. *Phillips' science of dental materials. (10th ed., pp583-618).* Philadelphia : WB Saunders.

Anusavice, K. J. (2003). Physical properties of dental materials. *Phillips' science of dental materials,* (11th ed. pp. 655-719). St. Louis, MO: Elsevier Saunders Co.

Anusavice, K. J. (2012). Standardizing failure, success, and survival decisions in clinical studies of ceramic and metal–ceramic fixed dental prostheses. *Dental Materials, 28*(1), 102-111.

Anusavice, K. J., Shen, C., Rawls, H. R. (2013). *Phillips' science of dental materials, (12th ed., pp.418-473). St. Louis, MO: Elsevier Saunders Co.*

Arami, S., Tabatabae, M. H., Namdar, S. F., Chiniforush, N. (2014). Effects of different lasers and particle abrasion on surface characteristics of zirconia ceramics. *Journal of Dentistry, 11*(2), 233.

Asgar, K. (1988). Casting metals in dentistry: past-present-future. *Advances in Dental Research, 2*(1), 33-43.

ASTM, E. (2003). 831-03. Standard test method for linear thermal expansion of solid materials by thermomechanical analysis. *ASTM International*.

Ausiello, P., Franciosa, P., Martorelli, M., Watts, D. C. (2011). *Mechanical behavior of post-restored upper canine teeth: A 3D FE Analysis.* (27).

Ausiello, P., Franciosa, P., Martorelli, M., Watts, D. C. (2011). Mechanical behavior of post-restored upper canine teeth: a 3D FE analysis. *Dental Materials, 27*(12), 1285-1294.

Bailer, W., 2006. Writing ImageJ Plugins–A Tutorial. Upper Austria University of Applied Sciences Dept. of Media Technology and Design Hagenberg, Austria (pp. 34-36).

Baino, F., Vitale-Brovarone, C. (2015). Feasibility of glass–ceramic coatings on alumina prosthetic implants by airbrush spraying method. *Ceramics International, 41*(2), 2150-2159.

Beckhoff, B., Kanngießer, B., Langhoff, N., Wedell, R., Wolff, H. (2007). *Handbook of practical X-ray fluorescence analysis*: Springer Science & Business Media, 85-129.

Beuer, F., Schweiger, J., Edelhoff, D. (2008). Digital dentistry: an overview of recent developments for CAD/CAM generated restorations. *British Dental Journal, 204*(9), 505-511.

Bigi, A., Boanini, E., Bracci, B., Facchini, A., Panzavolta, S., Segatti, F., Sturba, L. (2005). Nanocrystalline hydroxyapatite coatings on titanium: a new fast biomimetic method. *Biomaterials, 26*(19), 4085-4089.

Blarcom, C., Clifford, W. (2008). The glossary of prosthodontic terms. *Journal of Prosthetic Dentistry, 94*(1), 1-92.

Boccaccini, A., Keim, S., Ma, R., Li, Y., Zhitomirsky, I. (2010). Electrophoretic deposition of biomaterials. *Journal of the Royal Society Interface* 7. *S581–S613*.

Brochu, J. F., El-Mowafy, O. (2002). Longevity and clinical performance of IPS-Empress ceramic restorations-a literature review. *Journal Canadian Dental Association, 68*(4), 233-238.

Campos, R. E., Soares, P. V., Versluis, A., Júnior, O. B. d. O., Ambrosano, G. M., Nunes, I. F. (2015). Crown fracture: Failure load, stress distribution, and fractographic analysis. *Journal of Prosthetic Dentistry, 114*(3), 447-455.

Casucci, A., Mazzitelli, C., Monticelli, F., Toledano, M., Osorio, R., Osorio, E., Papacchini, F., Ferrari, M. (2010). Morphological analysis of three zirconium oxide ceramics: Effect of surface treatments. *Dental Materials, 26*(8), 751-760.

Casucci, A., Osorio, E., Osorio, R., Monticelli, F., Toledano, M., Mazzitelli, C., Ferrari, M. (2009). Influence of different surface treatments on surface zirconia frameworks. *Journal of Dentistry, 37*(11), 891-897.

Chang, M. S., Kim, J. H., Cho, S. K., Bok, W. M., Song, K. Y., Park, J. M. (2005). Bond strength of resin cements to zirconia ceramic. *Journal of Korean Academy of Prosthodontics, 43*(4), 426-437.

Chevalier, J. m., Gremillard, L., Virkar, A. V., Clarke, D. R. (2009). The tetragonal-monoclinic transformation in zirconia: lessons learned and future trends. *Journal of the American Ceramic Society, 92*(9), 1901-1920.

Chipera, S. J., Bish, D. L. (2002). FULLPAT: a full-pattern quantitative analysis program for X-ray powder diffraction using measured and calculated patterns. *Journal of Applied Crystallography, 35*(6), 744-749.

Christel, P., Meunier, A., DORLOT, J. M., CROLET, J. M., Witvoet, J., Sedel, L., Boutin, P. (1988). Biomechanical compatibility and design of ceramic implants for orthopedic surgery. *Annals of the New York Academy of Sciences, 523*(1), 234-256.

Christel, P., Meunier, A., Heller, M., Torre, J., Peille, C. (1989). Mechanical properties and short-term in vivo evaluation of yttrium-oxide-partially-stabilized zirconia. *Journal of Biomedical Materials Research, 23*(1), 45-61.

Claus, H. (1989). The structure and microstructure of dental porcelain in relationship to the firing conditions. *International Journal of Prosthodontics, 2*(4), 376-384.

Claus, H. (1990). Vita InCeram, a new system for producing aluminum oxide crown and bridge substructures. *Quintessenz Zahntech, 16*, 35-46.

Collins, T. J. (2007). ImageJ for microscopy. *Biotechniques, 43*(1 Suppl), 25-30.

Craig, R., Powers, J. (2002). Restorative dental materials, 2002. *Mosby, St Louis, MO, USA*, 332-340.

Craig, R., Powers, J., Wataha, J. (2004). Dental materials Properties and manipulation, China: Mosby. 161-166.

Curtis, A. R., Wright, A. J., Fleming, G. J. (2006). The influence of surface modification techniques on the performance of a Y-TZP dental ceramic. *Journal of Dentistry, 34*(3), 195-206.

da Silva, T. M., Salvia, A. C. R. D., de Carvalho, R. F., Pagani, C., da Rocha, D. M., da Silva, E. G. (2014). Polishing for glass ceramics: Which protocol? *Journal of Prosthodontic Research, 58*(3), 160-170.

Davidowitz, G., Kotick, P. G. (2011). The use of CAD/CAM in dentistry. *Dental Clinics of North America, 55*(3), 559-570.

De Jager, N., de Kler, M., van der Zel, J. M. (2006). The influence of different core material on the FEA-determined stress distribution in dental crowns. *Dental Materials, 22*(3), 234-242.

Dejak, B., Młotkowski, A., Langot, C. (2012). Three-dimensional finite element analysis of molars with thin-walled prosthetic crowns made of various materials. *Dental Materials, 28*(4), 433-441.

Dejak, B., Mlotkowski, A., Romanowicz, M. (2007). Strength estimation of different designs of ceramic inlays and onlays in molars based on the Tsai-Wu failure criterion. *Journal of Prosthetic Dentistry, 98*(2), 89-100.

Della Bona, A., Donassollo, T. A., Demarco, F. F., Barrett, A. A., Mecholsky, J. J. (2007). Characterization and surface treatment effects on topography of a glass-infiltrated alumina/zirconia-reinforced ceramic. *Dental Materials, 23*(6), 769-775.

Della Bona, A., Kelly, J. R. (2008). The clinical success of all-ceramic restorations. *Journal of the American Dental Association, 139,* S8-S13.

Della Bona, A., Mecholsky, J. J., Barrett, A. A., Griggs, J. A. (2008). Characterization of glass-infiltrated alumina-based ceramics. *Dental Materials, 24*(11), 1568-1574.

Denry, I., Holloway, J. A. (2010). Ceramics for dental applications: a review. *Materials, 3*(1), 351-368.

Denry, I., Kelly, J. R. (2008). State of the art of zirconia for dental applications. *Dental Materials, 24*(3), 299-307.

Denry, I., Mackert, J., Holloway, J., Rosenstiel, S. (1996). Effect of cubic leucite stabilization on the flexural strength of feldspathic dental porcelain. *Journal of Dental Research*, *75*(12), 1928-1935.

Deville, S., Chevalier, J., Gremillard, L. (2006). Influence of surface finish and residual stresses on the ageing sensitivity of biomedical grade zirconia. *Biomaterials, 27*(10), 2186-2192.

Dong, J., Luthy, H., Wohlwend, A., Schärer, P. (1992). Heat-pressed ceramics: technology and strength. *International Journal of Prosthodontics, 5*(1).

Dozić, A., Kleverlaan, C. J., Meegdes, M., van der Zel, J., Feilzer, A. J. (2003). The influence of porcelain layer thickness on the final shade of ceramic restorations. *Journal of Prosthetic Dentistry, 90*(6), 563-570.

Elsaka, S. E. (2013). Influence of surface treatments on the surface properties of different zirconia cores and adhesion of zirconia-veneering ceramic systems. *Dental Materials, 29*(10), e239-e251.

Everson, P., Addison, O., Palin, W. M., Burke, F. T. (2012). Improved bonding of zirconia substructures to resin using a “glaze-on” technique. *Journal of Dentistry, 40*(4), 347-351.

Ezazshahabi, N., Latifi, M., Madanipour, K. (2017). Modelling of surface roughness based on geometrical parameters of woven fabrics. *Indian Journal of Fibre & Textile Research (IJFTR), 42*(1), 43-50.

Farhan, F. A., Sulaiman, E., Kutty, M. G. (2017). Effect of new zirconia surface coatings on the surface properties and bonding strength of veneering zirconia substrate. *Surface and Coatings Technology*. doi: https://doi.org/10.1016/j.surfcoat.2017.10.030

Fathi, M., Doostmohammadi, A. (2009). Bioactive glass nanopowder and bioglass coating for biocompatibility improvement of metallic implant. *Journal of Materials Processing Technology, 209*(3), 1385-1391.

Filser, F., Lüthy, H., Schärer, P., Gauckler, L. (1997). *All-ceramic dental bridges by direct ceramic machining (DCM).* Paper presented at the Bioceramics Proceedings of the 10th International Symposium on Ceramics in Medicin (Vol. 10, pp. 433-436).

Fischer, J., Grohmann, P., Stawarczyk, B. (2008). Effect of zirconia surface treatments on the shear strength of zirconia/veneering ceramic composites. *Dental Materials Journal, 27*(3), 448-454.

Fischer, J., Stawarczyk, B., Hämmerle, C. (2008). Flexural strength of veneering ceramics for zirconia. *Journal of Dentistry, 36*(5), 316-321.

Fischer, J., Stawarzcyk, B., Trottmann, A., Hämmerle, C. H. (2009). Impact of thermal misfit on shear strength of veneering ceramic/zirconia composites. *Dental Materials, 25*(4), 419-423.

Fouquier, R. (2010). Master Craftsman Zirconia: With or without liner? *Dental Technologies*(89), 25.

Gadelmawla, E., Koura, M., Maksoud, T., Elewa, I., Soliman, H. (2002). Roughness parameters. *Journal of Materials Processing Technology, 123*(1), 133-145.

Garvie, R., Hannink, R., Pascoe, R. (1975). Ceramic steel? *Nature, 258*(5537), 703-704.

Ghumatkar, A., Budhe, S., Sekhar, R., Banea, M., Barros, S. d. (2016). Influence of Adherend Surface Roughness on the Adhesive Bond Strength. *Latin American Journal of Solids and Structures, 13*(13), 2356-2370.

Giordano, R. (2006). Materials for chairside CAD/CAM–produced restorations. *Journal of the American Dental Association, 137,* 14S-21S.

Goldstein, J., Newbury, D. E., Echlin, P., Joy, D. C., Romig Jr, A. D., Lyman, C. E., Fiori, C., Lifshin, E. (2012). *Scanning electron microscopy and X-ray microanalysis: a text for biologists, materials scientists, and geologists*: Springer Science & Business Media, 150-163.

Gorman, C. M., Hill, R. G. (2003). Heat-pressed ionomer glass-ceramics. Part I: an investigation of flow and microstructure. *Dental Materials, 19*(4), 320-326.

Gowida, M., Aboushelib, M. (2016). Bonding to Zirconia (A Systematic Review). *Journal of Dental Sciences, 1*(1), 1-19.

Griggs, J. A. (2007). Recent advances in materials for all-ceramic restorations. *Dental Clinics of North America, 51*(3), 713-727.

Guazzato, M., Albakry, M., Ringer, S. P., Swain, M. V. (2004). Strength, fracture toughness and microstructure of a selection of all-ceramic materials. Part I. Pressable and alumina glass-infiltrated ceramics. *Dental Materials, 20*(5), 441-448.

Guazzato, M., Albakry, M., Swain, M. V., Ironside, J. (2001). Mechanical properties of In-Ceram Alumina and In-Ceram Zirconia. *International Journal of Prosthodontics, 15*(4), 339-346.

Guess, P. C., Att, W., Strub, J. R. (2012). Zirconia in fixed implant prosthodontics. *Clinical Implant Dentistry and Related Research, 14*(5), 633-645.

Guess, P. C., Kuliš, A., Witkowski, S., Wolkewitz, M., Zhang, Y., Strub, J. R. (2008). Shear bond strengths between different zirconia cores and veneering ceramics and their susceptibility to thermocycling. *Dental Materials, 24*(11), 1556-1567.

Guess, P. C., Schultheis, S., Bonfante, E. A., Coelho, P. G., Ferencz, J. L., Silva, N. R. (2011). All-ceramic systems: laboratory and clinical performance. *Dental Clinics of North America, 55*(2), 333-352.

Habelitz, S., Carl, G., Rüssel, C. (2001). Processing, microstructure and mechanical properties of extruded mica glass-ceramics. *Materials Science and Engineering: A, 307*(1–2), 1-14.

Hallmann, L., Ulmer, P., Wille, S., Kern, M. (2014). Effect of differences in coefficient of thermal expansion of veneer and Y-TZP ceramics on interface phase transformation. *Journal of Prosthetic Dentistry, 112*(3), 591-599.

Heffernan, M. J., Aquilino, S. A., Diaz-Arnold, A. M., Haselton, D. R., Stanford, C. M., Vargas, M. A. (2002). Relative translucency of six all-ceramic systems. Part I: core materials. *Journal of Prosthetic Dentistry, 88*(1), 4-9.

Helmer, J., Driskell, T. (1969). *Research on bioceramics.* Paper presented at the Symposium on use of ceramics as surgical implants. South Carolina (USA): Clemson University.

Helvey, G. (2010). Ceramics. *Compendium of Continuing Education in Dentistry, 31*(4), 309-311.

Helvey, G. A. (2008). Zirconia and computer-aided design/computer-aided manufacturing (CAD/CAM) dentistry. *Inside Dentistry, 4*(4), 72-79.

Hisbergues, M., Vendeville, S., Vendeville, P. (2009). Zirconia: Established facts and perspectives for a biomaterial in dental implantology. *Journal of Biomedical Materials Research Part B: Applied Biomaterials, 88*(2), 519-529.

Höland, W., Beall, G. H. (2012). Composition Systems for Glass-Ceramics. *Glass-Ceramic Technology, Second Edition*, 75-206.

Höland, W., Rheinberger, V., Apel, E., van't Hoen, C., Höland, M., Dommann, A., Obrecht, M., Mauth, C., Graf-Hausner, U. (2006). Clinical applications of glass-ceramics in dentistry. *Journal of Materials Science: Materials in Medicine, 17*(11), 1037-1042.

Hu, J., Dai, N., Bao, Y., Gu, W., Ma, J., Zhang, F. (2013). Effect of different coping designs on all-ceramic crown stress distribution: A finite element analysis. *Dental Materials, 29*(11), e291-e298.

Hutchinson, J. (1989). Mechanisms of toughening in ceramics. *Theoretical and Applied Mechanics*, 139-144.

Hwang, J. W., Yang, J. H. (2001). Fracture strength of copy-milled and conventional In-Ceram crowns. *Journal of Oral Rehabilitation, 28*(7), 678-683.

Imanishi, A., Nakamura, T., Ohyama, T. (2003). 3-D Finite element analysis of all-ceramic posterior crowns. *Journal of Oral Rehabilitation, 30*(8), 818-822.

Isgrò, G., Kleverlaan, C. J., Wang, H., Feilzer, A. J. (2004). Thermal dimensional behavior of dental ceramics. *Biomaterials, 25*(12), 2447-2453.

ISO 9693, (2012). Metal-ceramic dental restorative systems. International Organization for Standardization, Geneva. ISO 6872.

ISO 25178-2, (2010). Geometrical product specifications (GPS)-Surface texture: Areal-Part. International Organization for Standardization, FDIS 25178-2. *2.*

James, J., Spittle, J., Brown, S., Evans, R. (2001). A review of measurement techniques for the thermal expansion coefficient of metals and alloys at elevated temperatures. *Measurement Science and Technology, 12*(3), R1-R15.

Jin, X.-J. (2005). Martensitic transformation in zirconia containing ceramics and its applications. *Current Opinion in Solid State and Materials Science, 9*(6), 313-318.

Jing, Z., Ke, Z., Yihong, L., Zhijian, S. (2014). Effect of Multistep Processing Technique on the Formation of Micro-defects and Residual Stresses in Zirconia Dental Restorations. *Journal of Prosthodontics, 23*(3), 206-212.

Jones, D. W. (1985). Development of dental ceramics. An historical perspective. *Dental Clinics of North America, 29*(4), 621-644.

Julien, K., Buschang, P., Throckmorton, G., Dechow, P. (1996). Normal masticatory performance in young adults and children. *Archives of Oral Biology, 41*(1), 69-75.

Juy, A., Anglada, M. (2007). Surface Phase Transformation During Grinding of Y-TZP. *Journal of the American Ceramic Society, 90*(8), 2618-2621.

Kelly, J. R. (1999). Clinically relevant approach to failure testing of all-ceramic restorations. *Journal of Prosthetic Dentistry, 81*(6), 652-661.

Kelly, J. R. (2007). Developing meaningful systematic review of CAD/CAM reconstructions and fiber-reinforced composites*. *Clinical Oral Implants Research, 18*(s3), 205-217.

Kelly, J. R., Nishimura, I., Campbell, S. D. (1996). Ceramics in dentistry: historical roots and current perspectives. *Journal of Prosthetic Dentistry, 75*(1), 18-32.

Kelly, P., Arnell, R. (2000). Magnetron sputtering: a review of recent developments and applications. *Vacuum, 56*(3), 159-172.

Kern, M., Thompson, V. (1993). Sandblasting and silica-coating of dental alloys: volume loss, morphology and changes in the surface composition. *Dental Materials, 9*(3), 155-161.

Kern, M., Thompson, V. P. (1995). Bonding to glass infiltrated alumina ceramic: adhesive methods and their durability. *Journal of Prosthetic Dentistry, 73*(3), 240-249.

Kern, M., Wegner, S. M. (1998). Bonding to zirconia ceramic: adhesion methods and their durability. *Dental Materials, 14*(1), 64-71.

Kim, H. J., Lim, H. P., Park, Y. J., Vang, M. S. (2011). Effect of zirconia surface treatments on the shear bond strength of veneering ceramic. *Journal of Prosthetic Dentistry, 105*(5), 315-322.

Kohal, R. J., Klaus, G., Strub, J. R. (2006). Zirconia-implant-supported all-ceramic crowns withstand long-term load: a pilot investigation. *Clinical Oral Implants Research, 17*(5), 565-571.

Komine, F., Saito, A., Kobayashi, K., Koizuka, M., Koizumi, H., Matsumura, H. (2010). Effect of cooling rate on shear bond strength of veneering porcelain to a zirconia ceramic material. *Journal of Oral Science, 52*(4), 647-652.

Komine, F., Strub, J. R., Matsumura, H. (2012). Bonding between layering materials and zirconia frameworks. *Japanese Dental Science Review, 48*(2), 153-161.

Kosmac, T., Oblak, C., Jevnikar, P., Funduk, N., Marion, L. (2000). Strength and reliability of surface treated Y-TZP dental ceramics. *Journal of Biomedical Materials Research, 53*(4), 304-313.

Kosmač, T., Oblak, C., Jevnikar, P., Funduk, N., Marion, L. (1999). The effect of surface grinding and sandblasting on flexural strength and reliability of Y-TZP zirconia ceramic. *Dental Materials, 15*(6), 426-433.

Kosmač, T., Oblak, Č., Marion, L. (2008). The effects of dental grinding and sandblasting on ageing and fatigue behavior of dental zirconia (Y-TZP) ceramics. *Journal of the European Ceramic Society, 28*(5), 1085-1090.

Land, C. H. (1904). *Porcelain dental art: No. II. Dental Cosmostics, 45, 615-620*.

Li, H., Li, J., Zou, Z., Fok, A. S.-L. (2011). Fracture simulation of restored teeth using a continuum damage mechanics failure model. *Dental Materials, 27*(7), e125-e133.

Li, R. W. K., Chow, T. W., Matinlinna, J. P. (2014). Ceramic dental biomaterials and CAD/CAM technology: state of the art. *Journal of Prosthodontic Research, 58*(4), 208-216.

Lin, J., Shinya, A., Gomi, H., Shinya, A. (2012). Finite element analysis to compare stress distribution of connector of lithia disilicate-reinforced glass–ceramic and zirconia-based fixed partial denture. *Odontology, 100*(1), 96-99.

Liu, D., Matinlinna, J. P., Tsoi, J. K.-H., Pow, E. H., Miyazaki, T., Shibata, Y., Kan, C. W. (2013). A new modified laser pretreatment for porcelain zirconia bonding. *Dental Materials, 29*(5), 559-565.

Liu, P. R. (2005). A panorama of dental CAD/CAM restorative systems. *Compendium, 26*(7), 507-513.

Lou, B., Chao, Q., Wang, M., Lu, Z., Chao, Y. (2004). Short-term follow-up study of Cercon all-ceramic crowns and bridges. *West China Journal of Stomatology, 22*(5), 402-403.

Luthardt, R., Weber, A., Rudolph, H., Schöne, C., Quaas, S., Walter, M. (2002). Design and production of dental prosthetic restorations: basic research on dental CAD/CAM technology. *International Journal of Computerized Dentistry, 5*(2-3), 165-176.

Luthardt, R. G., Holzhüter, M. S., Rudolph, H., Herold, V., Walter, M. H. (2004). CAD/CAM-machining effects on Y-TZP zirconia. *Dental Materials, 20*(7), 655-662.

Manicone, P. F., Iommetti, P. R., Raffaelli, L. (2007). An overview of zirconia ceramics: basic properties and clinical applications. *Journal of Dentistry, 35*(11), 819-826.

Mantri, S. S., Bhasin, A. S. (2010). CAD/CAM in dental restorations: an overview. *Annals and Essences of Dentistry, 2*(3), 123-128.

Marinis, A., Aquilino, S. A., Lund, P. S., Gratton, D. G., Stanford, C. M., Diaz-Arnold, A. M., Qian, F. (2013). Fracture toughness of yttria-stabilized zirconia sintered in conventional and microwave ovens. *Journal of Prosthetic Dentistry, 109*(3), 165-171.

Matinlinna, J. P., Heikkinen, T., Özcan, M., Lassila, L. V., Vallittu, P. K. (2006). Evaluation of resin adhesion to zirconia ceramic using some organosilanes. *Dental Materials*, *22*(9), 824-831.

Matyas, J., Caputo, A. (1982). Bond strength of spray-opaque porcelain to metal. *Journal of the Calefornia Dental Association, 10*(9), 37-39.

McCabe, J. F., Walls, A. W. (2008). *Applied dental materials. 9 Edition*: John Wiley & Sons. 6-18.

McLean, J., Hughes, T. (1965). The reinforcement of dental porcelain with ceramic oxides. *British Dental Journal, 119*(6), 251.

McLean, J. W. (2001). Evolution of dental ceramics in the twentieth century. *Journal of Prosthetic Dentistry, 85*(1), 61-66.

Meyenberg, K. H., Luthy, H., Scharer, P. (1995). Zirconia Posts: A New All-Ceramic Concept for Nonvital Abutment Teeth. *Journal of Esthetic and Restorative Dentistry, 7*(2), 73-80.

Miyazaki, T., Hotta, Y., Kunii, J., Kuriyama, S., Tamaki, Y. (2009). A review of dental CAD/CAM: current status and future perspectives from 20 years of experience. *Dental Materials Journal, 28*(1), 44-56.

Moeser, M., 2007. Fractography with the SEM (failure analysis). Materials Science Monographs. 366-385

Monmaturapoj, N., Lawita, P., Thepsuwan, W. (2013). Characterisation and properties of lithium disilicate glass ceramics in the SiO2-Li2O-K2O-Al2O3 system for dental applications. *Advances in Materials Science and Engineering*, 1-11.

Moon, J. E., Kim, S. H., Lee, J. B., Ha, S. R., Choi, Y. S. (2011). The effect of preparation order on the crystal structure of yttria-stabilized tetragonal zirconia polycrystal and the shear bond strength of dental resin cements. *Dental Materials, 27*(7), 651-663.

Mörmann, W. H., Brandestini, M., Lutz, F., Barbakow, F. (1989). Chairside computer-aided direct ceramic inlays. *Quintessence International, 20*(5), 329-339.

Mosharraf, R., Rismanchian, M., Savabi, O., Ashtiani, A. H. (2011). Influence of surface modification techniques on shear bond strength between different zirconia cores and veneering ceramics. *Journal of Advanced Prosthodontics, 3*(4), 221-228.

Naji, G. A. H., Omar, R. A., Yahya, R. (2017). Influence of sodalite zeolite infiltration on the coefficient of thermal expansion and bond strength of all-ceramic dental prostheses. *Journal of the Mechanical Behavior of Biomedical Materials, 67*, 135-143.

Naji, G. A. H., Omar, R. A., Yahya, R. (2016). The effect of sodalite zeolite infiltrated material on the fracture toughness, elastic modulus and optical properties of all-ceramic dental prostheses. *Ceramics International, 42*, 18737–18746.

Nishigori, A., Yoshida, T., Bottino, M. C., Platt, J. A. (2014). Influence of zirconia surface treatment on veneering porcelain shear bond strength after cyclic loading. *Journal of Prosthetic Dentistry, 112*(6), 1392-1398.

O'Brien, W. J. (2002). Dental materials and their selection. 3rd edition. *Quintessence Publishing Co*, 210-225.

Ohkuma, K., Kazama, M., Ogura, H. (2011). The grinding efficiency by diamond points developed for yttria partially stabilized zirconia. *Dental Materials Journal, 30*(4), 511-516.

Øilo, M., Gjerdet, N. R. (2013). Fractographic analyses of all-ceramic crowns: a study of 27 clinically fractured crowns. *Dental Materials, 29*(6), e78-e84.

Ono, T., Allaire, R. (2000). Fracture Analysis, a Basic Tool to Solve Breakage Issues. Taiwan FPD Expo 2000.

Özkurt, Z., Kazazoğlu, E. (2010). Clinical success of zirconia in dental applications. *Journal of Prosthodontics, 19*(1), 64-68.

Piconi, C., Maccauro, G. (1999). Zirconia as a ceramic biomaterial. *Biomaterials, 20*(1), 1-25.

Pittayachawan, P. (2009). *Comparative study of physical properties of zirconia based dental ceramics.* (Doctoral dissertation), UCL (University College London).

Piwowarczyk, A., Ottl, P., Lauer, H. C., Kuretzky, T. (2005). A Clinical Report and Overview of Scientific Studies and Clinical Procedures Conducted on the 3M ESPE Lava™ All-Ceramic System. *Journal of Prosthodontics, 14*(1), 39-45.

Pjetursson, B. E., Sailer, I., Zwahlen, M., Hämmerle, C. H. (2007). A systematic review of the survival and complication rates of all-ceramic and metal–ceramic reconstructions after an observation period of at least 3 years. Part I: single crowns. *Clinical Oral Implants Research, 18*(s3), 73-85.

Popa, D., Constantiniuc, M., Negucioiu, M., Ciobotea, L., Câmpian, R. S. (2015). Cercon-Smart Ceramics, From theory to practice. *International Journal of Medical Dentistry, 5*(1), 31.

Porter, D. A., Easterling, K E. (1992). Phase Transformations in Metals and Alloys,”. *London: Chapman k Hall*, 147.

Porter, D. L., Heuer, A. (1977). Mechanisms of toughening partially stabilized zirconia (PSZ). *Journal of the American Ceramic Society, 60*(3-4), 183-184.

Powers, J. M., Wataha, J. C. (2013). *Dental Materials Book: Properties and Manipulation* (Vol. 10th ed., pp.187-205). London: Mosby.

Pröbster, L. (1992). Survival rate of In-Ceram restorations. *International Journal of Prosthodontics, 6*(3), 259-263.

Pröbster, L., Diehl, J. (1992). Slip-casting alumina ceramics for crown and bridge restorations. *Quintessence International (Berlin, Germany: 1985), 23*(1), 25-31.

Qualtrough, A., Piddock, V. (1995). Dental CAD/CAM: a millstone or a milestone? *Dental Update, 22*(5), 200-204.

Qualtrough, A., Piddock, V. (2002). Dental ceramics: what's new? *Dental Update, 29*(1), 25-33.

Quinn, J. B., Quinn, G. D., Kelly, J. R., Scherrer, S. S. (2005). Fractographic analyses of three ceramic whole crown restoration failures. *Dental Materials, 21*(10), 920-929.

Quinn, J. B., Sundar, V., Lloyd, I. K. (2003). Influence of microstructure and chemistry on the fracture toughness of dental ceramics. *Dental Materials, 19*(7), 603-611.

Rad, A. T., Solati-Hashjin, M., Osman, N. A. A., Faghihi, S. (2014). Improved bio-physical performance of hydroxyapatite coatings obtained by electrophoretic deposition at dynamic voltage. *Ceramics International, 40*(8), 12681-12691.

Raigrodski, A. (2005). All-ceramic full-coverage restorations: concepts and guidelines for material selection. *Practical Procedures & Aesthetic Dentistry, 17*(4), 249-256; quiz 258.

Raigrodski, A. J. (2004). Contemporary materials and technologies for all-ceramic fixed partial dentures: a review of the literature. *Journal of Prosthetic Dentistry, 92*(6), 557-562.

Raigrodski, A. J., Hillstead, M. B., Meng, G. K., Chung, K.-H. (2012). Survival and complications of zirconia-based fixed dental prostheses: a systematic review. *Journal of Prosthetic Dentistry, 107*(3), 170-177.

Raposo, L. H., Armstrong, S. R., Maia, R. R., Qian, F., Geraldeli, S., Soares, C. J. (2012). Effect of specimen gripping device, geometry and fixation method on microtensile bond strength, failure mode and stress distribution: laboratory and finite element analyses. *Dental Materials, 28*(5), e50-e62.

Rasband, W., 1997. ImageJ. US National Institutes of Health, Bethesda, MD.

Reichelt, R. (2007). Scanning electron microscopy. *Science of Microscopy* (pp. 133-272): Springer.

Rezaei, S. M. M., Heidarifar, H., Arezodar, F. F., Azary, A., Mokhtarykhoee, S. (2011). Influence of connector width on the stress distribution of posterior bridges under loading. *Journal of Dentistry, 8*(2), 67.

Rizkalla, A., Jones, D. (2004). Mechanical properties of commercial high strength ceramic core materials. *Dental Materials, 20*(2), 207-212.

Rosentritt, M., Behr, M., van der Zel, J. M., Feilzer, A. J. (2009). Approach for evaluating the influence of laboratory simulation. *Dental Materials, 25*(3), 348-352.

Sadoun, M. (1988). *All ceramic bridges with the slip casting technique.* Paper presented at the 7th International Symposium on Ceramics, Paris, September 1988.

Sailer, I., Gottner, J., Känel, S., Franz Hämmerle, C. H. (2009a). Randomized controlled clinical trial of zirconia-ceramic and metal-ceramic posterior fixed dental prostheses: a 3-year follow-up. *International Journal of Prosthodontics, 22*(6), 553.

Sailer, I., Holderegger, C., Jung, R. E., Suter, A., Thiévent, B., Pietrobon, N., Gebhard-Achilles, W., Hämmerle, C. H. F. (2007a). Clinical study of the color stability of veneering ceramics for zirconia frameworks. *International Journal of Prosthodontics, 20*(3).

Sailer, I., Philipp, A., Zembic, A., Pjetursson, B. E., Hämmerle, C. H., Zwahlen, M. (2009b). A systematic review of the performance of ceramic and metal implant abutments supporting fixed implant reconstructions. *Clinical Oral Implants Research, 20*(s4), 4-31.

Sailer, I., Pjetursson, B. E., Zwahlen, M., Hämmerle, C. H. (2007b). A systematic review of the survival and complication rates of all-ceramic and metal–ceramic reconstructions after an observation period of at least 3 years. Part II: fixed dental prostheses. *Clinical Oral Implants Research, 18*(s3), 86-96.

Saint-Jean, S. J. (2013). Dental Glasses and Glass-ceramics. In J. Z. Shen & T. Kosmač (Eds.), *Advanced Ceramics for Dentistry* (1st ed., pp. 255-277). St. Wyaman: Elsevier Inc.

Salem, N. A., Taleb, A., Ahmed, L., Aboushelib, M. N. (2013). Biomechanical and Histomorphometric Evaluation of Osseointegration of Fusion-Sputtered Zirconia Implants. *Journal of Prosthodontics, 22*(4), 261-267.

Santos Jr, G. C., Santos Jr, M., Rizkalla, A. S., Madani, D., El-Mowafy, O. (2013). Overview of CEREC CAD/CAM chairside system. *General Dentistry, 61*(1), 36-40.

Scardaci, V., Coull, R., Lyons, P. E., Rickard, D., Coleman, J. N. (2011). Spray deposition of highly transparent, low-resistance networks of silver nanowires over large areas. *Small, 7*(18), 2621-2628.

Scherrer, S. S., Cattani-Lorente, M., Vittecoq, E., de Mestral, F., Griggs, J. A., Wiskott, H. A. (2011). Fatigue behavior in water of Y-TZP zirconia ceramics after abrasion with 30µm silica-coated alumina particles. *Dental Materials, 27*(2), e28-e42.

Scherrer, S. S., Quinn, G. D., Quinn, J. B. (2008). Fractographic failure analysis of a Procera® AllCeram crown using stereo and scanning electron microscopy. *Dental Materials, 24*(8), 1107-1113.

Scherrer, S. S., Quinn, J. B., Quinn, G. D., Wiskott, H. A. (2007). Fractographic ceramic failure analysis using the replica technique. *Dental Materials, 23*(11), 1397-1404.

Schneider, C. A., Rasband, W. S., Eliceiri, K. W. (2012). NIH Image to Image J: 25 years of image analysis. *Nature Methods, 9*(7), 671.

Schuetz, G. (2013). Measuring for Flatness, Thickness and Parallelism. *Modern Machine Shop, 85*(11), 56-58.

Seghi, R., Denry, I., Rosenstiel, S. (1995). Relative fracture toughness and hardness of new dental ceramics. *Journal of Prosthetic Dentistry, 74*(2), 145-150.

Shenoy, A., Shenoy, N. (2010). Dental ceramics: An update. *Journal of Conservative Dentistry: JCD, 13*(4), 195.

Soares, C. J., Soares, P. V., Pereira, J. C., Fonseca, R. B. (2005). Surface Treatment Protocols in the Cementation Process of Ceramic and Laboratory-Processed Composite Restorations: A Literature Review. *Journal of Esthetic and Restorative Dentistry, 17*(4), 224-235.

Spinell, Vita In-Ceram. (2002). Directions for use fabrication of framework in the slip-casting technique. Site: www. vitazahnfabrik. com. br, 1-17.

Springate, S., Winchester, L. (1991). An evaluation of zirconium oxide brackets: a preliminary laboratory and clinical report. *British Journal of Orthodontics, 18*(3), 203-209.

Sun, L., Berndt, C. C., Gross, K. A., Kucuk, A. (2001). Material fundamentals and clinical performance of plasma-sprayed hydroxyapatite coatings: a review. *Journal of Biomedical Materials Research, 58*(5), 570-592.

Sundh, A., Sjögren, G. (2004). A comparison of fracture strength of yttrium-oxide-partially-stabilized zirconia ceramic crowns with varying core thickness, shapes and veneer ceramics. *Journal of Oral Rehabilitation, 31*(7), 682-688.

Teng, J., Wang, H., Liao, Y., Liang, X. (2012). Evaluation of a conditioning method to improve core-veneer bond strength of zirconia restorations. *Journal of Prosthetic Dentistry, 107*(6), 380-387.

Tholey, M. J., Berthold, C., Swain, M. V., Thiel, N. (2010). XRD 2 micro-diffraction analysis of the interface between Y-TZP and veneering porcelain: role of application methods. *Dental Materials, 26*(6), 545-552.

Thompson, J. Y., Stoner, B. R., Piascik, J. R. (2007). Ceramics for restorative dentistry: critical aspects for fracture and fatigue resistance. *Materials Science and Engineering: C, 27*(3), 565-569.

Thompson, V. P., Rekow, D. E. (2004). Dental ceramics and the molar crown testing ground. *Journal of Applied Oral Science, 12*(SPE), 26-36.

Tinschert, J., Natt, G., Hassenpflug, S., Spiekermann, H. (2004). Status of current CAD/CAM technology in dental medicine. *International Journal of Computerized Dentistry, 7*(1), 25-45.

Triwatana, P., Nagaviroj, N., Tulapornchai, C. (2012). Clinical performance and failures of zirconia-based fixed partial dentures: a review literature. *Journal of Advanced Prosthodontics, 4*(2), 76-83.

Valíček, J., Držík, M., Hryniewicz, T., Harničárová, M., Rokosz, K., Kušnerová, M., Barčová, K., Bražina, D. (2012). Non-contact method for surface roughness measurement after machining. *Measurement Science Review, 12*(5), 184-188.

Van Noort, R., Barbour, M. E. (2013). *Introduction to Dental Materials. 4th edition* Elsevier Health Sciences.

van Noort, R., Gjerdet, N. R., Schedle, A., Björkman, L., Berglund, A. (2004). An overview of the current status of national reporting systems for adverse reactions to dental materials. *Journal of Dentistry, 32*(5), 351-358.

Vivadent, I. (2009). IPS e. max lithium disilicate: The future of all ceramic dentistry material science, Practical Applications, keys to success. *Amherst, NY: Ivoclar Vivadent,* 1-15.

Waetjen, A. M., Polsakiewicz, D. A., Kuhl, I., Telle, R., Fischer, H. (2009). Slurry deposition by airbrush for selective laser sintering of ceramic components. *Journal of the European Ceramic Society, 29*(1), 1-6.

Wakabayashi, N., Ona, M., Suzuki, T., Igarashi, Y. (2008). Nonlinear finite element analyses: advances and challenges in dental applications. *Journal of Dentistry, 36*(7), 463-471.

Walter, M. H., Wolf, B. H., Wolf, A. E., Boening, K. W. (2006). Six-year clinical performance of all-ceramic crowns with alumina cores. *International Journal of Prosthodontics, 19*(2), 162-163.

Wang, G., Zhang, S., Bian, C., Kong, H. (2014). Interface toughness of a zirconia-veneer system and the effect of a liner application. *Journal of Prosthetic Dentistry, 112*(3), 576-583.

Wang, X., Li, X., Onuma, K., Ito, A., Sogo, Y., Kosuge, K., Oyane, A. (2010). Mesoporous bioactive glass coatings on stainless steel for enhanced cell activity, cytoskeletal organization and AsMg immobilization. *Journal of Materials Chemistry, 20*(31), 6437-6445.

White, S., Miklus, V., McLaren, E., Lang, L., Caputo, A. (2005). Flexural strength of a layered zirconia and porcelain dental all-ceramic system. *Journal of Prosthetic Dentistry, 94*(2), 125-131.

Winchester, L. (1991). Bond strengths of five different ceramic brackets: an in vitro study. *European Journal of Orthodontics, 13*(4), 293-305.

Window, B. (1996). Issues in magnetron sputtering of hard coatings. *Surface and Coatings Technology, 81*(1), 92-98.

Wolfart, S., Harder, S., Eschbach, S., Lehmann, F., Kern, M. (2009). Four-year clinical results of fixed dental prostheses with zirconia substructures (Cercon): end abutments vs. cantilever design. *European Journal of Oral Sciences, 117*(6), 741-749.

Wollman, D., Irwin, K. D., Hilton, G. C., Dulcie, L., Newbury, D. E., Martinis, J. M. (1997). High-resolution, energy-dispersive microcalorimeter spectrometer for X-ray microanalysis. *Journal of Microscopy, 188*(3), 196-223.

Yang, B., Barloi, A., Kern, M. (2010). Influence of air-abrasion on zirconia ceramic bonding using an adhesive composite resin. *Dental Materials, 26*(1), 44-50.

Yang, Y., Kim, K. H., Ong, J. L. (2005). A review on calcium phosphate coatings produced using a sputtering process-an alternative to plasma spraying. *Biomaterials, 26*(3), 327-337.

Yasuno, K., Kakura, K., Taniguchi, Y., Yamaguchi, Y., Kido, H. (2014). Zirconia implants with laser surface treatment: peri-implant bone response and enhancement of osseointegration. *Journal of Hard Tissue Biology, 23*(1), 93-100.

Yeo, I. S., Yang, J. H., Lee, J. B. (2003). In vitro marginal fit of three all-ceramic crown systems. *Journal of Prosthetic Dentistry, 90*(5), 459-464.

Yilmaz, H., Aydin, C., Gul, B. E. (2007). Flexural strength and fracture toughness of dental core ceramics. *Journal of Prosthetic Dentistry, 98*(2), 120-128.

Yoon, H. I., Yeo, I. S., Yi, Y. J., Kim, S. H., Lee, J. B., Han, J. S. (2014). Effect of surface treatment and liner material on the adhesion between veneering ceramic and zirconia. *Journal of the Mechanical Behavior of Biomedical Materials, 40,* 369-374.

Yoshinari, M., Dérand, T. (1994). Fracture strength of all-ceramic crowns. *International Journal of Prosthodontics, 7*(4), 329-338.

Zhang, Y., Sun, T., Liu, R., Feng, X., Chen, A., Shao, L. (2014). An in vitro evaluation of the zirconia surface treatment by mesoporous zirconia coating on its bonding to resin cement. *Bio-Medical Materials and Engineering, 24*(6), 2109-2116.

LIST OF PUBLICATION AND PAPERS PRESENTED

Published papers

1. Farhan, F. A., Sulaiman, E., Kutty, M. G. (2018). Effect of new zirconia surface coatings on the surface properties and bonding strength of veneering zirconia substrate. Surface and Coatings Technology, 333, 247-258. (Q_1 - ISI cited publication).

Submitted paper

1. Farhan, F. A., Sulaiman, E., Abbood, A. I. & Kutty, M. G. Influence of new zirconia surface coatings on the fracture strength and stress distribution of zirconia-ceramic restoration. *Journal of Materials science: Journal of the European Ceramic Society*.

Manuscript in preparation

1. Farhan, F. A., Sulaiman E., Kutty, M. G. Influence of technique and particle sizes of zirconia powder on the coating properties.

Conference presentation

Farhan, F.A., Sulaiman, E., & Kutty, M.G. Development of a new coating on dental zirconia substrate using airbrush technique. The 2nd International Conference on Innovative Dentistry (ICID), 13th - 14th August 2016.